Evaluation of Liquefaction Potential of Impounded Class F Fly Ash

Thesis Write-Up

The Ohio State University Research Project # 60024835

December 2009 - March 2013

Submitted to: The Ohio State University Knowledge Bank

Department of Civil and Environmental Engineering and Geodetic Science

The Ohio State University
470 Hitchcock Hall, 2070 Neil Avenue
Columbus, Ohio 43210

March 22, 2013

Abstract

The purpose of this study was to evaluate the liquefaction potential of impounded Class F fly ash and compare the results to a 2005 study at the Ohio State University by Zand et al. A computer ground response analysis program, SHAKE, was used to obtain the cyclic stress ratios and equivalent number of cycles during several variations of a design earthquake. The profiles are based upon an actual impounded fly ash unit at an American Electric Power (AEP) plant. Cyclic triaxial tests were also performed on reconstituted specimens. The tests were performed at varying cyclic stress ratios, sample densities, and confining stresses. The results of the computer analyses were compared with laboratory testing which found the design seismic loading to be lower than the cyclic strength of the fly ash. This result is consistent with the 2005 study; however, the correlation between confining stress and liquefaction potential was not.

Acknowledgements

I would like to thank my research advisors, Dr. William Wolfe and Dr. Tarunjit Butalia for all their support and guidance over the past three years. I would also like to thank Nathan Yencho and Brian Dudley for their work during laboratory testing. Their hard work was invaluable to this project.

Table of Contents

List of Figures and Tables

List of Equations

Chapter 1 Introduction

1.1 Motivation

In 2011, approximately 60 million tons of fly ash was produced in the United States alone. Of this total, 38% was reused and the remainder left in landfills or storage ponds (AACA 2013). When designing these containment areas, liquefaction potential during seismic events is a key piece of knowledge. Liquefaction of soils can cause severe and costly structural damage. Combining this fact with environmental hazards associated with industrial by-products such as fly ash, understanding the liquefaction potential of soil-like materials becomes hyper critical.

By the mid-1970's, many studies on the liquefaction characteristics of sand and clay had been completed. Seed et al (1975-1) completed a study to determine the effects of small versus large scale testing on the liquefaction resistance of sand. Previous studies had already suggested that intact and reconstituted specimens typically have different soil structures which can have a significant effect on liquefaction resistance. Typically, intact specimen test results are more accurate to in-field results; however, obtaining these specimens and maintaining their in-situ characteristics is difficult. Although yielding different results, Seed et al developed correlations to normalize random earthquake data and relate them to response data obtained on reconstituted laboratory specimens. Seed et al (1970) compiled the results of many ground response analyses to provide a guide for selecting the dynamic shear moduli and the damping ratios. This data compilation aided in the selection of the dynamic shear moduli and damping ratios for this study. Because fly ash is a non-plastic material like sands, much of the testing protocol is based upon

equations and conclusions developed for sand. Also, the moduli and ratios for fly ash were based on those for sand.

Limited liquefaction potential testing has been performed on Class F fly ash. In 2005, a study completed at the Ohio State University sought to expand the available information. The objective of the study was to evaluate the liquefaction potential of fly ash from an American Electric Power plant (Zand et al. 2005). The study combined cyclic triaxial laboratory testing with computer simulation through SHAKE software to determine the threat an earthquake would impose on a fly ash storage pond. The study resulted in a strong correlation between the onset of liquefaction and initial dry density of specimen and a weaker correlation between the onset of liquefaction and confining stress.

The purpose of this project was to evaluate the liquefaction potential of fly ash from a different American Electric Power facility and follow similar methodology to the 2005 study. This will establish whether or not the correlations between liquefaction and different fly ash characteristics apply to different types of fly ash.

Chapter 2 Methodology

All laboratory tests and numerical modeling was carried out in the Soil Mechanics Laboratory of the Department of Civil and Environmental Engineering and Geodetic Science at The Ohio State University

2.1 Laboratory Tests

Laboratory testing consisted of creating reconstituted Class F fly ash specimens, saturating the specimens, and testing the specimens under various cyclic stress ratios.

2.1.1 Sample Preparation

Reconstituted Class F fly ash specimens were prepared from a fly ash sample provided by American Electric Power because intact specimens could not be recovered. A wet depositional method was used to simulate how fly ash is stored in the field. 500 g of oven-dried fly ash was weighed and placed in a mixing bowl. Distilled water was added to the ash and mixed until a paste was formed. The paste was fluviated into large triaxial chamber in layers to create a bulk sample. Typically, five, 500 g layers were used to make a sample. Layers were scarified with a spatula to ensure bonding between layers. After placing the last layer, the triaxial chamber was fully assembled with the addition of a circular plate which rested on top of the sample. The initial height of the sample was measured and noted.

The bulk sample was left to cure for 24 hours. After the cure period, samples were either consolidated under a 71.55 psi stress or not consolidated at all. This was done to determine how density affected liquefaction potential. If the sample was consolidated, a final sample height was measured.

2.1.2 Specimen Preparation

After the sample was fully prepared and cured, the top of the triaxial chamber was removed. Four copper pipe segments approximately 3-1/2 inches in length and 1-1/2 inches in diameter were inserted into the top of the sample. A PVC pipe segment of similar dimensions was also inserted into the top of the sample. The copper pipe molds provided stability for and prevented damage of specimens when installing them into the triaxial cell. The PVC pipe mold had a thinner wall thickness which allowed it to fit in the same bulk sample with four copper molds. After the molds were fully inserted into the top of the bulk sample, the cell was carefully removed to expose the bulk sample. A moisture content sample was removed from the bulk sample, weighed and placed in an oven with a temperature of 40˚C to 45˚C. The specimen in the PVC extruder was removed, weighed, and placed in the same oven as measure of dry density and moisture content. Each copper tube specimen was removed from the sample. The ends of each specimen were smoothed with excess portions of the bulk sample. The specimens were weighed and installed in a triaxial chamber with a surrounding membrane. The installed specimens were then attached to a pressure panel. A pressure gradient was established with slightly higher pressure on the bottom of the specimen than the top. This was done to saturate the specimen.

2.1.3 Cyclic Test

Specimens were left to saturate for at least 24 hours. The degree of saturation was judged by the measure B-value. The B-value is found by measuring the pore pressure differential when the cell pressure was increased. The pore pressure differential is then divided by the increased cell pressure. Once the B-value reached at least 95% or two weeks of saturation had occurred, the specimen was secured in a MTS hydraulic load frame controlled by an MTS Test Star Controller. An effective confining stress of approximately 20 or 40 psi was applied to the specimen.

The MTS machine applied a specified cyclic loading which was measured with a 200 lb capacity load cell. The loading was derived from the selected cyclic stress ratio (CSR). The CSR is defined as follows (Kramer, 1996):

$$CSR = \frac{\tau_{cyc}}{\sigma_0'} \qquad (2.1)$$

τ_{cyc} is the applied cyclic stress, and σ_0' is the effective confining stress.

Pore pressure was measured with a Honeywell 100 psig capacity pressure transducer. The pore pressure measurements are used to determine when liquefaction occurs which is detailed in the next chapter. Displacement was measured with the internal linear variable differential transformer (LVTD) of the MTS load frame.

The onset of liquefaction was defined as the point at which the excess pore pressure was equivalent to the initial confining stress or the point at which the axial stress readings were no longer equal to or greater than 95% of the programmed load. Whichever event occur first defined the onset of liquefaction. The criteria coupled with a significant increase in strain amplitude completed the definition. An example of the onset of liquefaction can be found in Figure 2.1 below. All tests were performed until either the onset of liquefaction or 500 loading cycles had occurred.

2.2 Computer Modeling

The computer modeling used a program called SHAKE. This program is a one-dimensional wave propagation, earthquake analysis program. Several soil profiles and inputs were created and analyzed using this program.

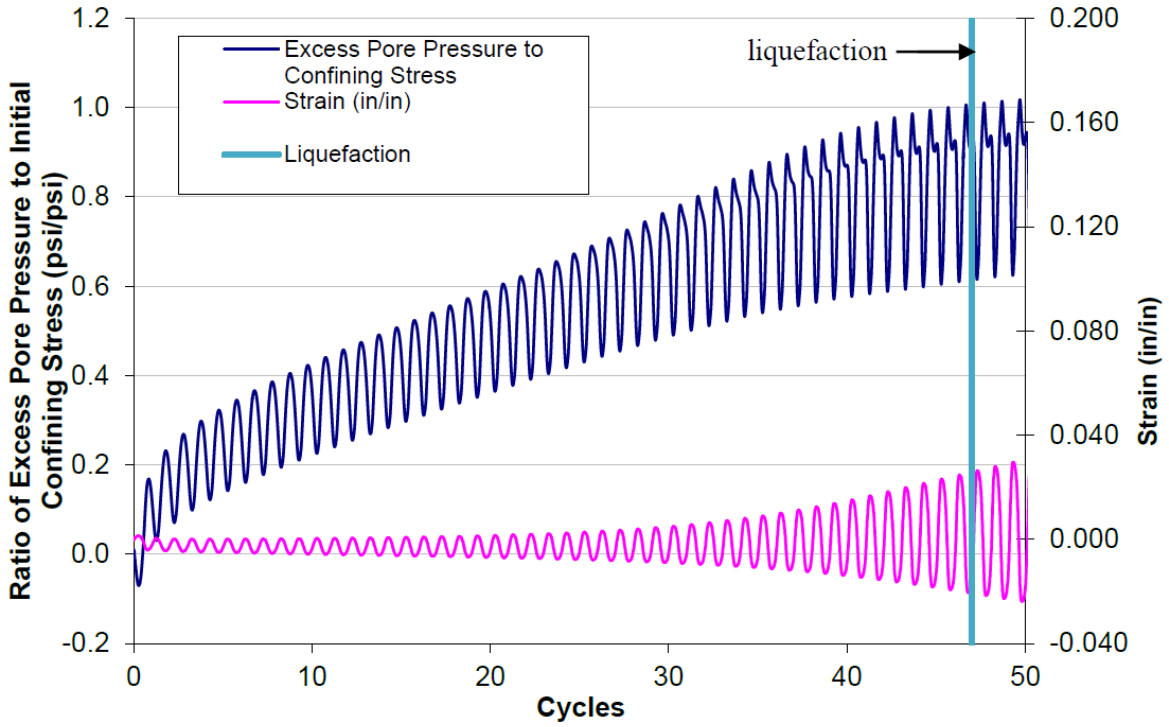

Figure 2.1: Visual definition of the Liquefaction

2.2.1 Soil Profile Inputs

To begin the modeling process, a private communication with AEP provided a previous study to be analyzed. The study used a two-dimensional modeling program known as QUAKE to study several soil profiles. Both this project and the AEP study are of the same fly ash pond.

Two, one-dimensional profiles were created in SHAKE based upon one of the two-dimensional profiles provided in the private communication. The profiles were selected based on vicinity to the original and current dikes which are considered critical structures. Also, each of the created profiles has a different total thickness of fly ash. The profile characteristics including layer thickness, unit weight, water table level, and the small strain shear modulus were provided by the AEP private communication.

The modulus reduction curve and damping curve were selected based upon the soil description from the AEP private communication and the available data from Seed et al (1970). These curves are meant to relate shear strain amplitude to shear moduli and damping ratio respectively. When differences in material description from the original OSU study occurred, curves were selected based upon the following principles ("EduPro Civil Systems, Inc.").

1. The modulus reduction curve is a measure of how non-linear a soil's stress-strain relationship is. A decrease in the plasticity index will increase the non-linear behavior.
2. The damping curve is a measure of how oscillations in a system will decay with variation in the shear strain. A decrease in plasticity index will increase soil damping.

Two input earthquake motions were selected for these models: the El Centro earthquake and the Taft earthquake. Because the ground acceleration amplitude of these earthquakes is much larger than the predicted amplitudes in the area of the power plant, the ground acceleration was scaled down to 0.08g or 0.15 g. Similar decisions were made for the previous OSU study.

2.2.2 Soil Profile Analysis

After applying the input motion to the soil profiles, results graphs were selected from the output module. A table containing the peak stress values in the center of each layer of interest was compared with the normalized stress time history of that layer. The details of this analysis will be explained in the chapter 3.

Chapter 3 Results and Discussion

The cyclic test results are presented in Appendix A. The detailed computer model analyses results can be found in Appendix B. A summary and discussion of results of the ground response analysis and laboratory tests are presented in this chapter.

3.1 Cyclic Test Results

Table 3.1 contains the tabulated results of the cyclic tests. These results are plotted in Figure 3.1 according to the number of cycles to liquefaction and the cyclic stress ratio. The data are separated by confining stress. Based upon these results, upper and lower results bounds were established. A red dashed lined marks the 500 cycle test limit at which a specimen was considered not liquefied.

Table 3.1: Cyclic Test Results

Specimen	Cyclic Stress Amplitude (psi)	Confining Pressure (psi)	Cyclic Stress Ratio	Cycles to Liquefaction
2R	7.800	18.90	0.206	146
3	10.820	20.00	0.271	7
6	5.250	20.00	0.131	DNL
7	7.180	20.00	0.179	87
8	17.610	40.00	0.220	12
10	6.160	18.00	0.171	DNL
11	14.820	20.00	0.371	8
18	15.480	40.00	0.194	52
21	6.450	20.00	0.161	62
81	5.240	20.00	0.131	132
84	7.845	20.00	0.395	13
85	8.064	20.00	0.400	12
86	10.291	40.00	0.194	47
87	8.311	20.00	0.161	99
109	6.360	20.00	0.159	DNL
111	4.000	20.00	0.100	DNL
114	4.000	20.00	0.100	97
116	16.000	20.00	0.400	191
117	4.000	20.00	0.100	DNL
119	6.360	20.00	0.159	28
120	16.007	40.00	0.200	5
122	16.002	20.00	0.400	13
123	15.522	40.00	0.194	8

DNL = Did not liquefy within 500 cycles.

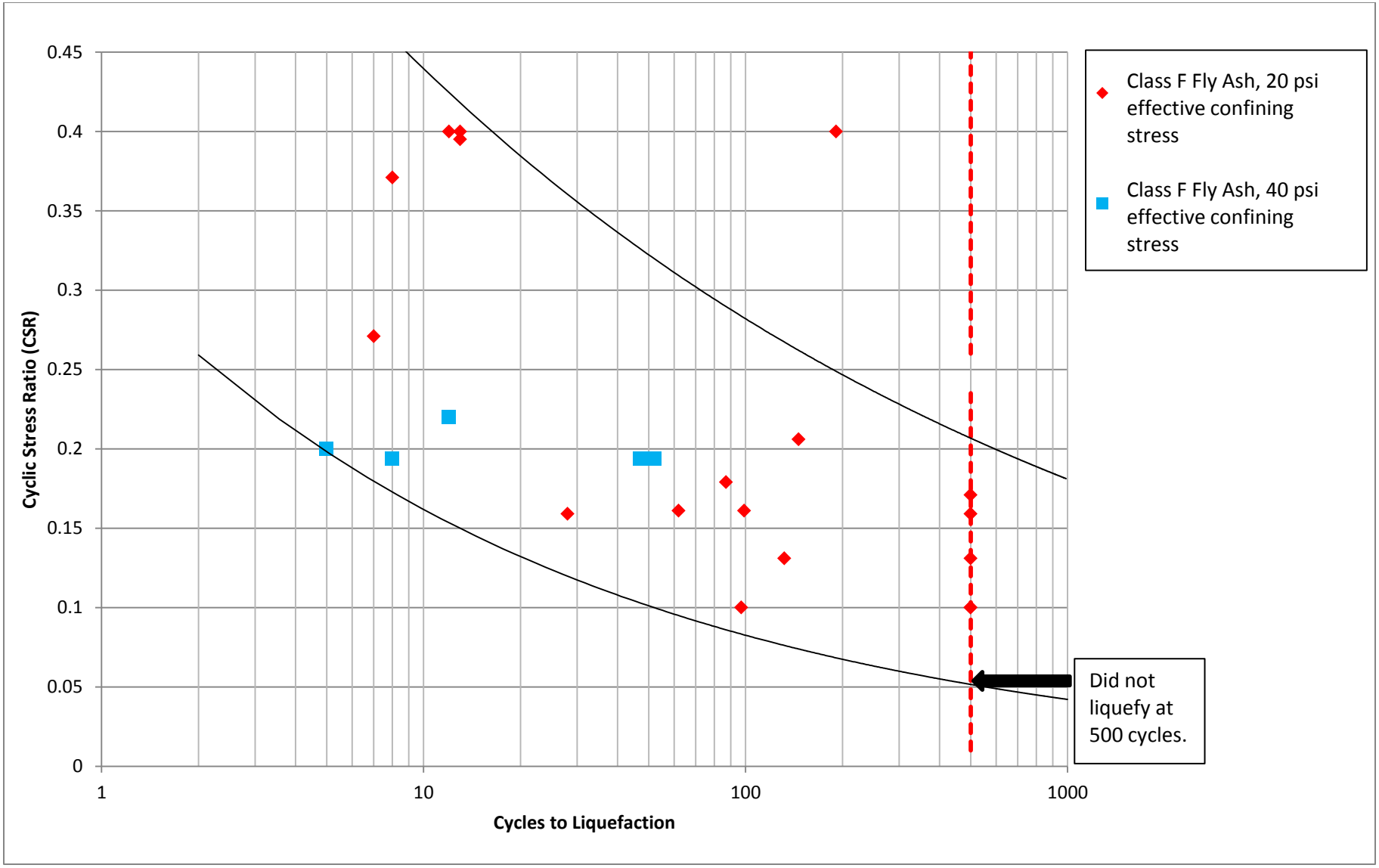

Figure 3.1: Plotted Liquefaction Result

3.2 Computer Model Results

Tables 3.2 and 3.3 detail the site characteristics of profile KK-1 and KK-2 respectively. Figures 3.2 and 3.3 below are illustrations of profiles KK-1 and KK-2. The profiles show relative profile thickness, soil descriptions, location of motion application, output motion measurement locations, relative shear wave velocity, and relative unit weight. The red dots indicate where the earthquake motion was applied. The green dots show where the output motions were analyzed.

Amplitude of the ground motion depends on the shear modulus (G) or shear wave velocity (Vs). Measurements of the maximum shear modulus were provided by the ground motion analysis done by AEP in the two-dimensional software, QUAKE. These values relate to shear wave velocity as follows.

$$G_{max} = \rho V_s^2 \qquad (3.1)$$

G_{max} is the maximum shear modulus and ρ is the density. SHAKE is able to produce the shear wave velocity when the maximum shear modulus is provided or vise versa.

Table 3.4 lists the computer model results at the center of each fly ash layer. The test name is structured as follows. The first half indicates what profile, KK-1 or KK-2, was tested. The letters in the second half indicate which earthquake motion was used. "EL" stands for El Centro and "T" stands for Taft. Lastly, the two-digit number shows which ground acceleration, 0.08g or 0.15 g, was applied in each test. The overburden stress (σ_0) was calculated based upon the density and thickness of each layer above the point of interest. The maximum shear stress for each fly ash

layer was taken from the table of maximum shear stress produced for each test. These tables may be found in Appendix B.

The cyclic stress method of liquefaction potential evaluation is one of the most common methods used. Because the stress-time history for each layer is irregular, the data had to be normalized in order to analyze the equivalent number of uniform cycles, N_{equ}. If a cycle exceeded 65% of the maximum shear stress amplitude, τ_{max}, that cycle counted for one equivalent uniform cycle. Seed et al. (1975-1) developed this relationship which is expressed in equation 3.2.

$$\tau_{cyc} = 0.65\tau_{max} \qquad (3.2)$$

65% is the most common value used for this purpose (Kramer, 1996). The cyclic shear stress amplitude (τ_{cyc}) was then applied to equation 2.1 to determine the laboratory cyclic stress ratio (CSR_{LAB}). Seed et al. (1975-2) suggested a correction to the laboratory results to yield a predication for the field results. Equation 3.3 below was used to correct the laboratory data.

$$CSR_{FIELD} = 0.9CSR_{LAB} \qquad (3.3)$$

The final field shear stress ratio and the equivalent number of cycles was plotted on the same chart as the laboratory results. This chart is contained in Figure 3.4. The numbers of equivalent cycles under field cyclic stress ratios were lower than the cyclic liquefaction tests. This implies that the critical layers of fly ash will not liquefy.

Table 3.2: Site Characteristics of Profile KK-1

Layer Number	Material Description	Thickness (ft)	Unit Weight (pcf)	Gmax (ksf)	Vs (ft/sec)	Modulus Reduction Curve	Damping Curve
1	Gravelly Silty Sand	2	108	3213	978	Sand (Seed and Idriss) - Average	Sand (Seed and Idriss) - Average
2	Sand and Gravel	13	114	3391	978	Sand (Seed and Idriss) - Upper	Sand (Seed and Idriss) - Upper
3	Sand and Gravel	5	114	3391	978	Sand (Seed and Idriss) - Upper	Sand (Seed and Idriss) - Upper
4	Silty Clay	2	125	3718	978	Clay (Seed and Sun 1989)	Clay - Average (Sun et al.)
5	Fly Ash	5	98	690	478	Sand (Seed and Idriss 1970)	Sand (Idriss 1990)
6	Fly Ash	5	98	690	478	Sand (Seed and Idriss 1970)	Sand (Idriss 1990)
7	Fly Ash	5	98	690	478	Sand (Seed and Idriss 1970)	Sand (Idriss 1990)
8	Fly Ash	5	98	690	478	Sand (Seed and Idriss 1970)	Sand (Idriss 1990)
9	Fly Ash	5	98	690	478	Sand (Seed and Idriss 1970)	Sand (Idriss 1990)
10	Fly Ash	5	98	690	478	Sand (Seed and Idriss 1970)	Sand (Idriss 1990)
11	Fly Ash	5	98	690	478	Sand (Seed and Idriss 1970)	Sand (Idriss 1990)
12	Clay Foundation	10	130	1944	694	Clay (Seed and Sun 1989)	Clay - Average (Sun et al.)
13	Silty Clay Foundaton	20	125	1870	694	Clay (Seed and Sun 1989)	Clay - Average (Sun et al.)
14	Foundation Soil	20	130	1944	694	Clay (Seed and Sun 1989)	Clay - Average (Sun et al.)
15	Sandstone Bedrock	Infinite	140	135360	5577	Rock (Idriss)	Rock (Idriss)

Table 3.3 Site Characteristics of Profile KK-2

Layer Number	Material Description	Thickness (ft)	Unit Weight (pcf)	Gmax (ksf)	Vs (ft/sec)	Modulus Reduction Curve	Damping Curve
1	Silty Clay	1	125	3718	978	Clay (Seed and Sun 1989)	Clay (Idriss 1990)
2	Bottom Ash	2	100	2975	978	Sand (Seed and Idriss 1970)	Sand (Idriss 1990)
3	Gravelly Silty Sand	13	110	3391	996	Sand (Seed and Idriss) - Average	Sand (Seed and Idriss) - Average
4	Silty Clay	6	128	1915	694	Clay (Seed and Sun 1989)	Clay - Average (Sun et al.)
5	Fly Ash	6	98	690	478	Sand (Seed and Idriss 1970)	Sand (Idriss 1990)
6	Fly Ash	6	98	690	478	Sand (Seed and Idriss 1970)	Sand (Idriss 1990)
7	Bottom Ash	8	100	2975	978	Sand (Seed and Idriss 1970)	Sand (Idriss 1990)
8	Silty Clay Foundation	20	125	1870	694	Clay (Seed and Sun 1989)	Clay - Average (Sun et al.)
9	Foundation Soil	20	130	1944	694	Clay (Seed and Sun 1989)	Clay - Average (Sun et al.)
10	Sandstone Bedrock	Infinite	140	135360	5577	Rock (Idriss)	Rock (Idriss)

Figure 3.2: Soil Profile KK-1

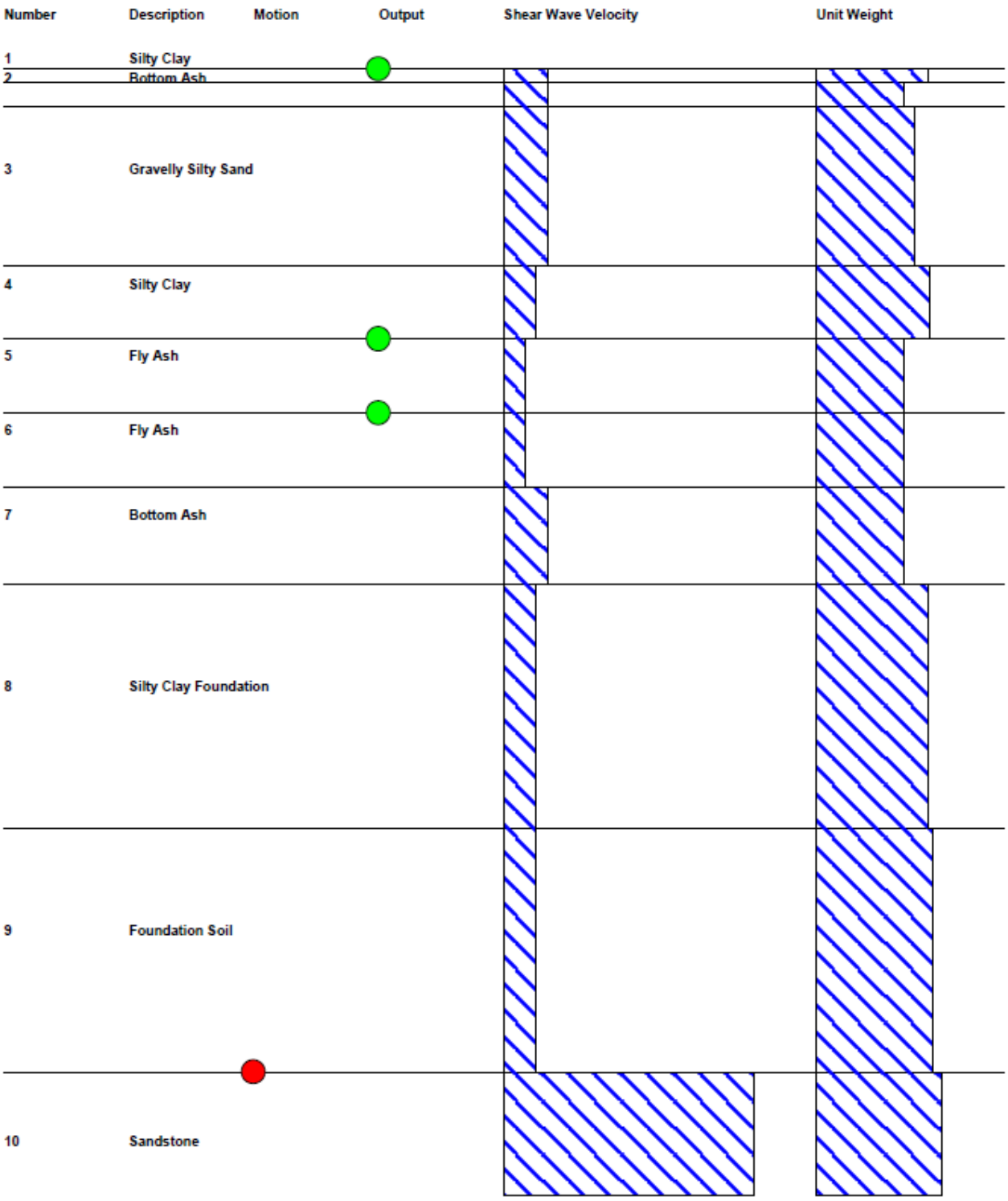

Figure 3.3: Soil Profile KK-2

Table 3.4: Computer Model Results Analysis

Test Name	Layer #	Depth (ft)	Ƭ max (PSF)	Ƭ cyc (PSF)	N_{equ}	σ_0 (PSF)	CSR LAB	CSR FIELD
KK1_EL08	5	24.5	357	232	3	2763	0.083938	0.076
	6	29.5	398	259	3	3253	0.079593	0.072
	7	34.5	439	285	3	3743	0.076149	0.069
KK1_T08	5	24.5	367	238	3	2763	0.086302	0.078
	6	29.5	406	264	2	3253	0.081065	0.073
	7	34.5	431	280	3	3743	0.074885	0.067
KK1_EL15	5	24.5	472	307	2	2763	0.111152	0.100
	6	29.5	521	338	2	3253	0.104034	0.094
	7	34.5	548	356	2	3743	0.095227	0.086
KK1_T15	5	24.5	537	349	2	2763	0.126342	0.114
	6	29.5	569	370	2	3253	0.113733	0.102
	7	34.5	574	373	2	3743	0.099759	0.090
KK2_EL08	5	25	551	358	1	2817	0.12715	0.114
	6	31	580	377	1	3405	0.110655	0.100
KK2_T08	5	25	392	255	6	2817	0.090395	0.081
	6	31	446	290	7	3405	0.085099	0.077
KK2_EL15	5	25	729	474	1	2817	0.168303	0.151
	6	31	742	482	2	3405	0.141656	0.127
KK2_T15	5	25	617	401	2	2817	0.142294	0.128
	6	31	674	438	4	3405	0.128746	0.116

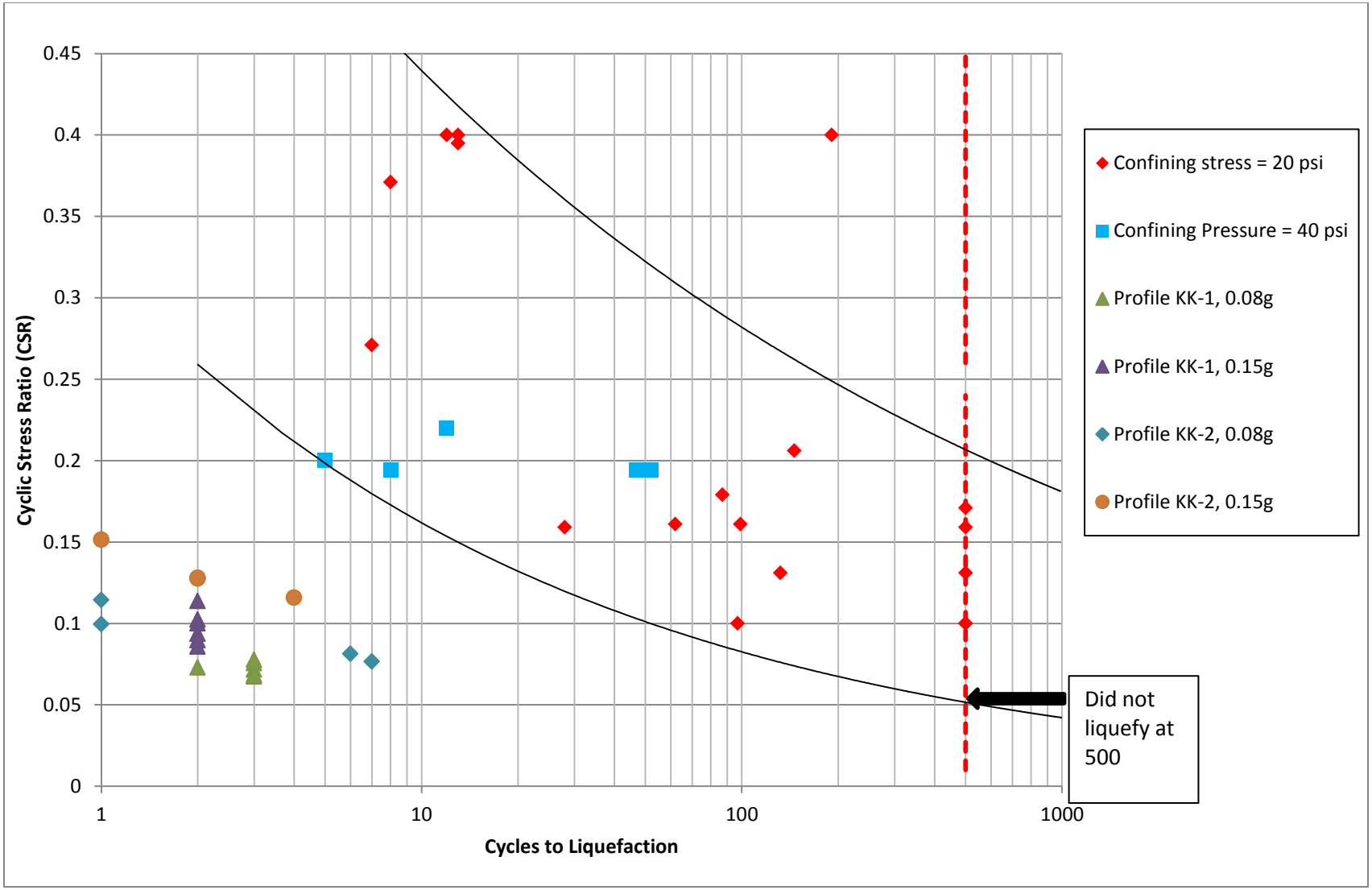

Figure 3.4: Combined Results of Laboratory Tests and Computer Models

Chapter 4 Summary and Conclusion

4.1 Summary

Liquefaction can cause extreme structural damage to infrastructure. Since the 1970's, extensive research has been done into the liquefaction potential of natural soils. This study examines the liquefaction potential of Class F fly ash in a storage pond through laboratory experiments and computer model analysis. Cyclic tests were performed with reconstituted specimens from an AEP fly ash pond. The results of these tests were used to establish upper and lower bounds of a liquefaction zone. Computer models of two pond profiles based upon a study provided by AEP were created. Each profile was analyzed four times using different combinations of ground acceleration amplitude and earthquake motion. The results from the top layers of fly ash were plotted on the cyclic laboratory test results to determine if liquefaction would occur and damage the dike of the pond.

4.2 Conclusions

The following conclusions can be made based on the laboratory testing and numerical analysis results.

1. The cyclic loading imposed by the input earthquake motion was found to be lower than the cyclic strength of the Class F fly ash material found in laboratory tests.

2. As the cyclic stress ratio increase, the number of stress cycles to liquefaction decreases.

3. The 2005 OSU Class F fly ash study suggested that there was a relationship between the confining stress and liquefaction potential unlike previous studies of sand. The results of the current study suggest that liquefaction potential is not significantly dependent on the confining pressure based upon the range of confining pressures used.

Further study should be done on Class F fly ash from other sources to determine if the suggested relationship between cycles to liquefaction and confining stress exists in the 2005 OSU study is valid. Also, further studies with Class F fly ash from other sources will determine if there is variation in liquefaction potential within this fly ash class.

List of References

1. ASTM Designation: ASTM D5311, “Standard Test Method for Load Controlled Cyclic Triaxial Strength of Soil”, Annual Book of ASTM Standards, 2004, pp. 1167-1176.

2. Kramer, S.L. (1996). Geotechnical Earthquake Engineering, Prentice Hall, Inc., Upper Saddle River, New Jersey, 653 pp.

3. Seed, H. B. and I. M. Idriss “Soil Moduli and Damping Factors for Dynamic Response Analysis”. Report No. UCB/EERC-70/10, Earthquake Engineering Research Center, University of California, Berkeley, 1970.

4. Seed, H.B., K. Mori and C.K. Chan, “Influence of Seismic History on the Liquefaction Characteristics of Sands”, Report No. UCB/EERC-75/25, Earthquake Engineering Research Center, University of California, Berkeley, 1975-1.

5. Seed, H.B., K.L. Lee, I.M. Idriss and F.I. Makdisi, “The Slides in the San Fernando Dams During the Earthquake of February 9, 1971 ”, Journal of Geotechnical Engineering Division, ASCE, Vol. 101, No. GT7, pp. 651-688, 1975-2.

6. Haldar, A., and W.H. Tang, “Statistical Study of Uniform Cycles in Earthquake Motion”, Journal of the Geotechnical Engineering Division, ASCE, Vol. 107, No. GT5, pp. 577-589, 1981.

7. Zand, Behrad, et al. "An Experimental Investigation on Liquefaction Potential and Post-Liquefaction Shear Strength of Impounded Fly Ash." Fuel. 88.7 (2009): 1160-1166. Web. 28 Jan. 2013. <http://www.sciencedirect.com/science/article/pii/S0016236108004018>.

8. . "2011 Fly Ash Production and Use Statistics." AACA: Advancing the Management and Use of Coal Combustion Products. AACA: Advancing the Management and Use of Coal Combustion Products, 25 Jan 2013. Web. 4 Feb 2013. <http://acaa.affiniscape.com/associations/8003/files/1966-2011_FlyAsh_Prod_and_Use_Charts.pdf>.

9. . "ProShake: Ground Response Analysis Program, User's Manual." EduPro Civil Systems, Inc.. EduPro Civil Systems, Inc., 2 Apr 2012. Web. 4 Feb 2013. <http://www.proshake.com/>.

Appendix A: Laboratory Test Results

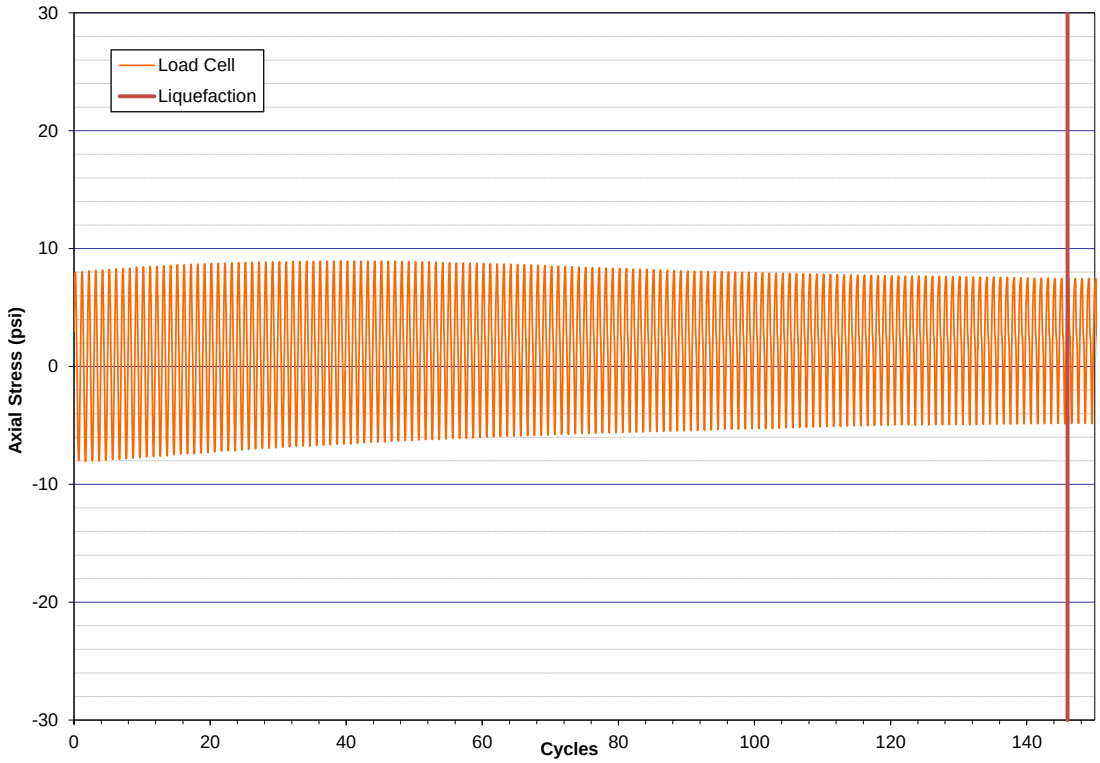

Figure A.1a: Specimen 2R Cyclic Loading

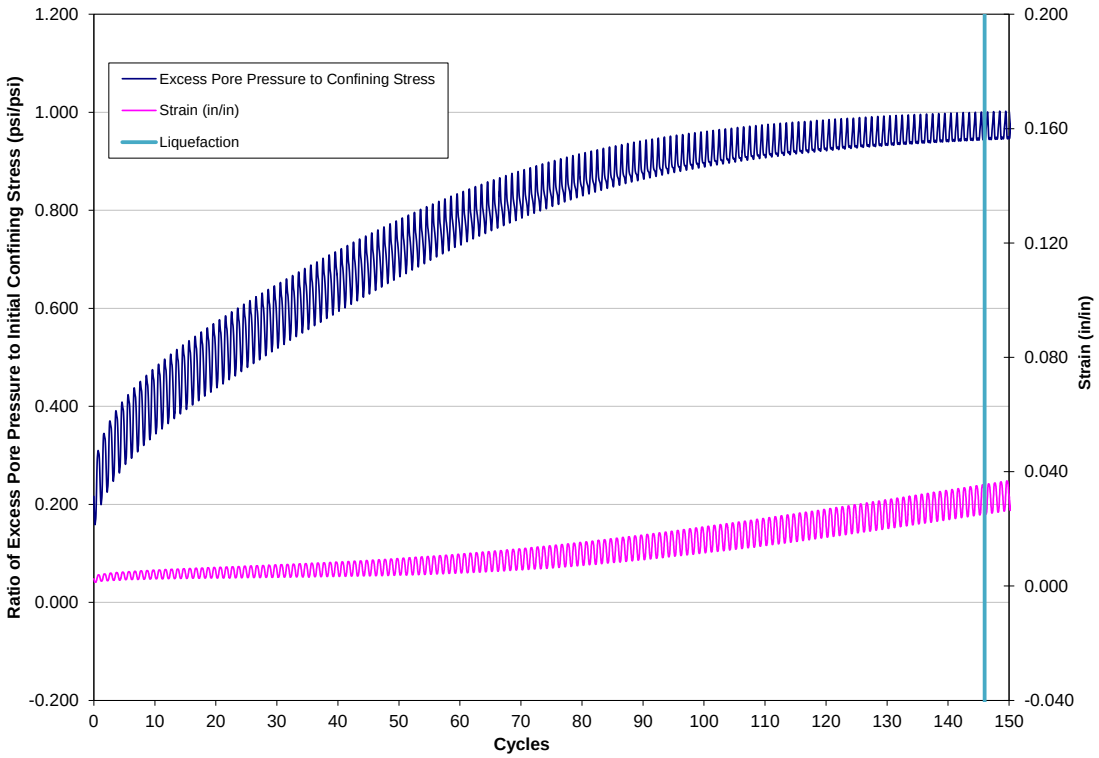

Figure A.1b: Specimen 2R Pore Water Pressure Build-up and Cyclic Displacement

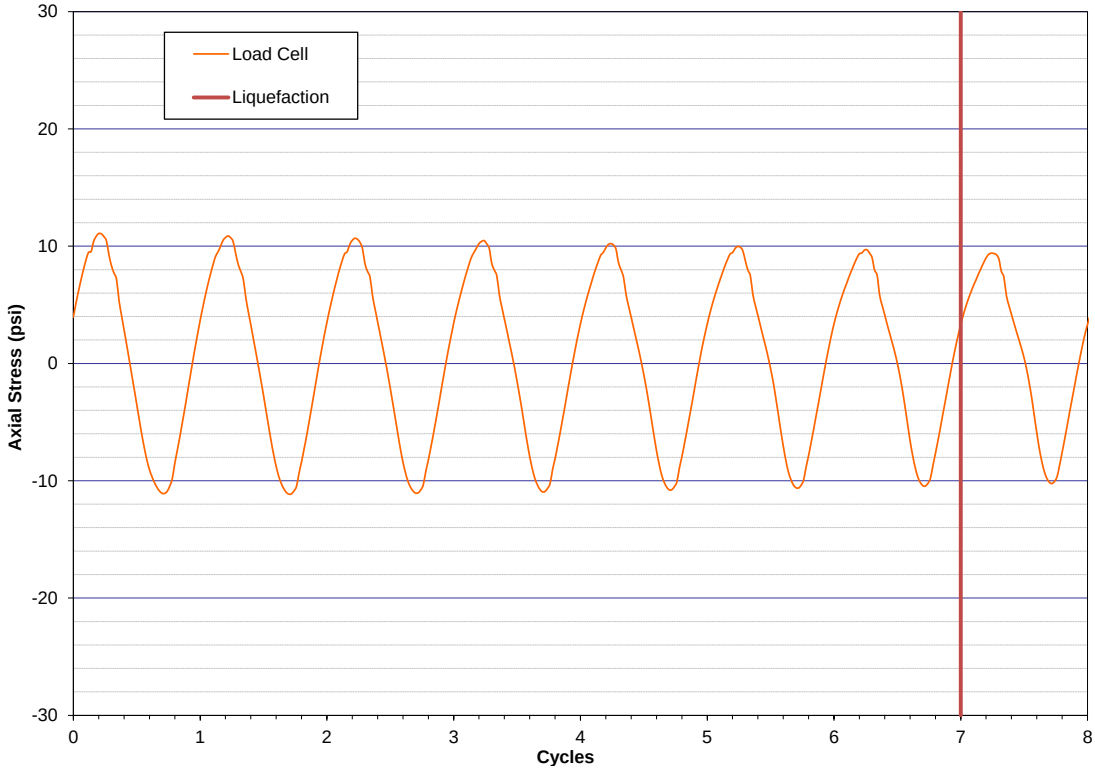

Figure A.2a: Specimen 3Cyclic Loading

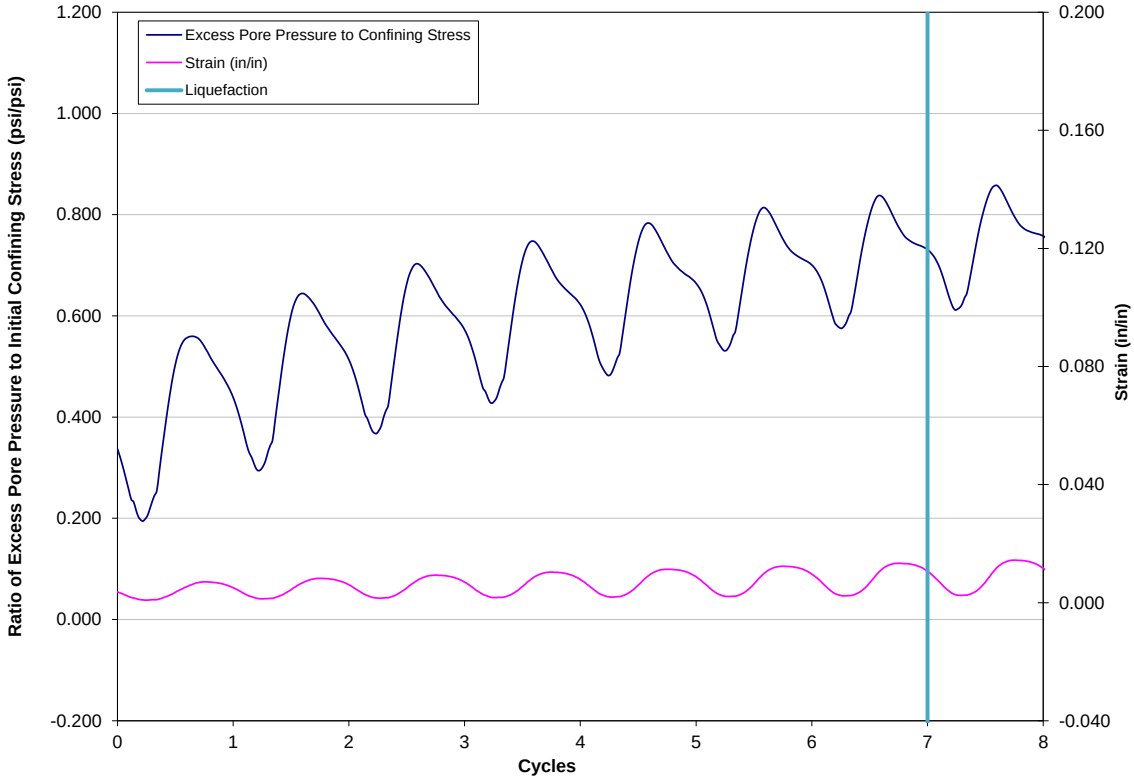

Figure A.2b: Specimen 3Pore Water Pressure Build-up and Cyclic Displacement

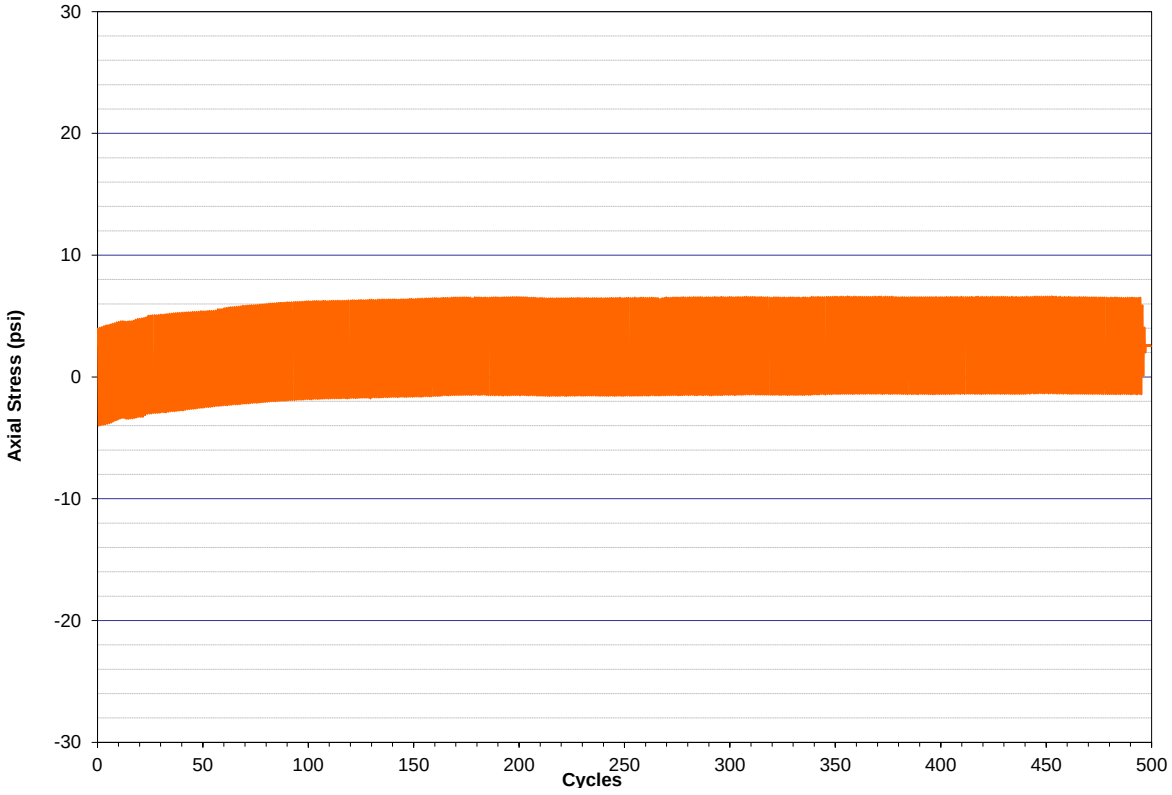

Figure A.3a: Specimen 6 Cyclic Loading (Load Cell Response)

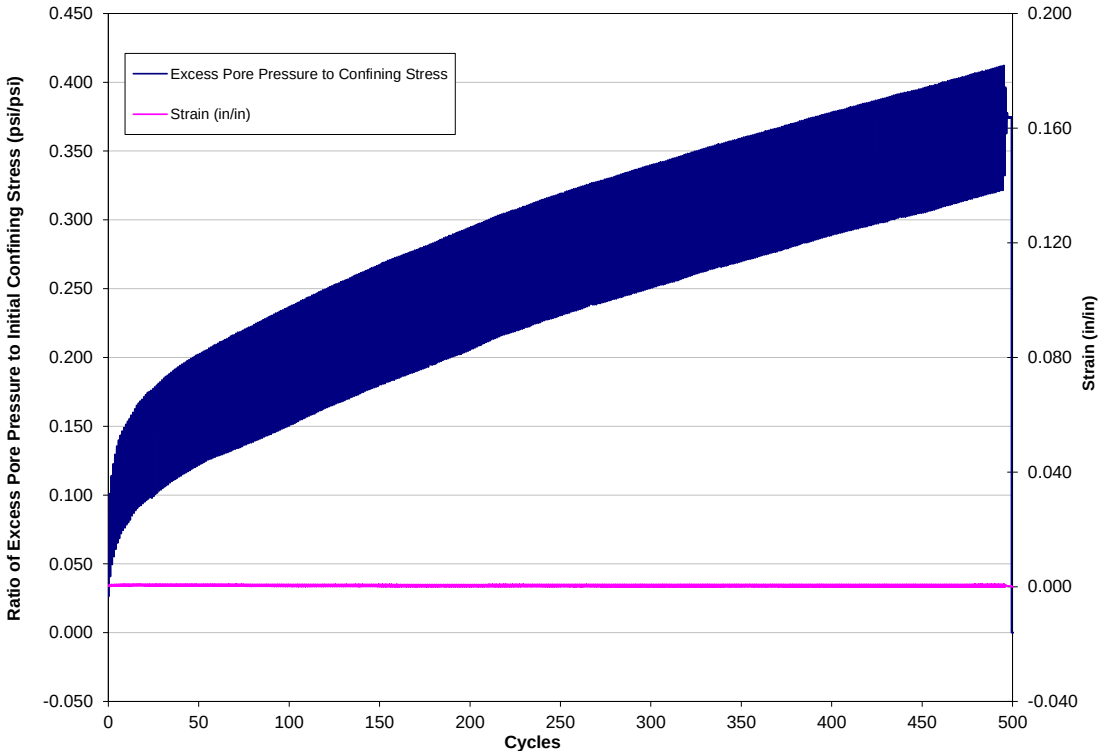

Figure A.3b: Specimen 6 Pore Water Pressure Build-up and Cyclic Displacement

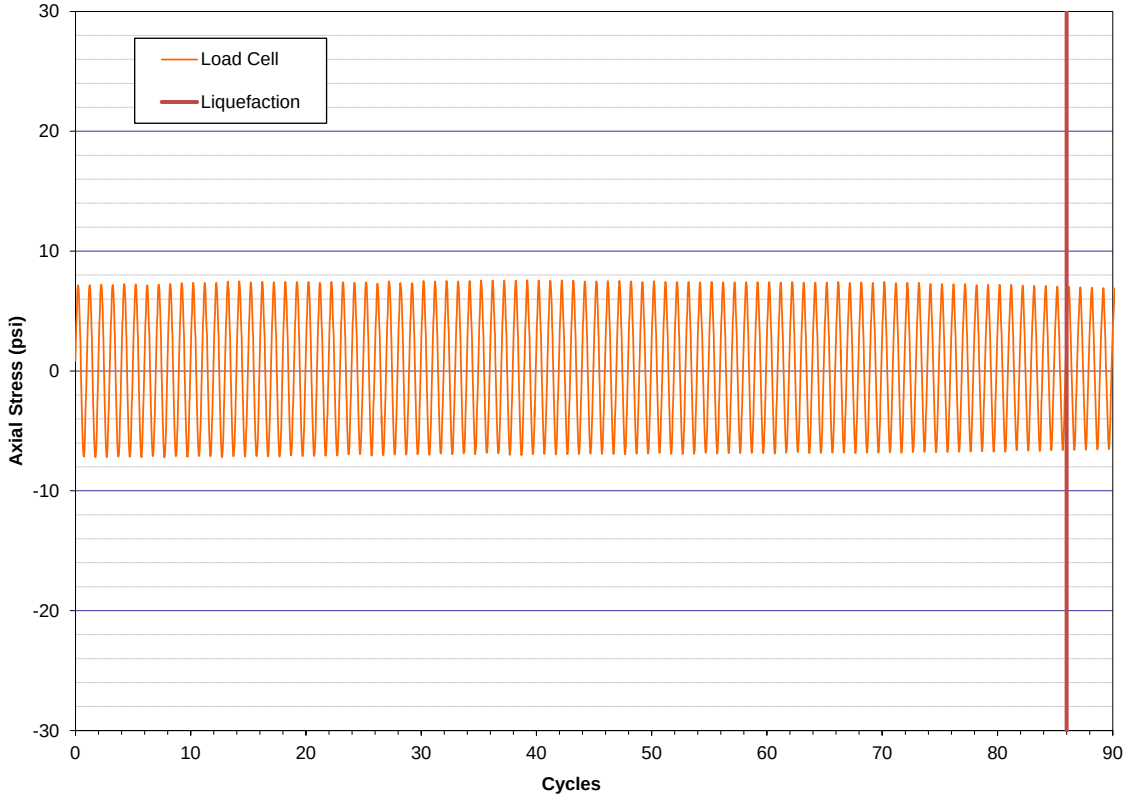

Figure A.4a: Specimen 7 Cyclic Loading

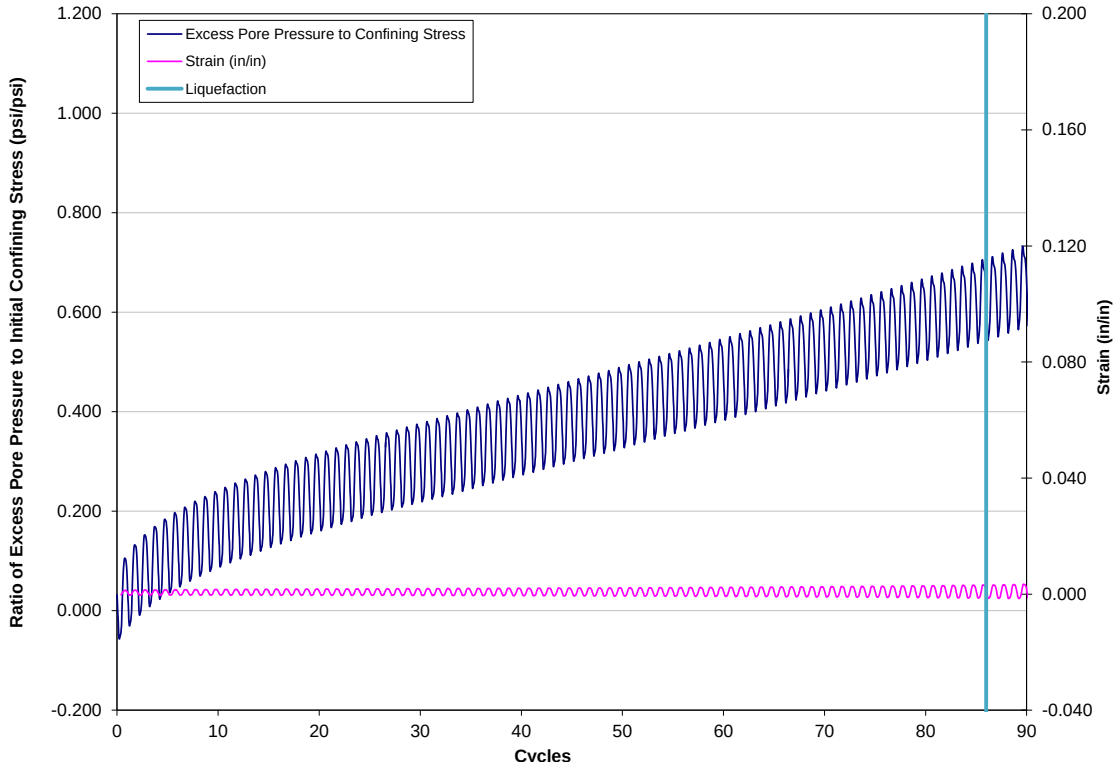

Figure A.4b: Specimen 7 Pore Water Pressure Build-up and Cyclic Displacement

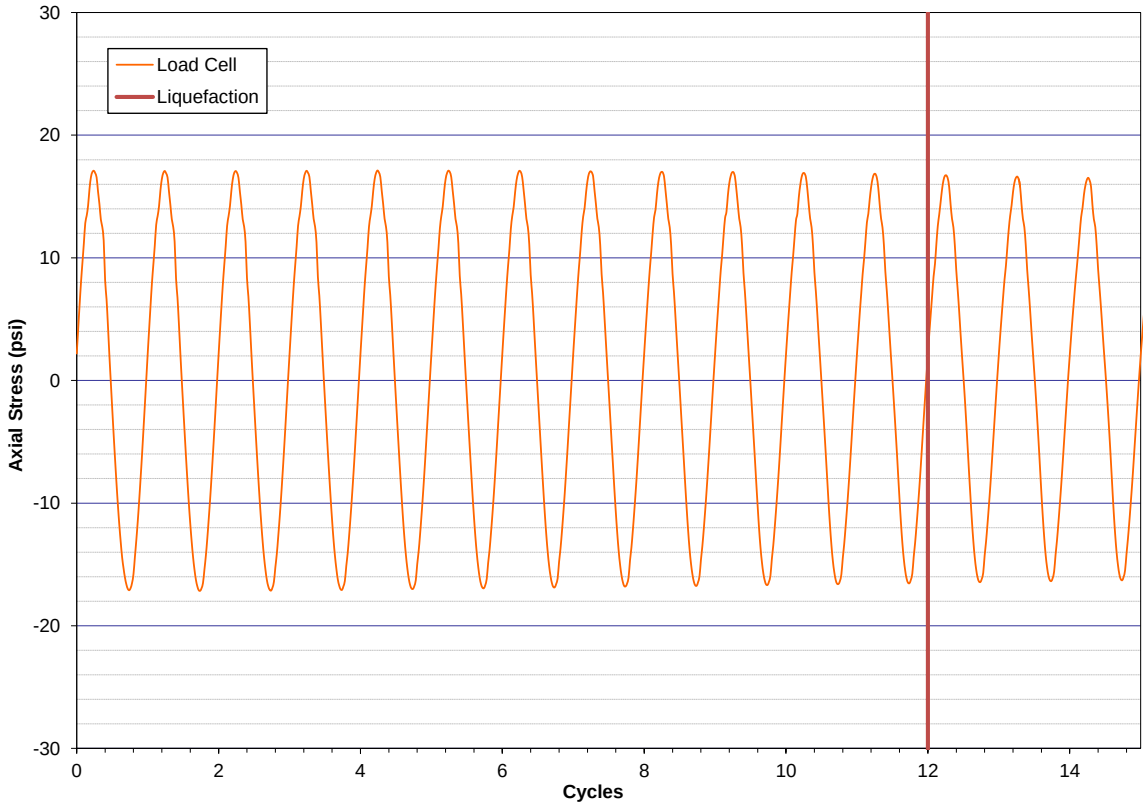

Figure A.5a: Specimen 8 Cyclic Loading

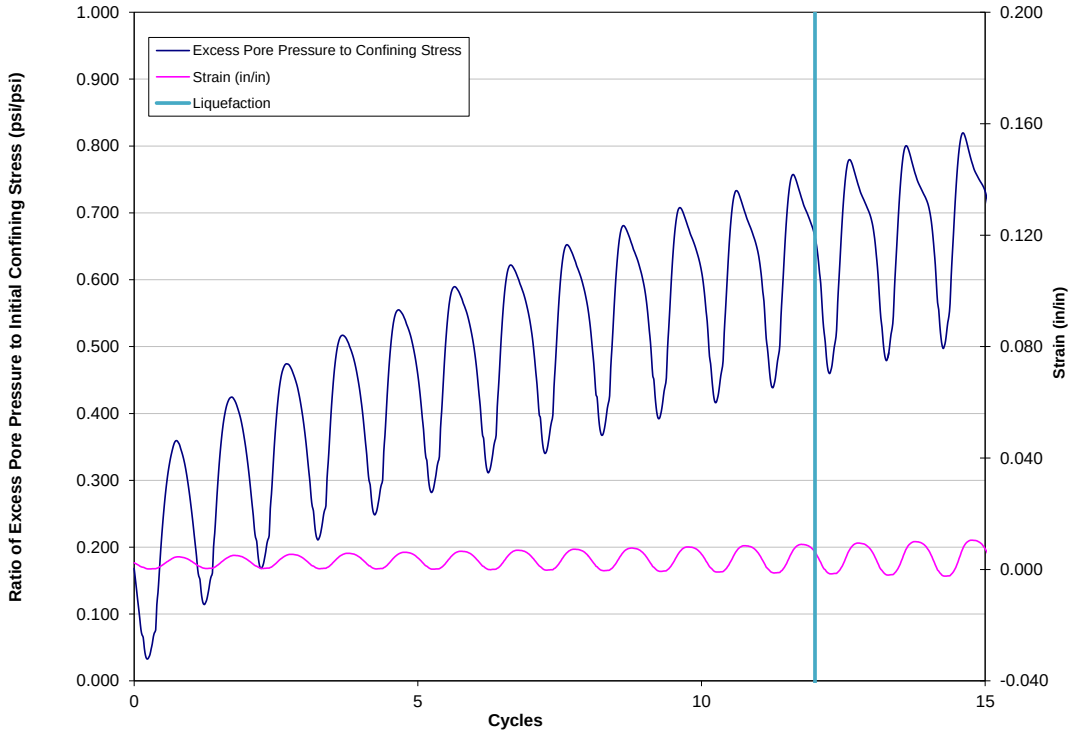

Figure A.5b: Specimen 8Pore Water Pressure Build-up and Cyclic Displacement

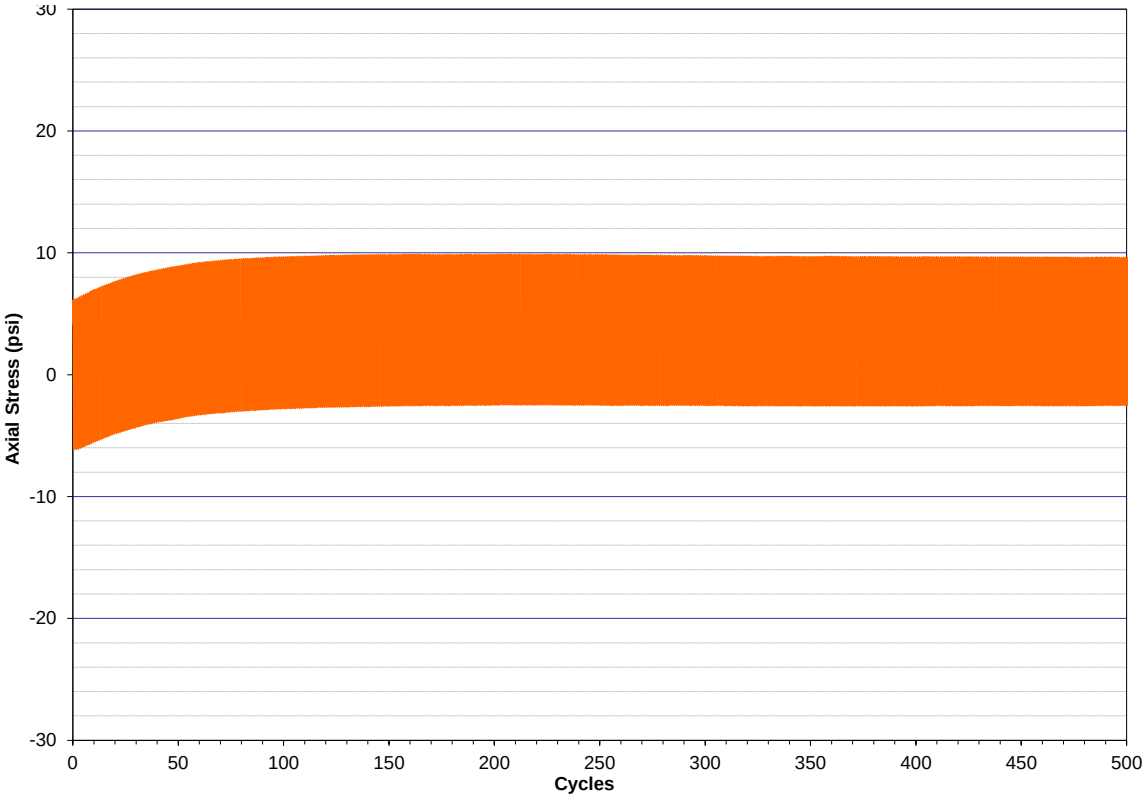

Figure A.6a: Specimen 10 Cyclic Loading (Load Cell Response)

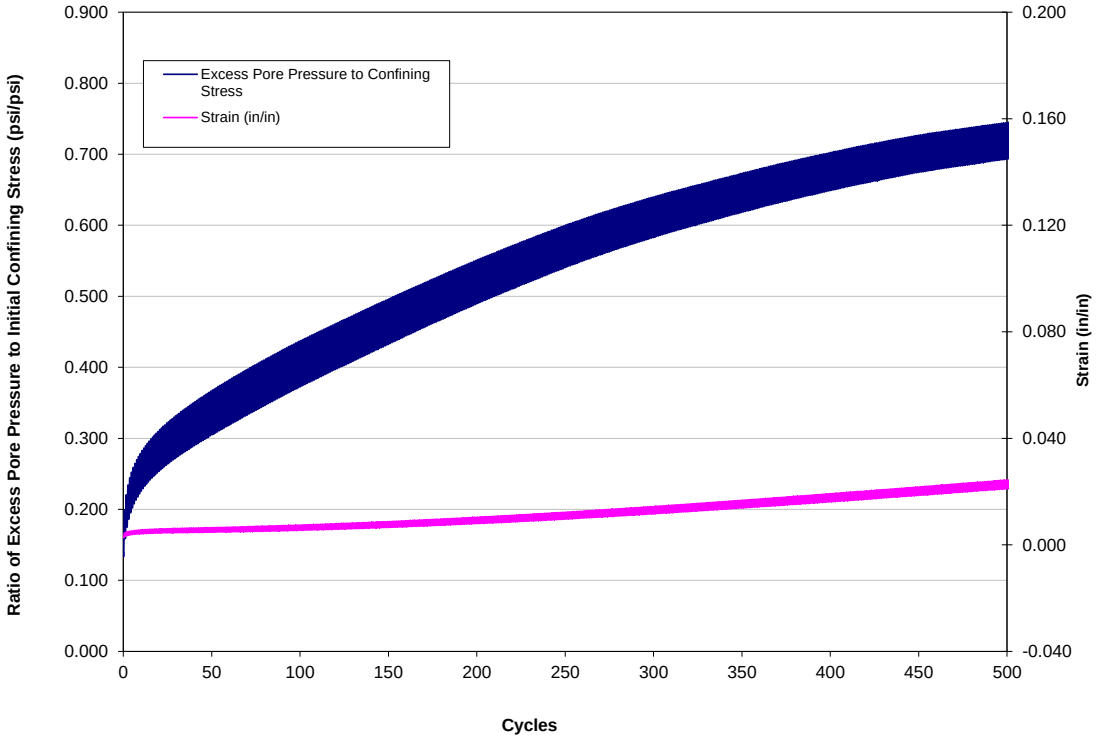

Figure A.6b: Specimen 10 Pore Water Pressure Build-up and Cyclic Displacement

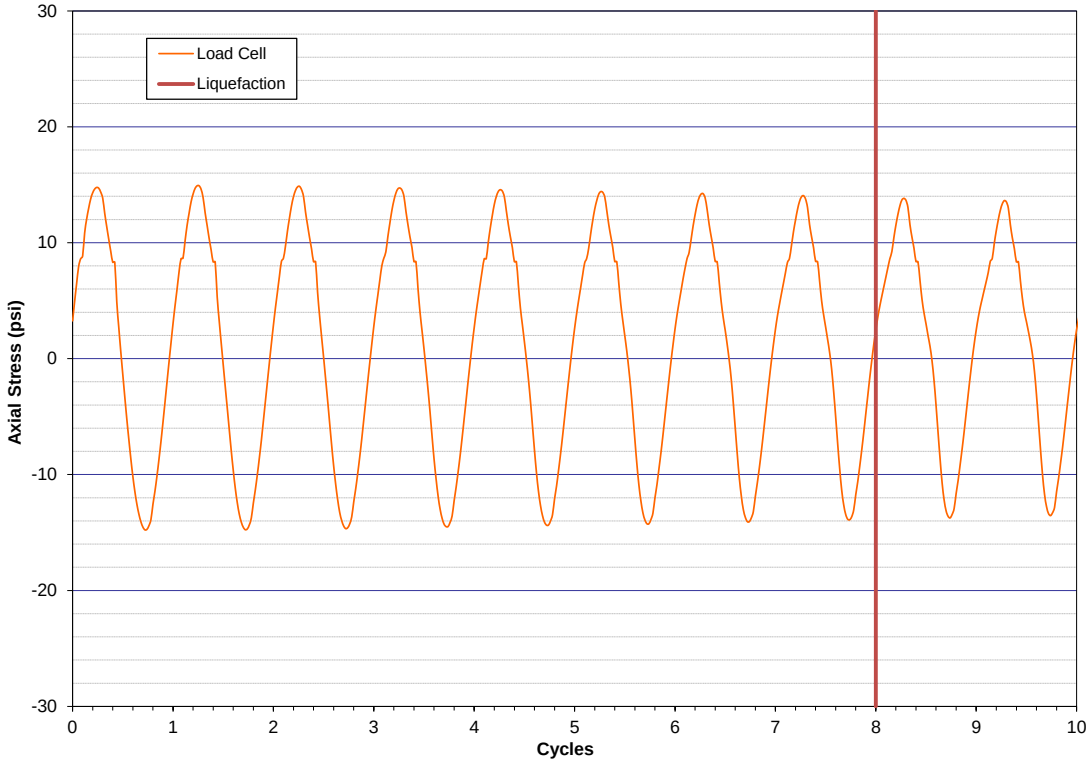

Figure A.7a: Specimen 11 Cyclic Loading

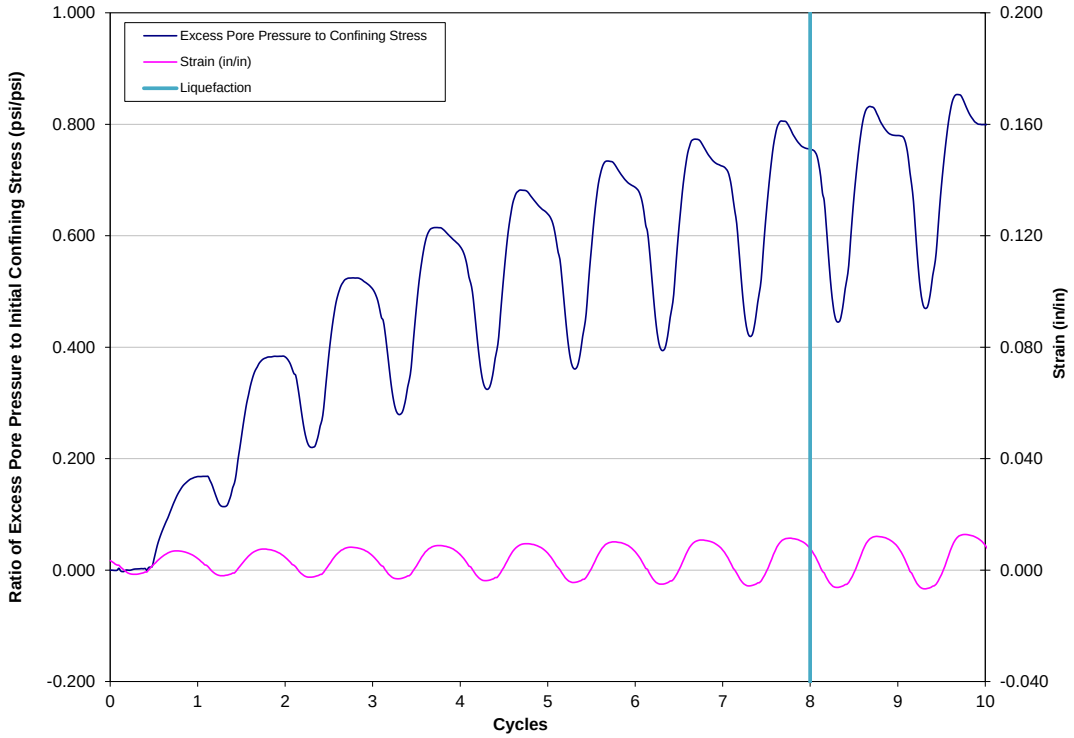

Figure A.7a: Specimen 11 Pore Water Pressure Build-up and Cyclic Displacement

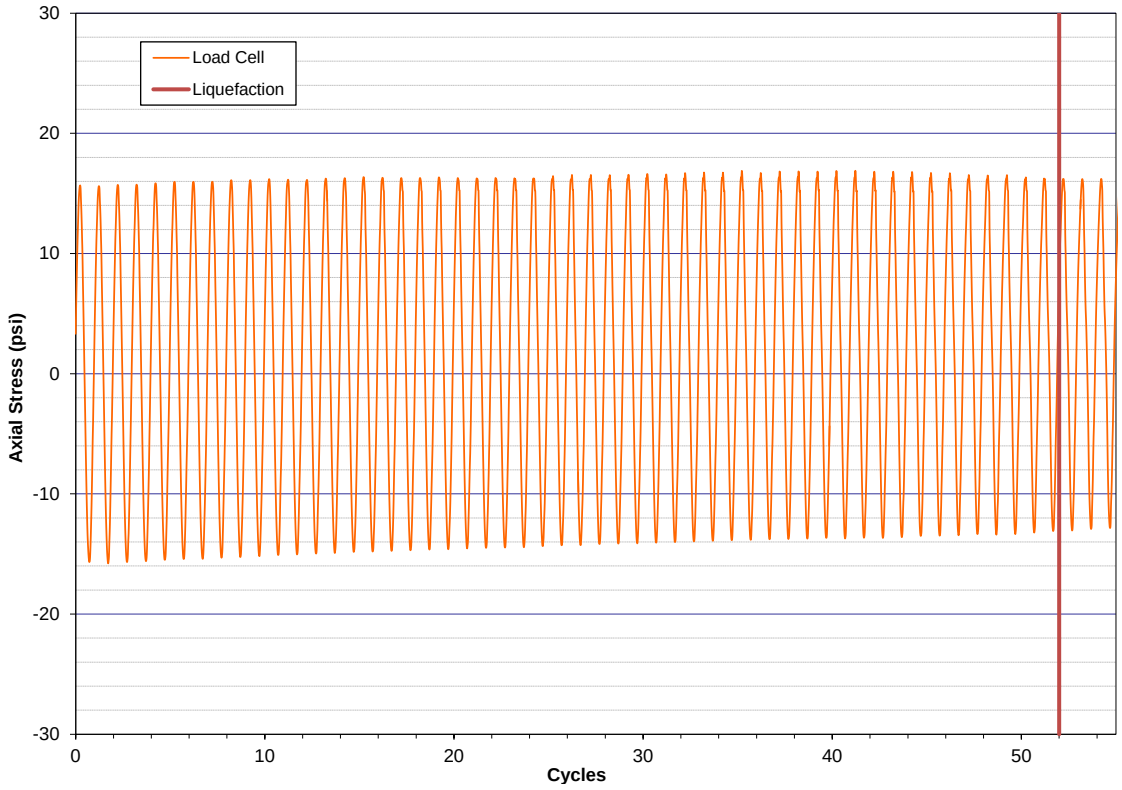

Figure A.8a: Specimen 18 Cyclic Loading

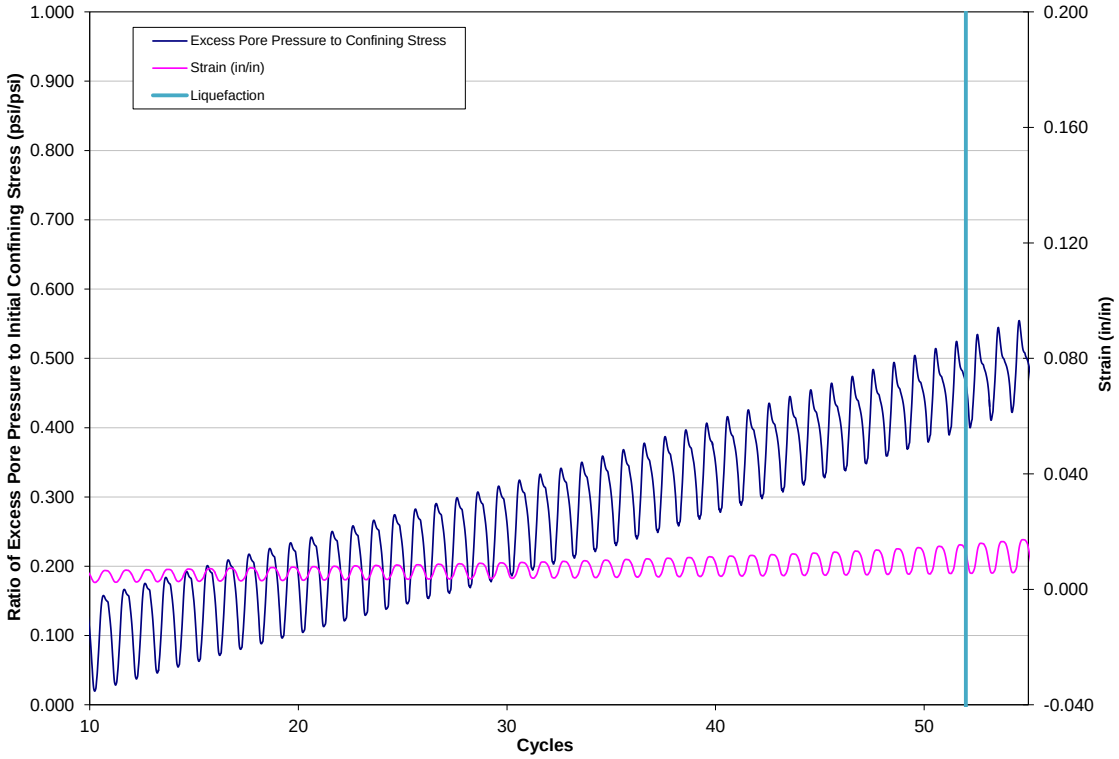

Figure A.8b: Specimen 18 Pore Water Pressure Build-up and Cyclic Displacement

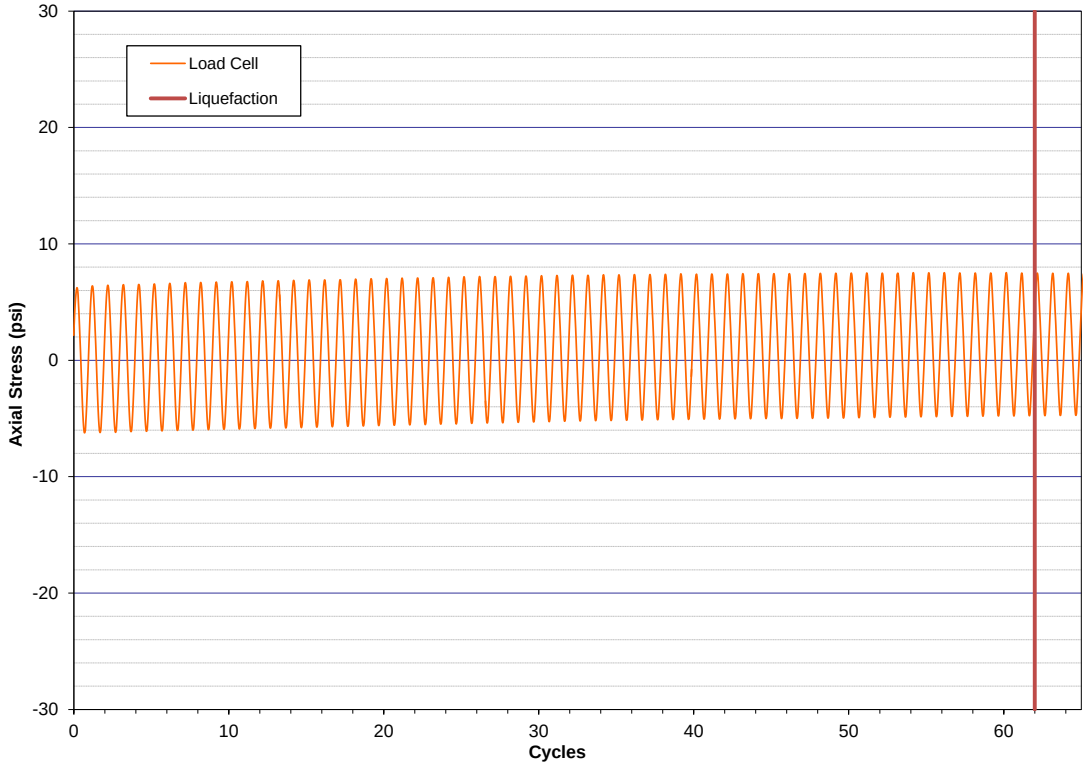

Figure A.9a: Specimen 21 Cyclic Loading

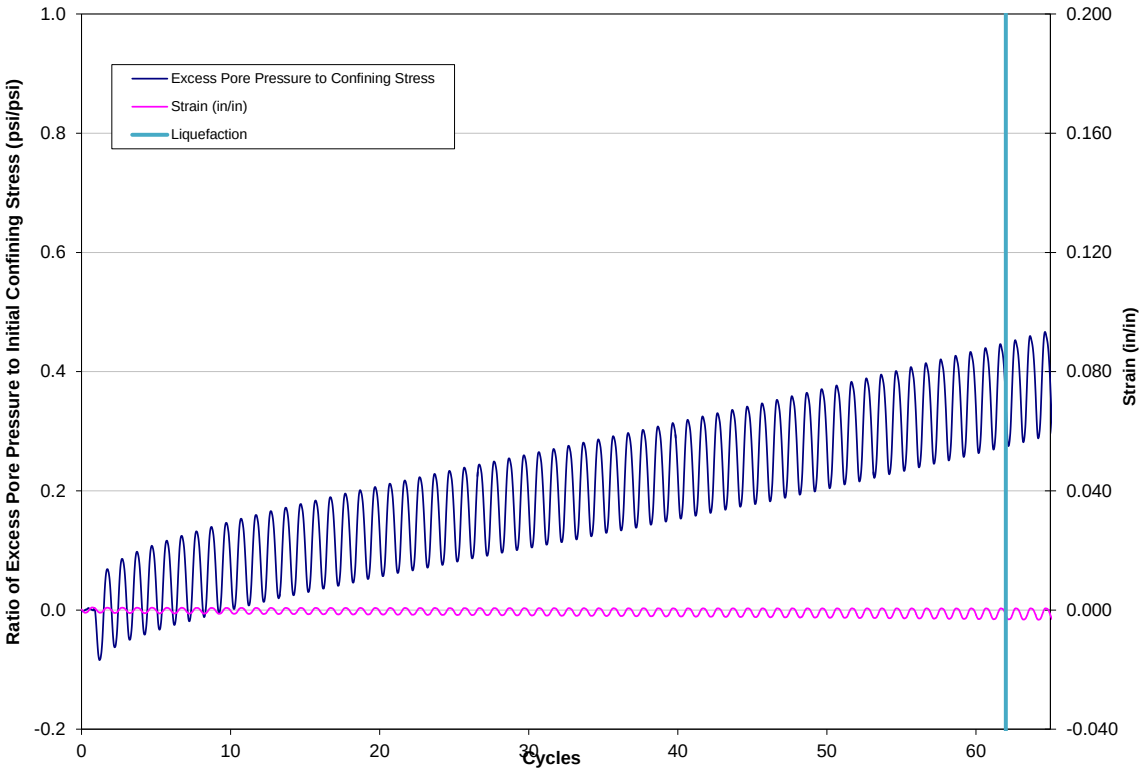

Figure A.9b: Specimen 21 Pore Water Pressure Build-up and Cyclic Displacement

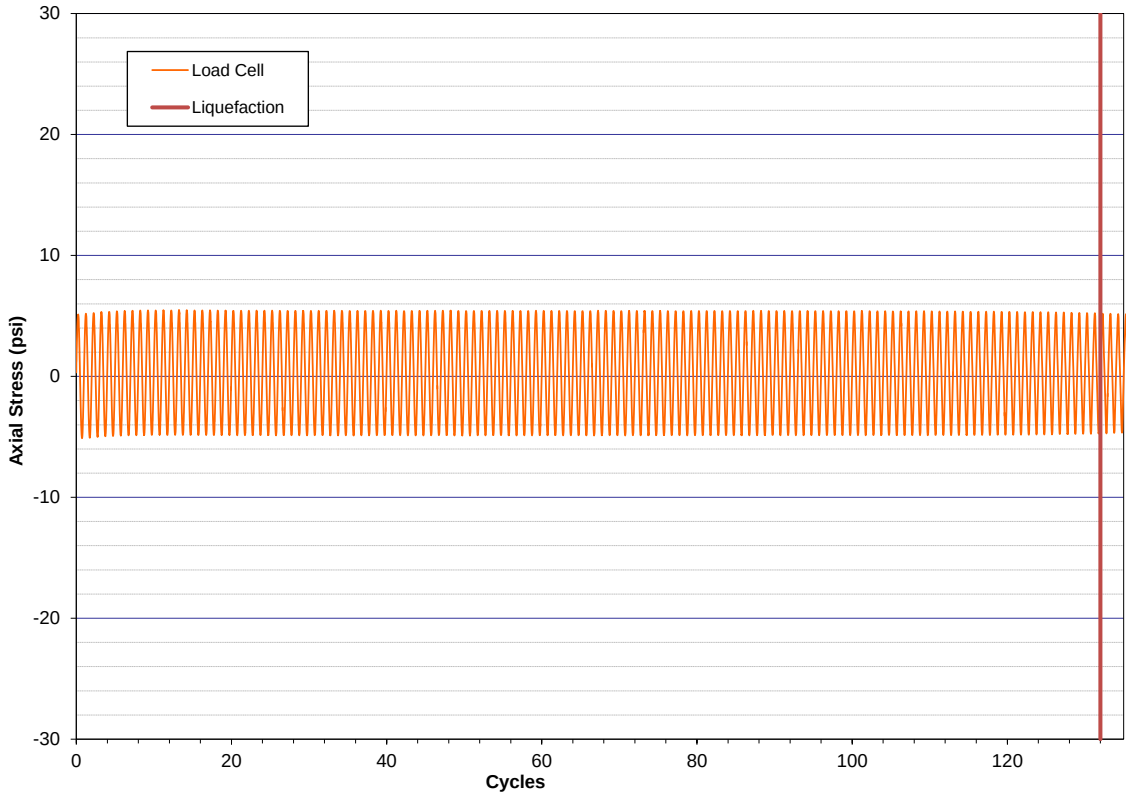

Figure A.10a: Specimen 81 Cyclic Loading

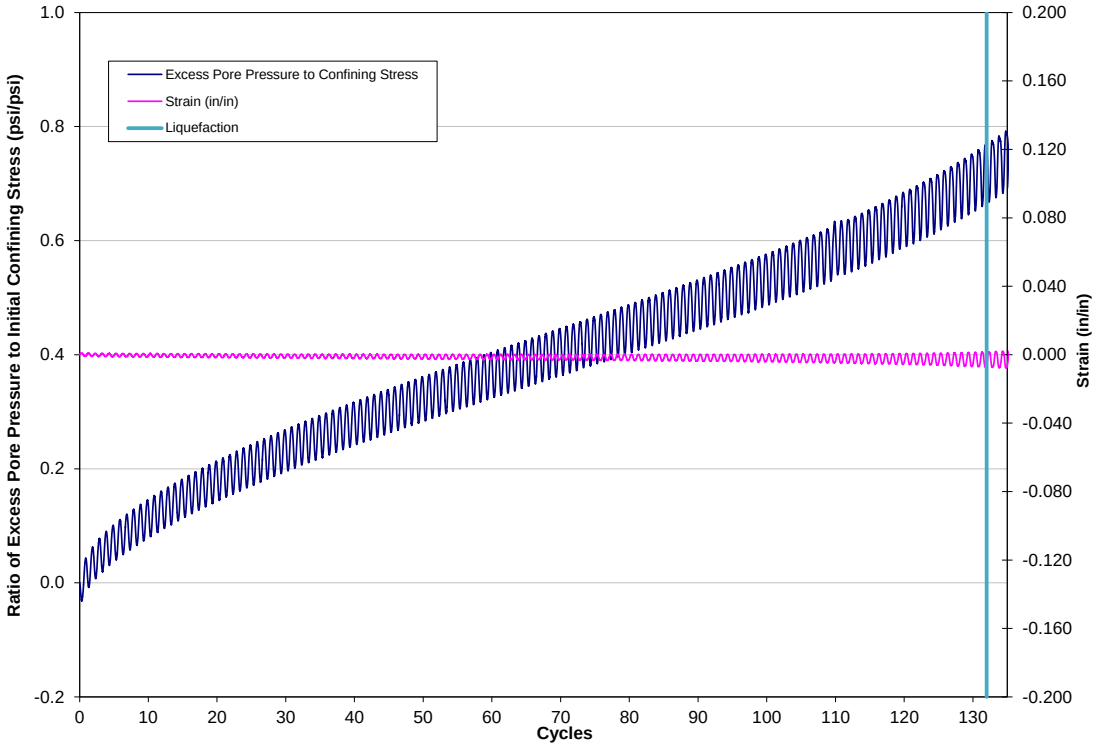

Figure A.10b: Specimen 81 Pore Water Pressure Build-up and Cyclic Displacement

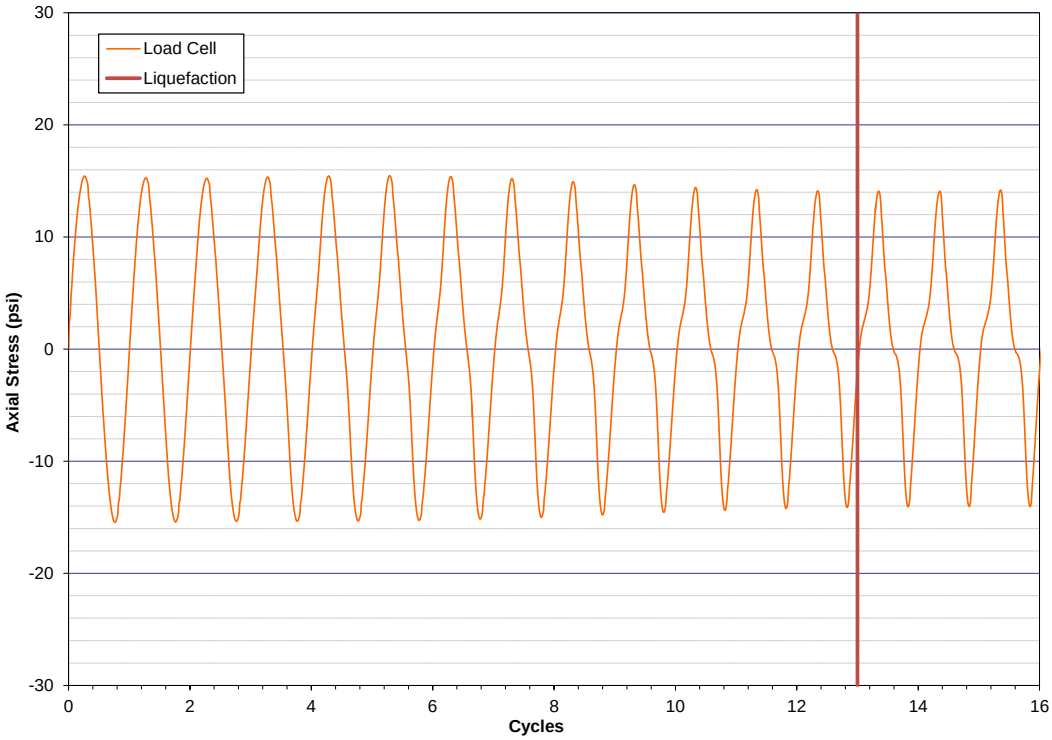

Figure A.11a: Specimen 84 Cyclic Loading

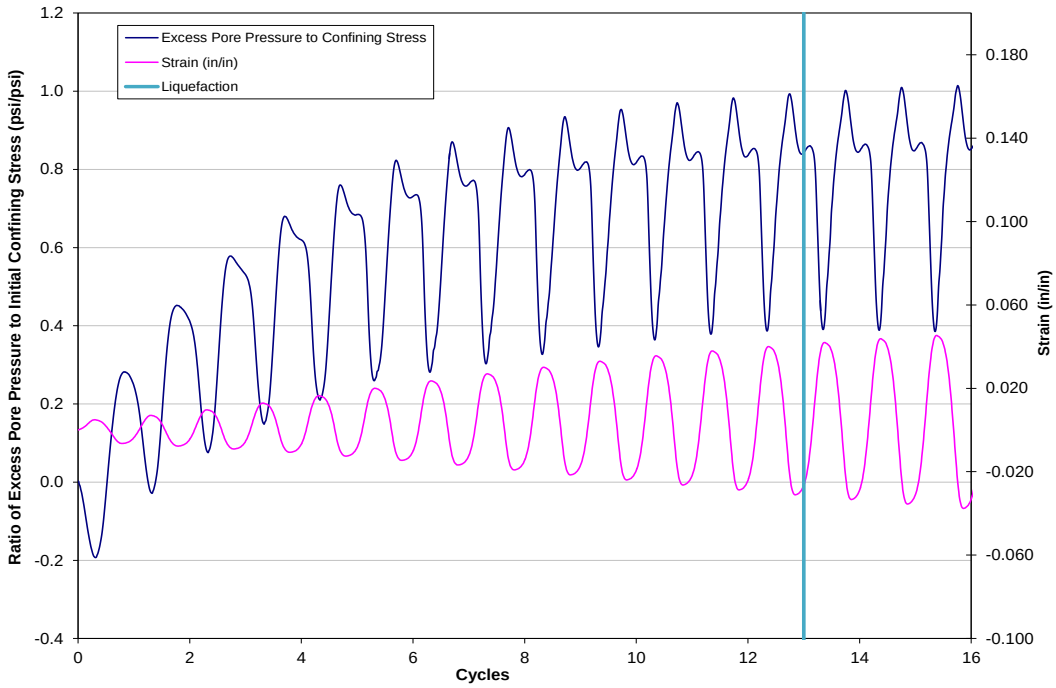

Figure A.11b: Specimen 84 Pore Water Pressure Build-up and Cyclic Displacement

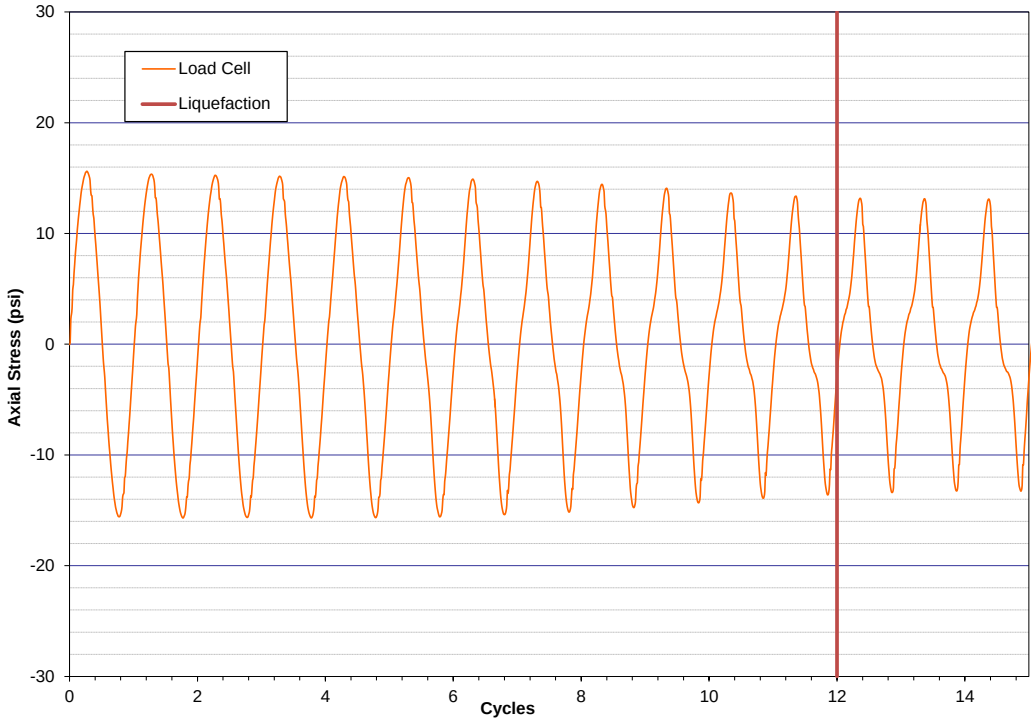

Figure A.12a Specimen 85 Cyclic Loading

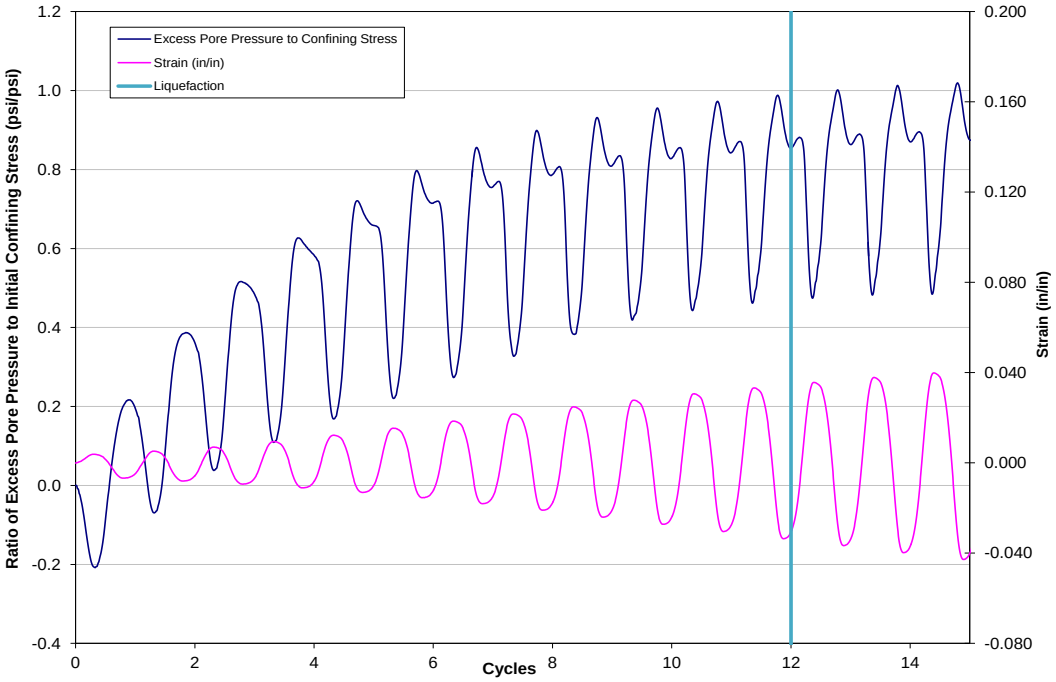

Figure A.12b Specimen 85 Pore Water Pressure Build-up and Cyclic Displacement

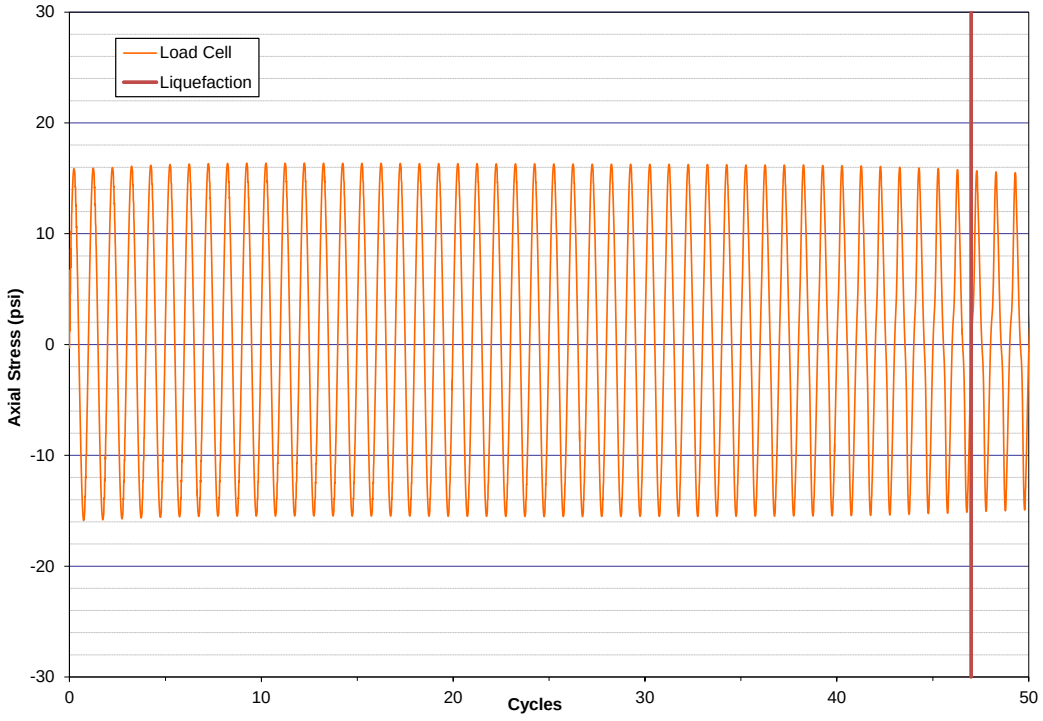

Figure A.13a Specimen 86 Cyclic Loading

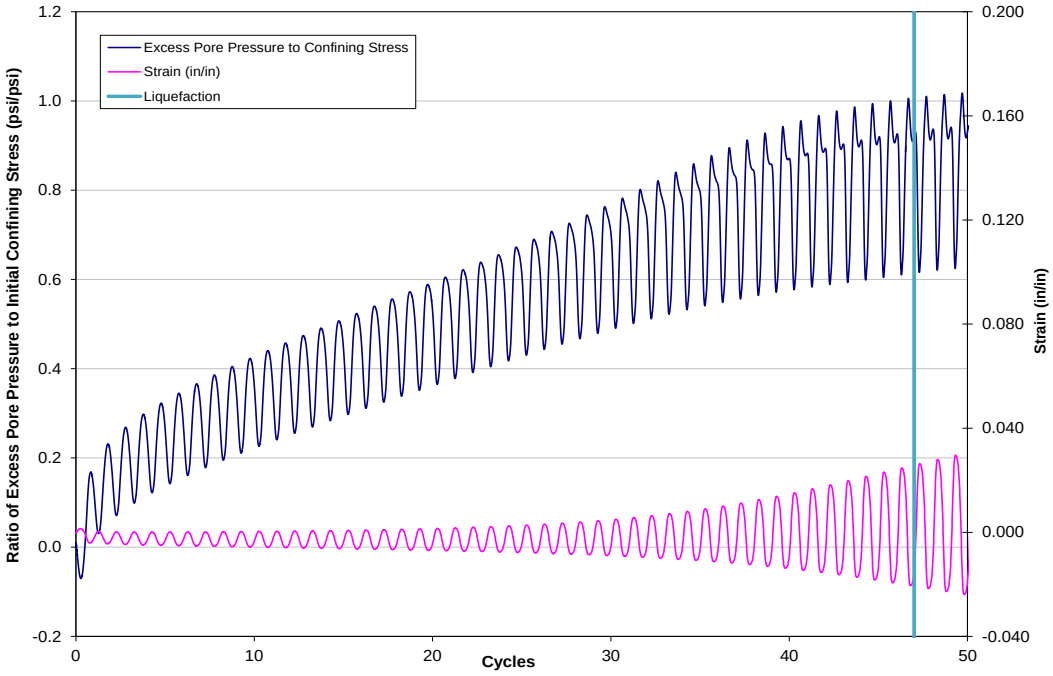

Figure A.13b Specimen 86 Pore Water Pressure Build-up and Cyclic Displacement

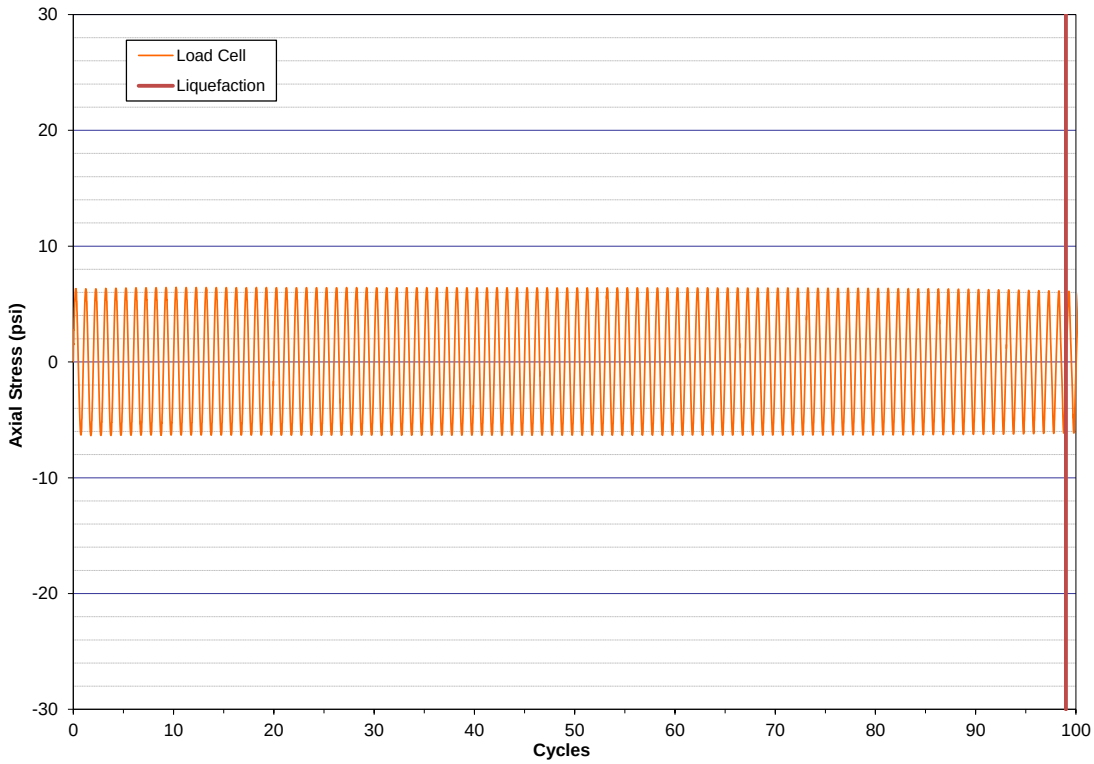

Figure A.14a Specimen 87 Cyclic Loading

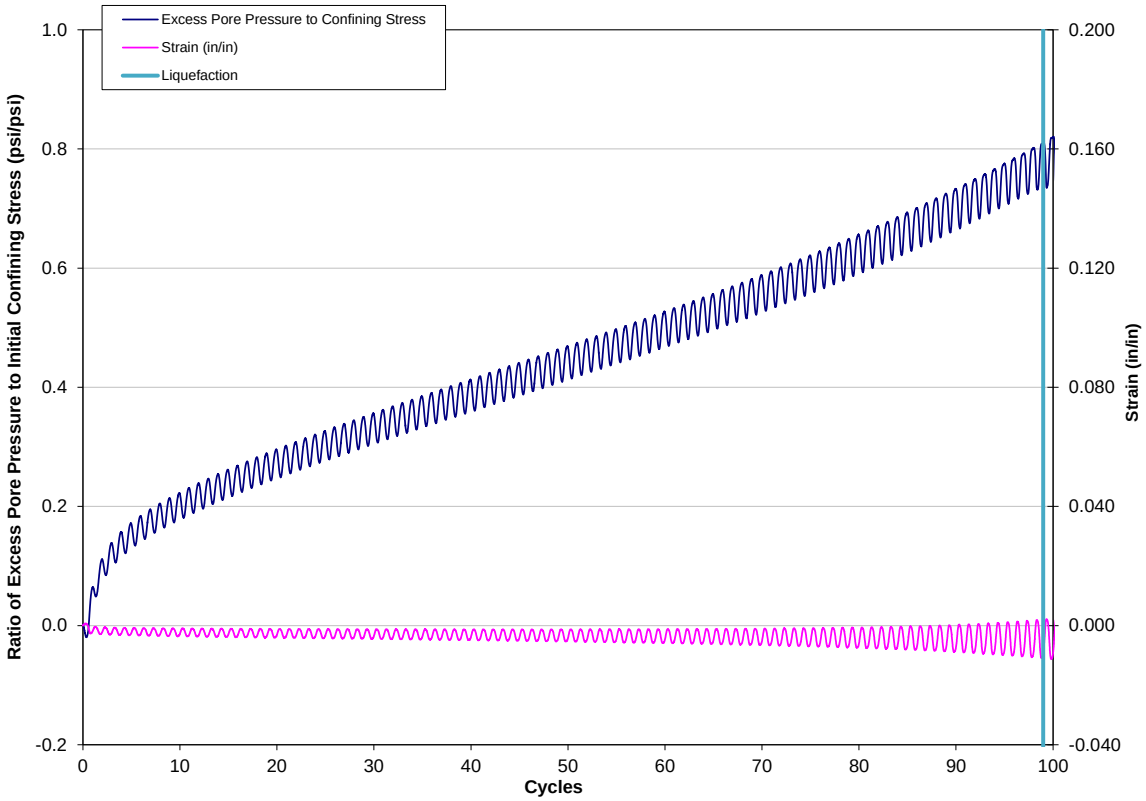

Figure A.14b Specimen 87 Pore Water Pressure Build-up and Cyclic Displacement

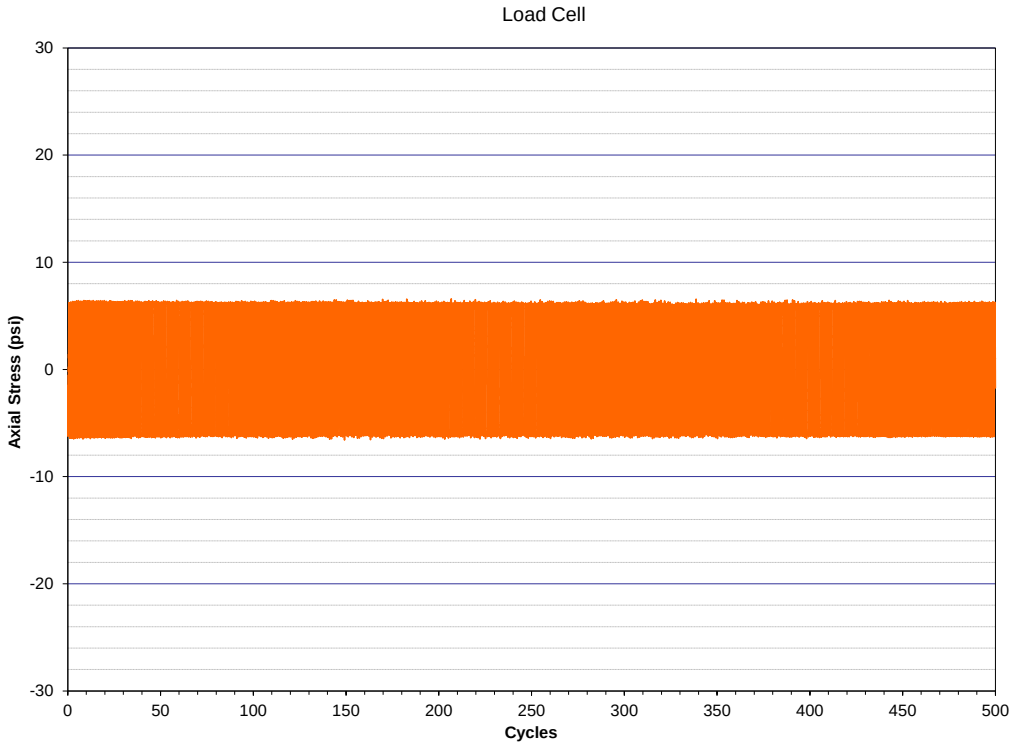

Figure A.15a Specimen 109 Cyclic Loading

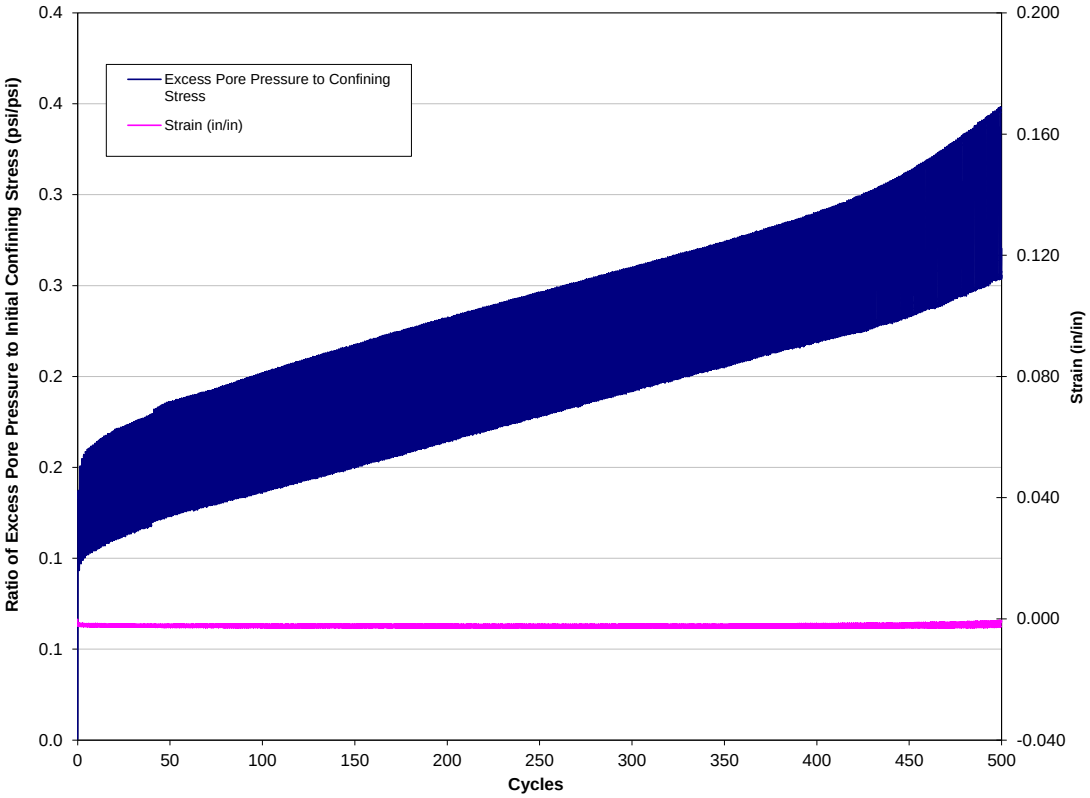

Figure A.15b Specimen 109 Pore Water Pressure Build-up and Cyclic Displacement

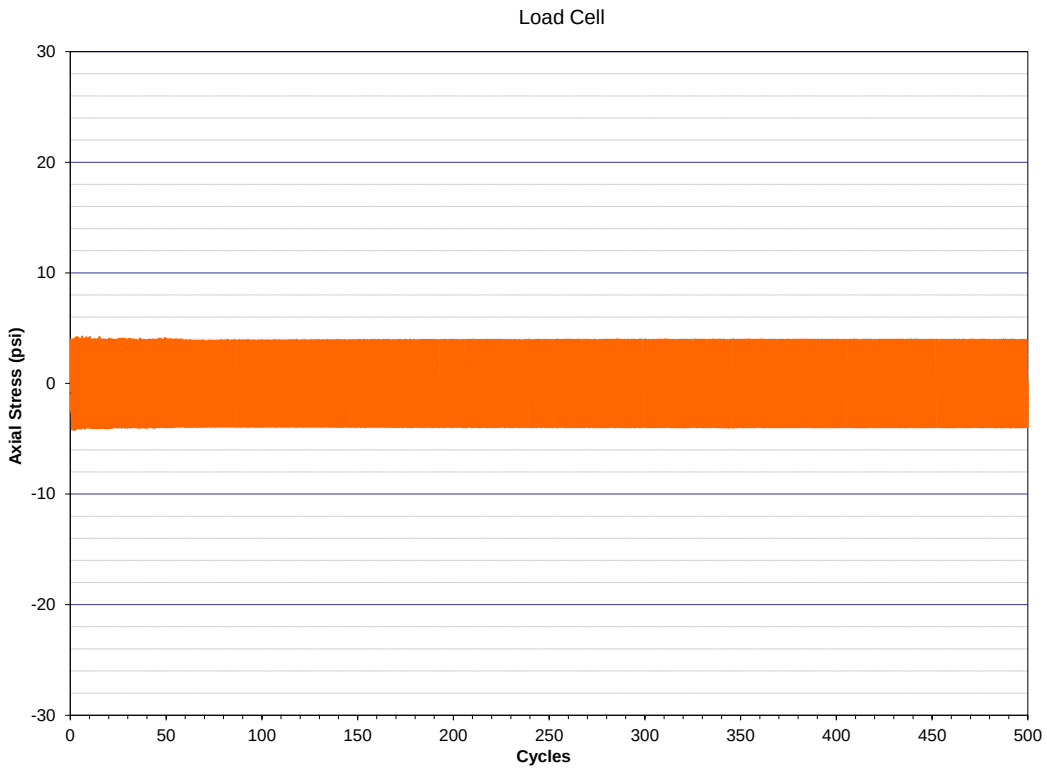

Figure A.16a Specimen 111 Cyclic Loading

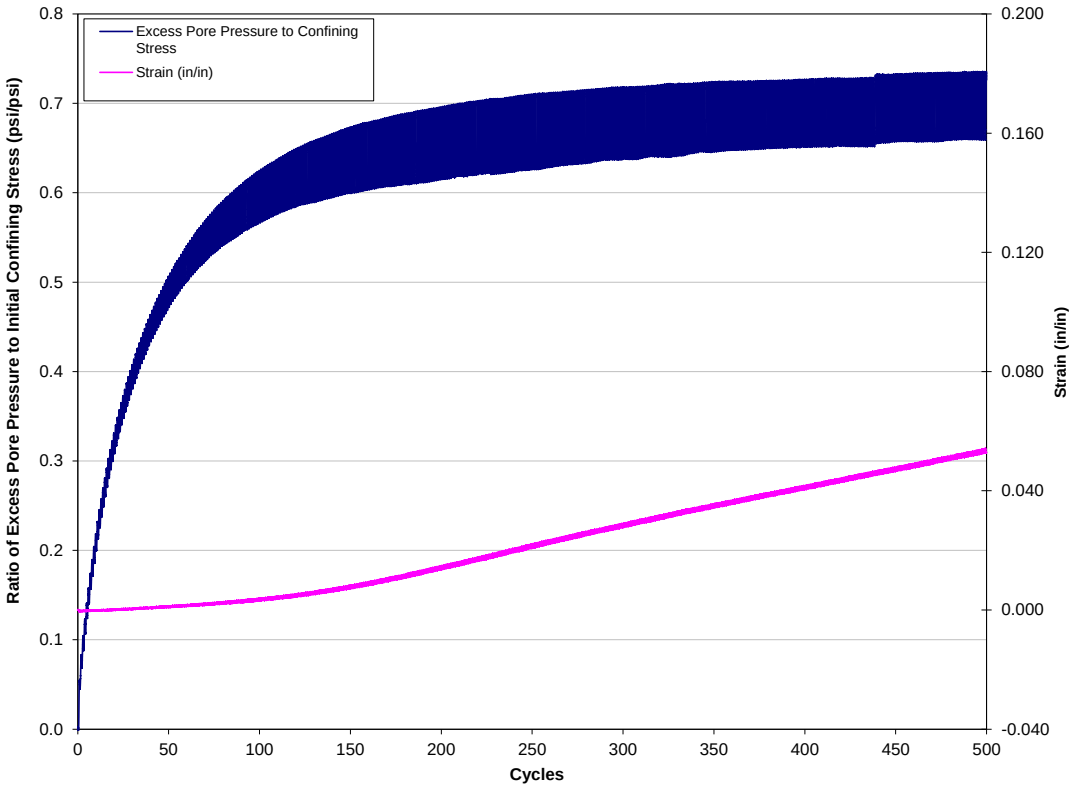

Figure A.16b Specimen 111 Pore Water Pressure Build-up and Cyclic Displacement

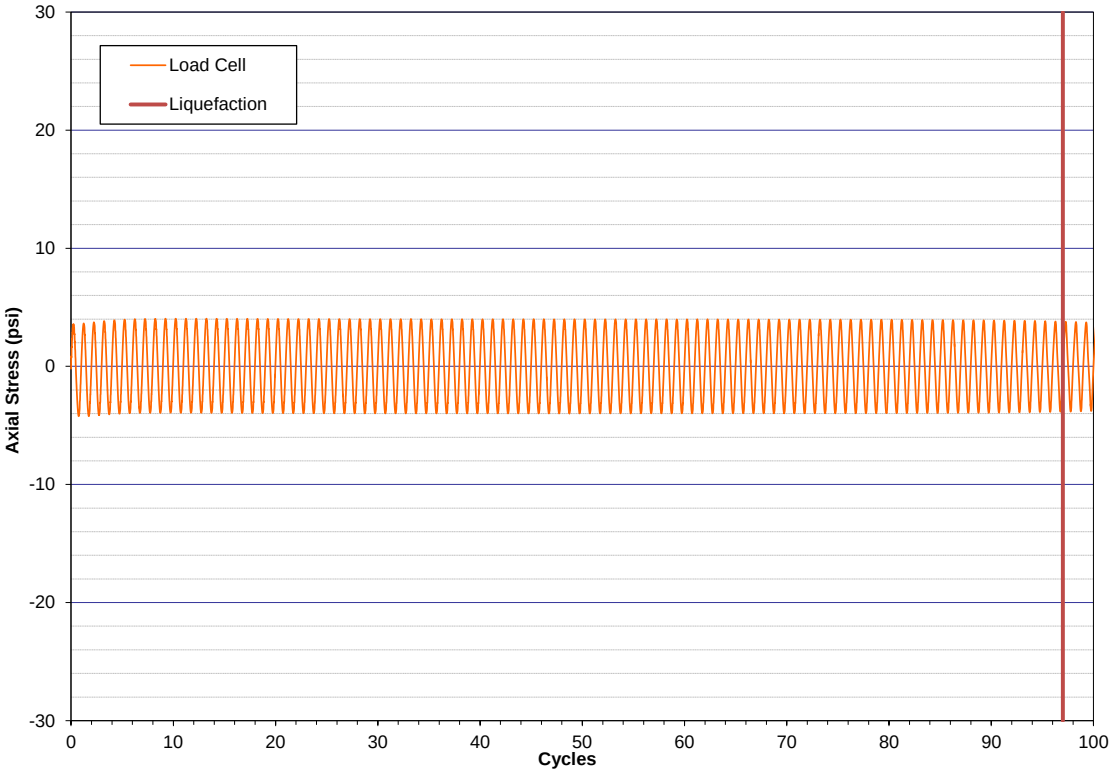

Figure A.17a Specimen 114 Cyclic Loading

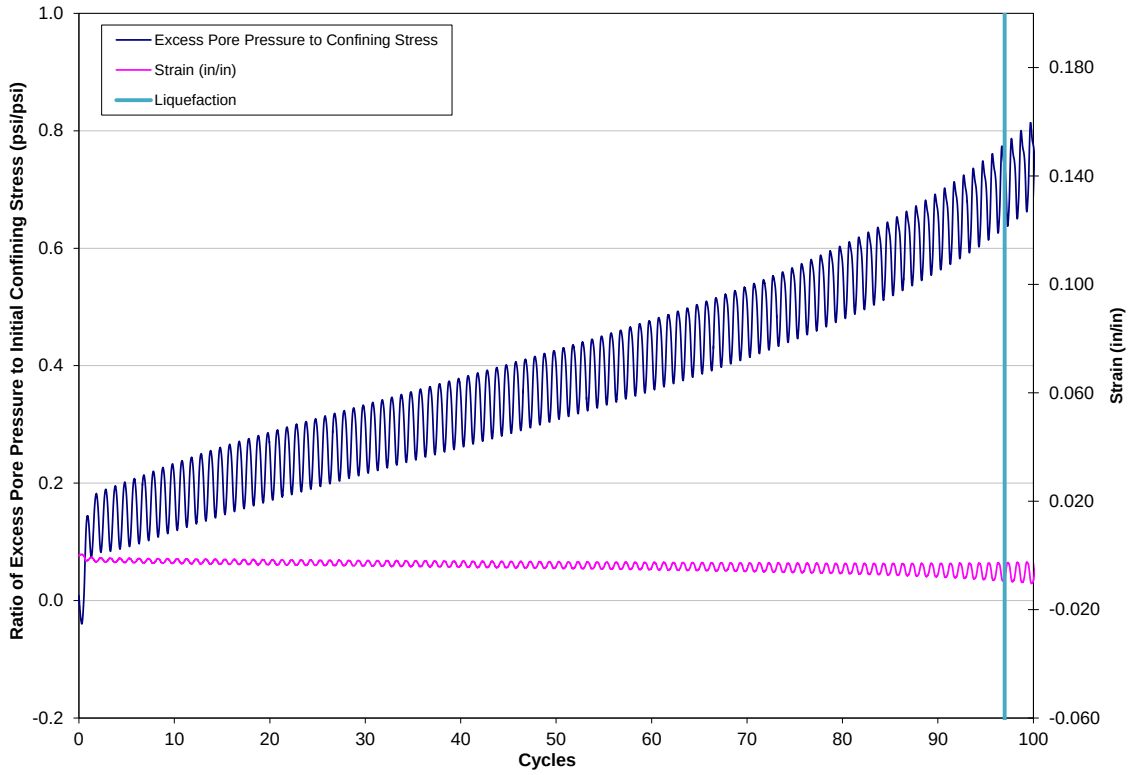

Figure A.17b Specimen 114 Pore Water Pressure Build-up and Cyclic Displacement

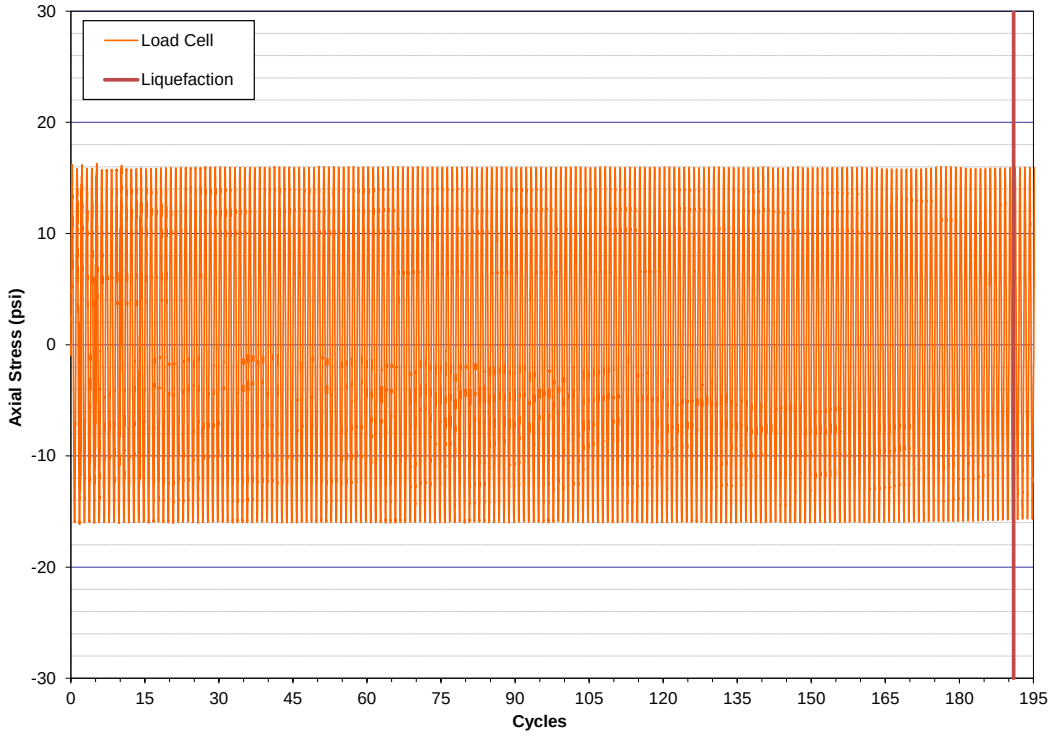

Figure A.18a Specimen 116 Cyclic Loading

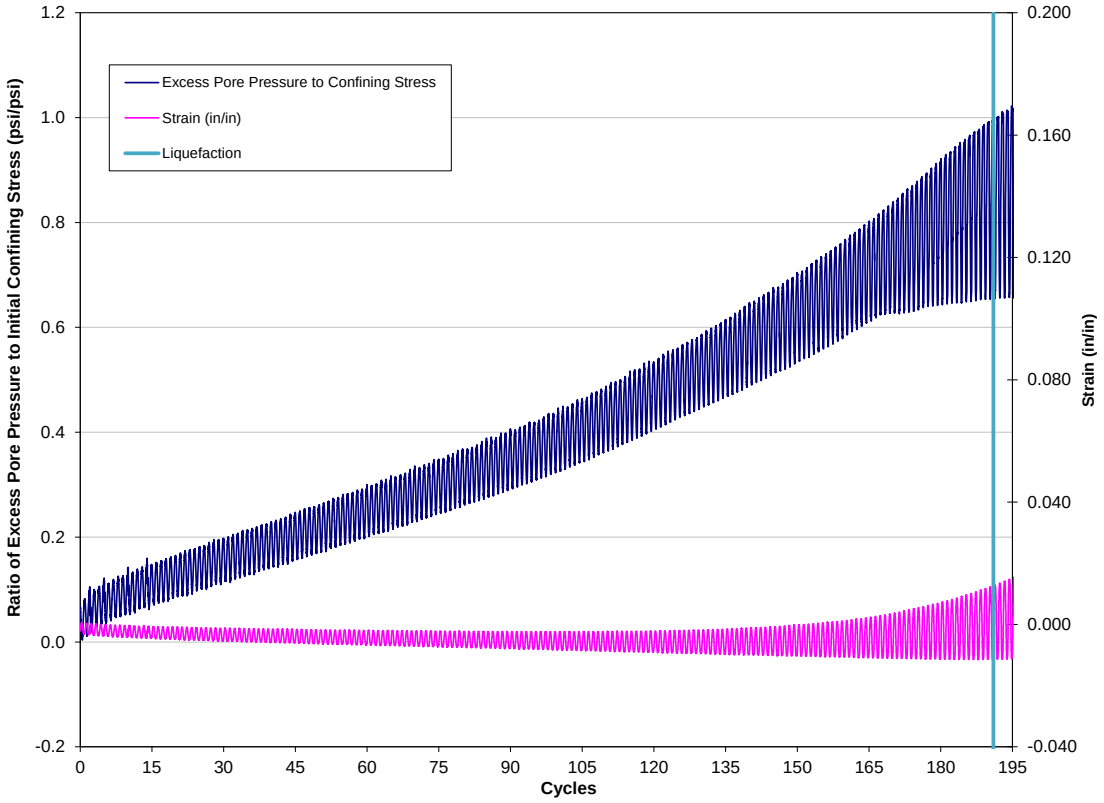

Figure A.18b Specimen 116 Pore Water Pressure Build-up and Cyclic Displacement

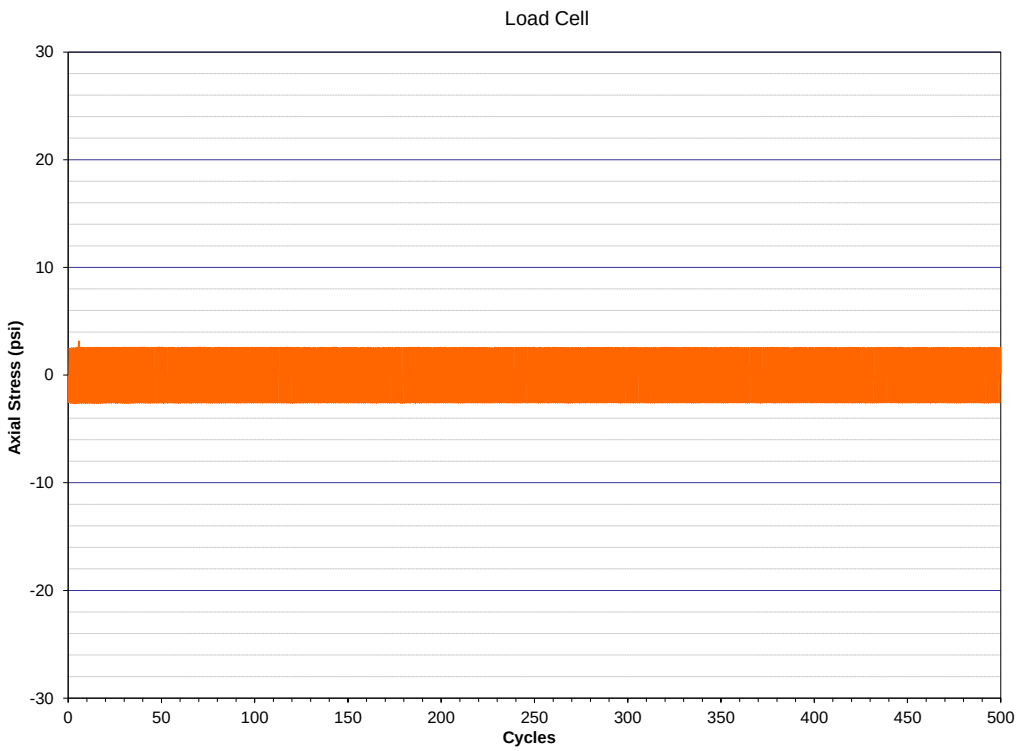

Figure A.19a Specimen 117 Cyclic Loading

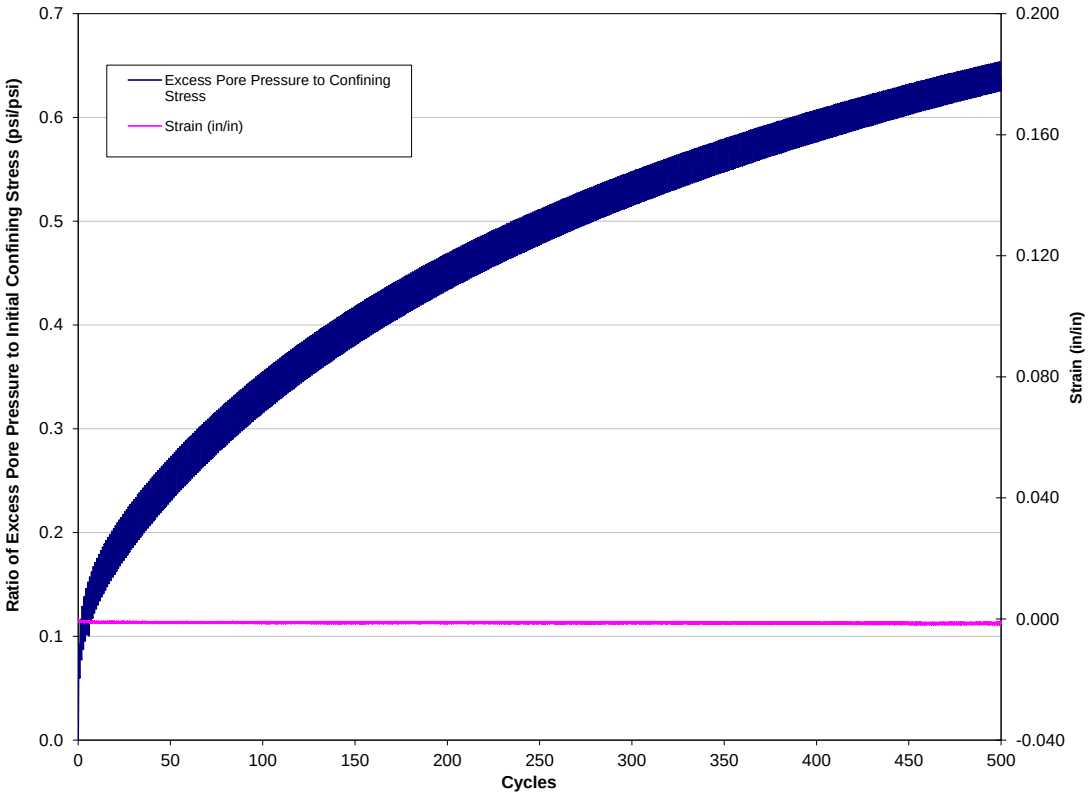

Figure A.19b Specimen 117 Pore Water Pressure Build-up and Cyclic Displacement

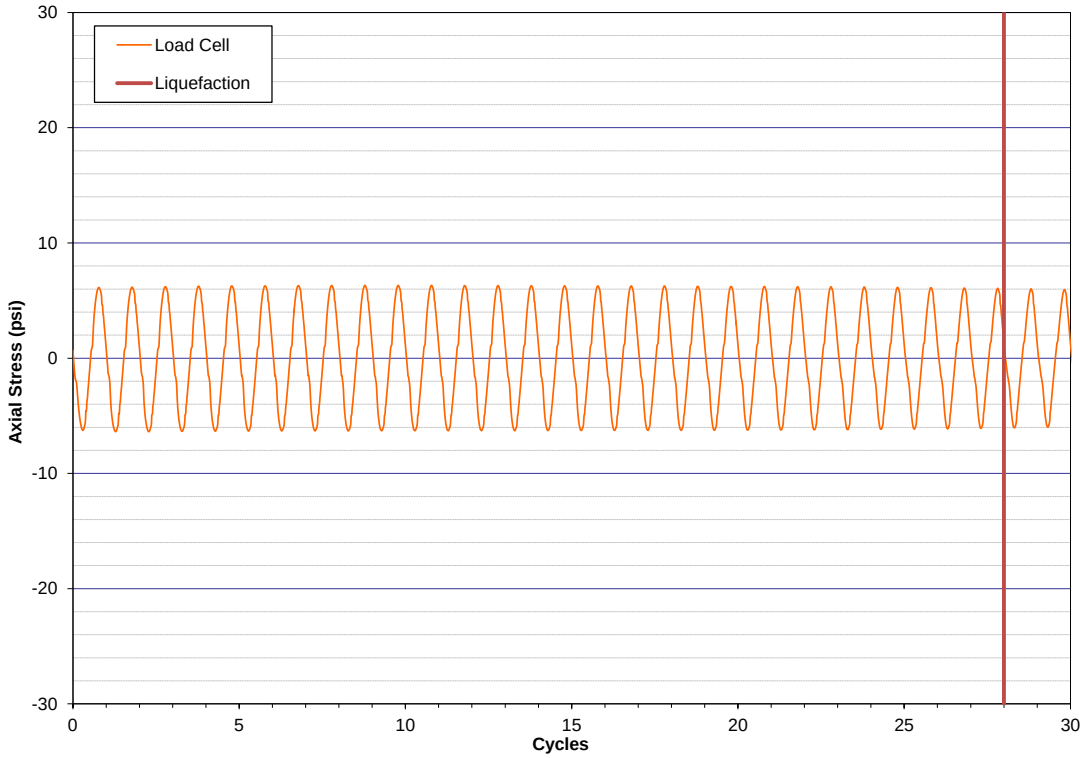

Figure A.20a Specimen 119 Cyclic Loading

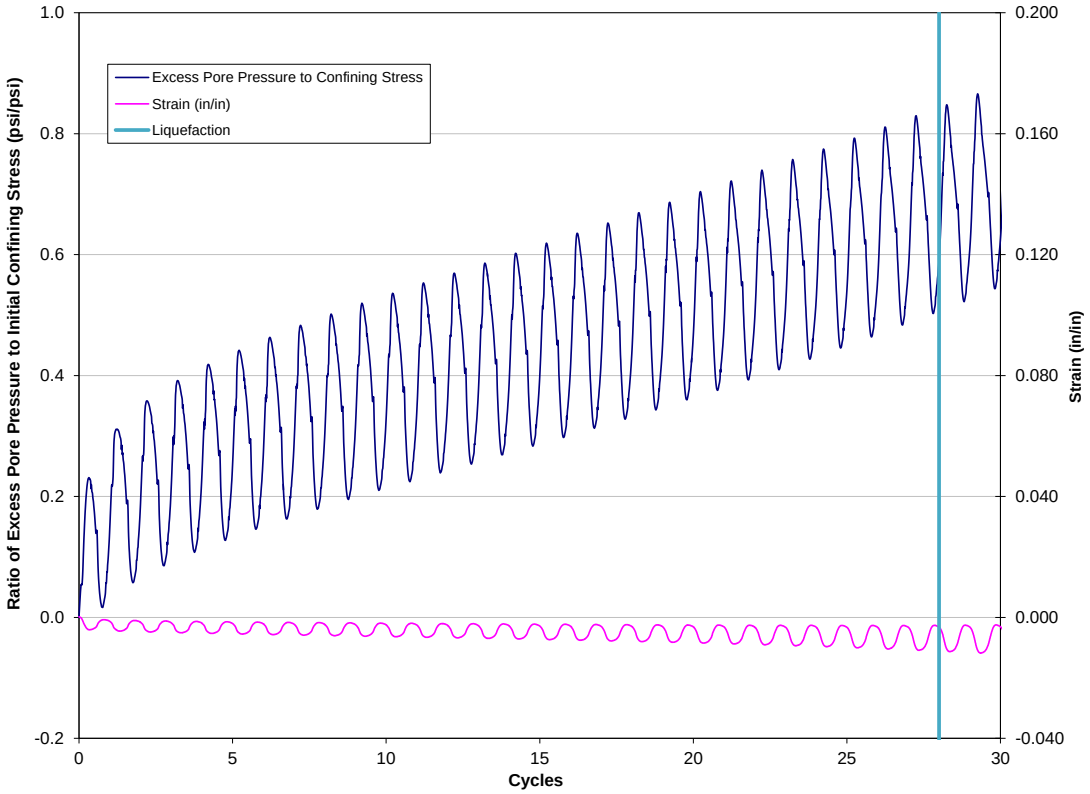

Figure A.20b Specimen 119 Pore Water Pressure Build-up and Cyclic Displacement

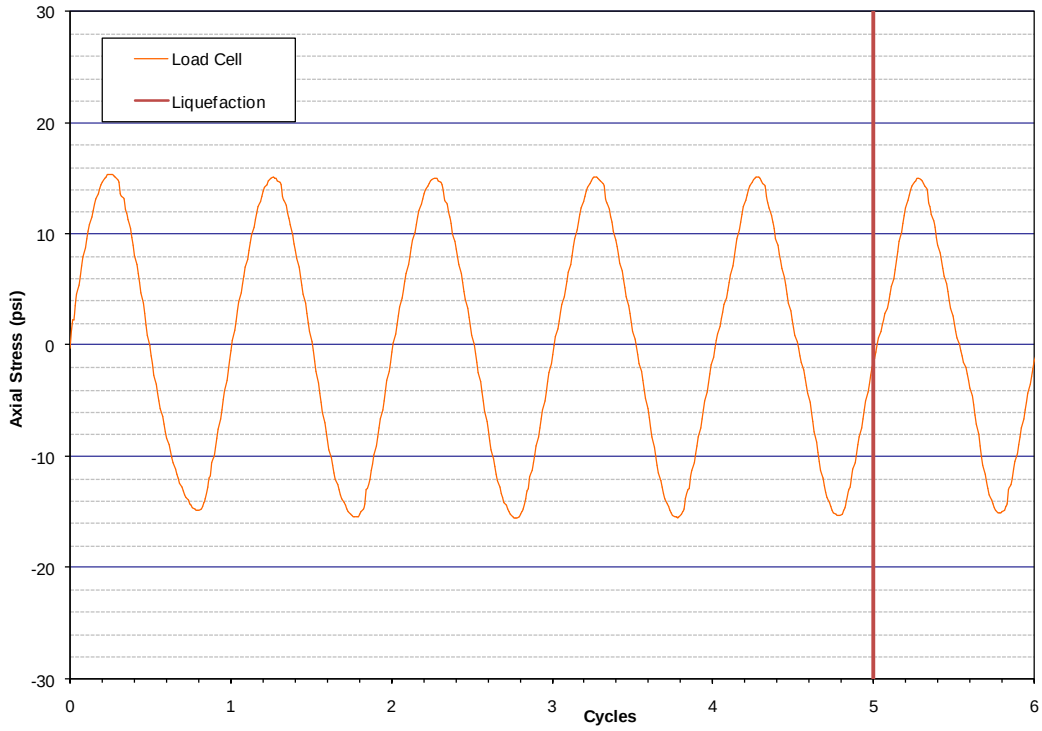

Figure A.21a Specimen 120 Cyclic Loading

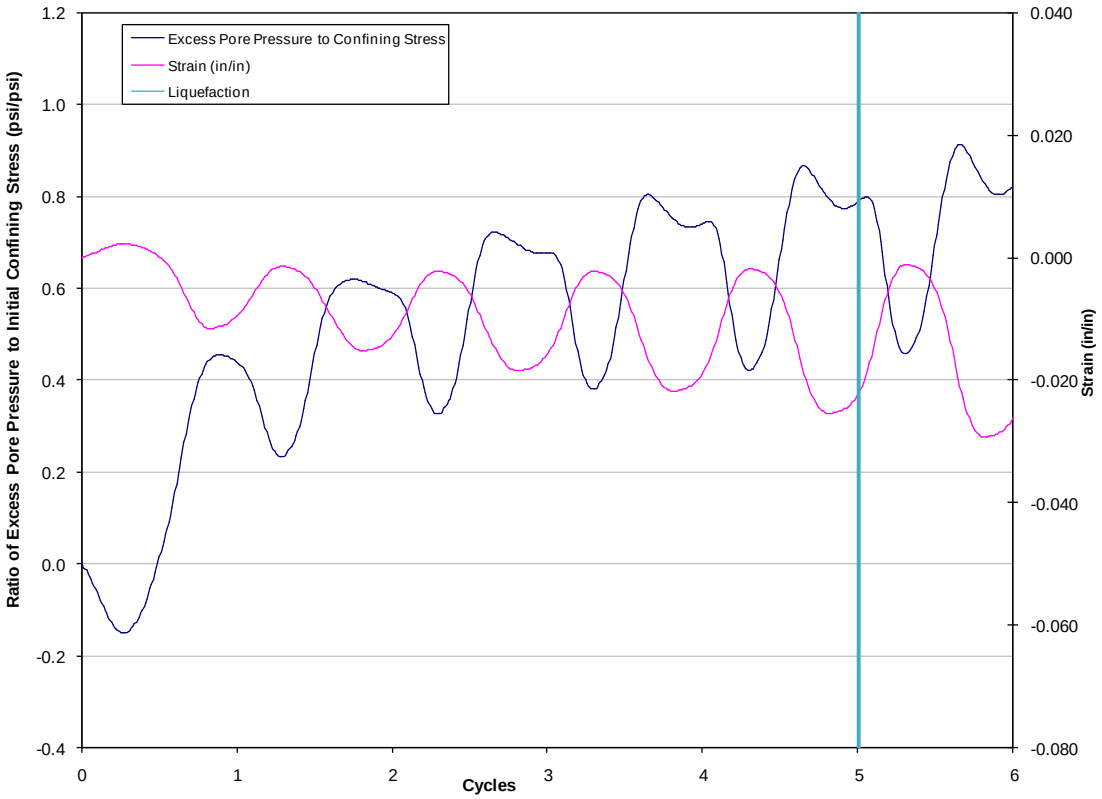

Figure A.21b Specimen 120 Pore Water Pressure Build-up and Cyclic Displacement

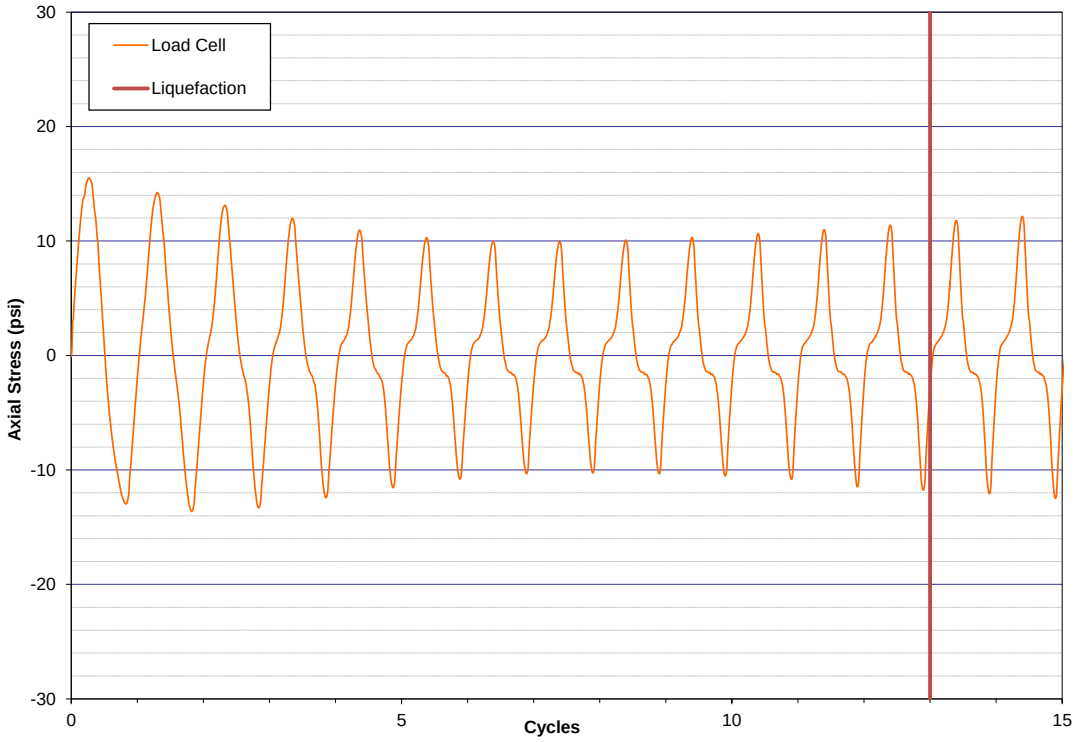

Figure A.22a Specimen 122 Cyclic Loading

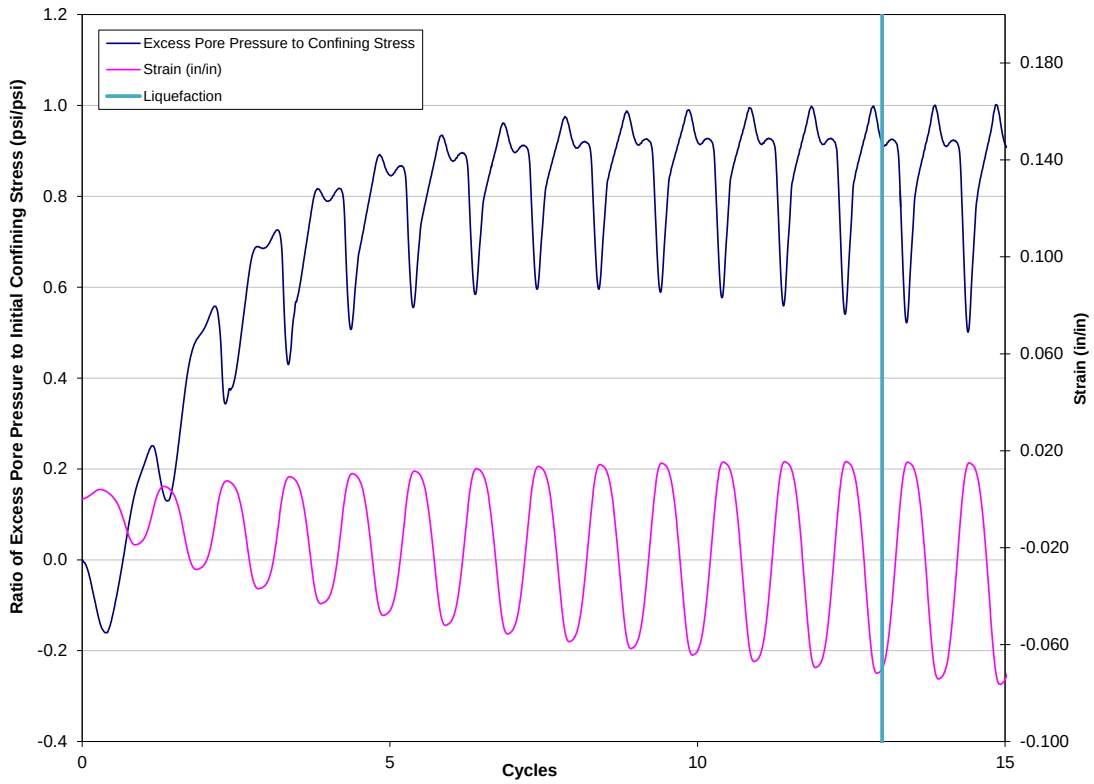

Figure A.22b Specimen 122 Pore Water Pressure Build-up and Cyclic Displacement

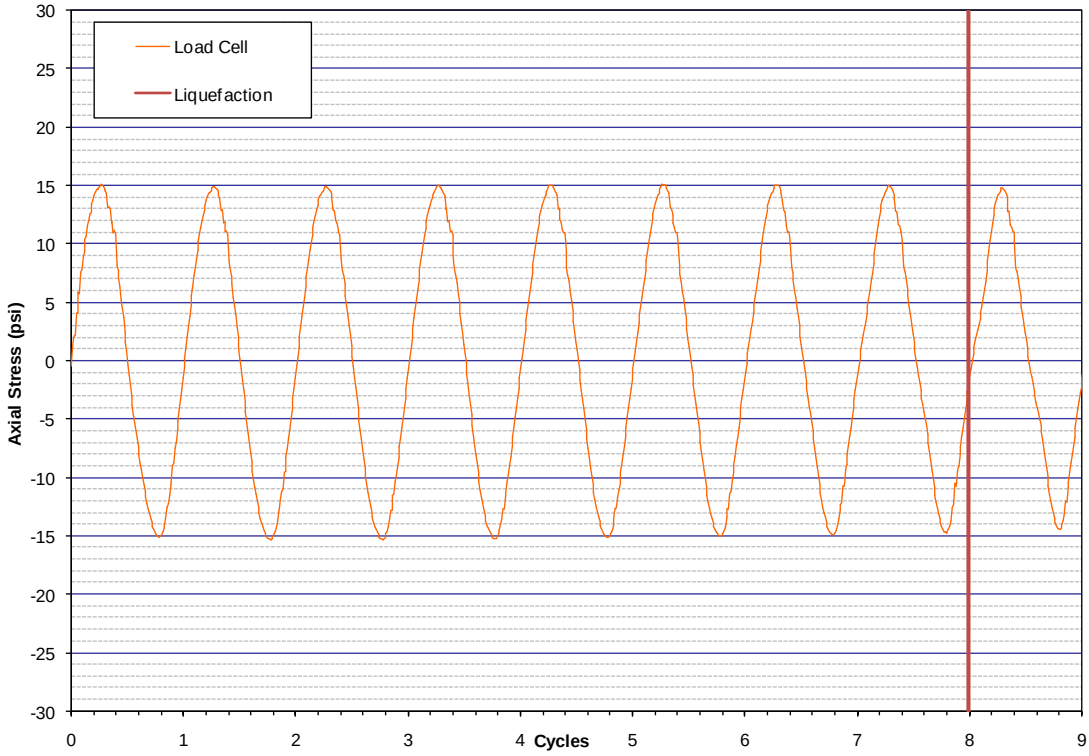

Figure A.23a Specimen 123 Cyclic Loading

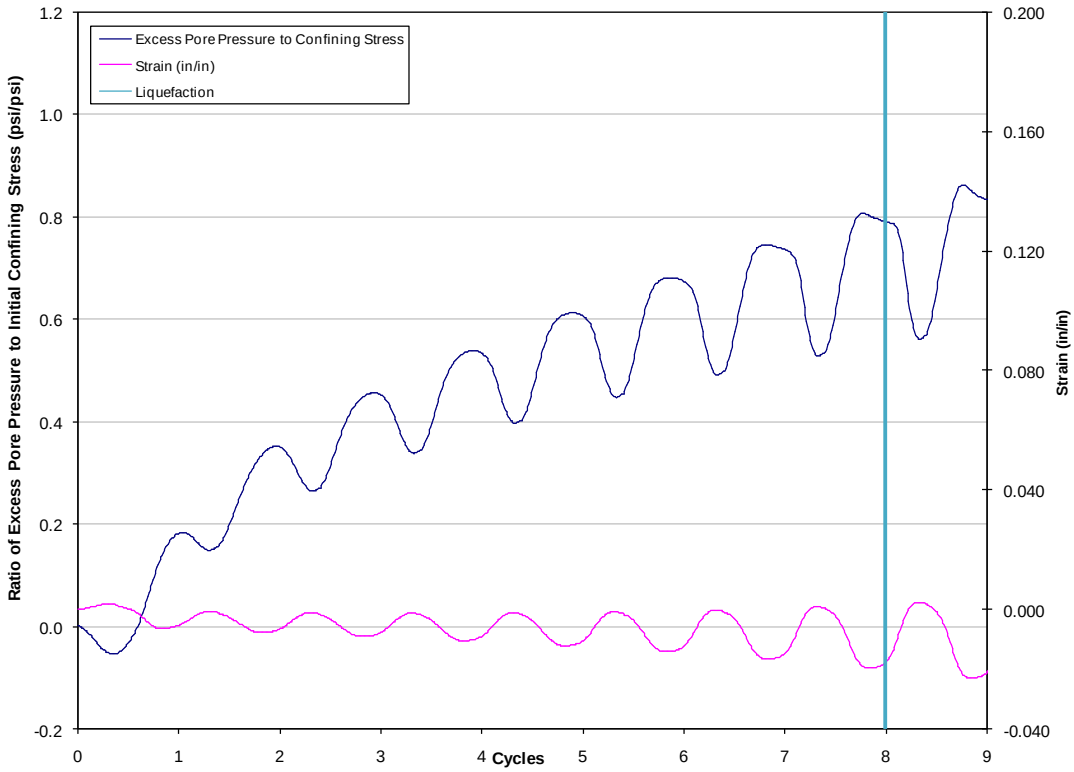

Figure A.23b Specimen 123 Pore Water Pressure Build-up and Cyclic Displacement

Appendix B: Ground Response Analysis Results

Input B.1: KK-1 Soil Profile Input Results

EduShake Report

Data File: C:\EDUSHAKE\KK1_08.DAT

Soil Profile

Profile Name: K-K Mesh - Profile 1
Water Table: 15.00 ft
Number of Layers: 15

Layer Number	Material Name	Thickness (ft)	Unit Weight (pcf)	Gmax (ksf)	Vs (ft/sec)	Modulus Curve	Damping Curve	Mod. Parameter	Damp. Parameter
1	Gravelly Silty Sand	2.00	108.00	3,213.00	978.35	Sand (Seed & Idriss) - A	Sand (Seed & Idriss) - Ave		
2	Sand and Gravel	13.00	114.00	3,391.00	978.28	Sand (Seed & Idriss) - U	Sand (Seed & Idriss) - Upp		
3	Sand and Gravel	5.00	114.00	3,391.00	978.28	Sand (Seed & Idriss) - U	Sand (Seed & Idriss) - Upp		
4	Silty Clay	2.00	125.00	3,718.00	978.26	Clay (Seed and Sun 198	Clay - Average (Sun et al.)		
5	Fly Ash	5.00	98.00	690.00	475.95	Sand (Seed and Idriss 1	Sand (Idriss 1990)		
6	Fly Ash	5.00	98.00	690.00	475.95	Sand (Seed and Idriss 1	Sand (Idriss 1990)		
7	Fly Ash	5.00	98.00	690.00	475.95	Sand (Seed and Idriss 1	Sand (Idriss 1990)		
8	Fly Ash	5.00	98.00	690.00	475.95	Sand (Seed and Idriss 1	Sand (Idriss 1990)		
9	Fly Ash	5.00	98.00	690.00	475.95	Sand (Seed and Idriss 1	Sand (Idriss 1990)		
10	Fly Ash	5.00	98.00	690.00	475.95	Sand (Seed and Idriss 1	Sand (Idriss 1990)		
11	Fly Ash	5.00	98.00	690.00	475.95	Sand (Seed and Idriss 1	Sand (Idriss 1990)		
12	Clay Foundation	10.00	130.00	1,944.00	693.63	Clay (Seed and Sun 198	Clay - Average (Sun et al.)		
13	Silty Clay Foundatic	20.00	125.00	1,870.00	693.77	Clay (Seed and Sun 198	Clay - Average (Sun et al.)		
14	Foundation Soil	20.00	130.00	1,944.00	693.63	Clay (Seed and Sun 198	Clay - Average (Sun et al.)		
15	Sandstone Bedrock	Infinite	140.00	135,360.0(	5,577.42	Rock (Idriss)	Rock (Idriss)		

Input Motion

Number of Motions: 1
Numeber of Iterations: 5
Strain Ratio: 0.65
Tolerance: 5.00%

File Name	No of Acc. Values	Max. Acc. (g)	Time Step (sec)	Cuttoff Freq. (Hz)	No of Fourier Terms	Layer	Outcrop
C:\EDUSHAKE\TAFT.EQ	4220	0.080	0.020	20.00	8192	15	No

Output Locations

Layer No	Depth (ft)	Outcrop
1	0.00	No
5	22.00	No
6	27.00	No
7	32.00	No

K-K Mech - Profile 1

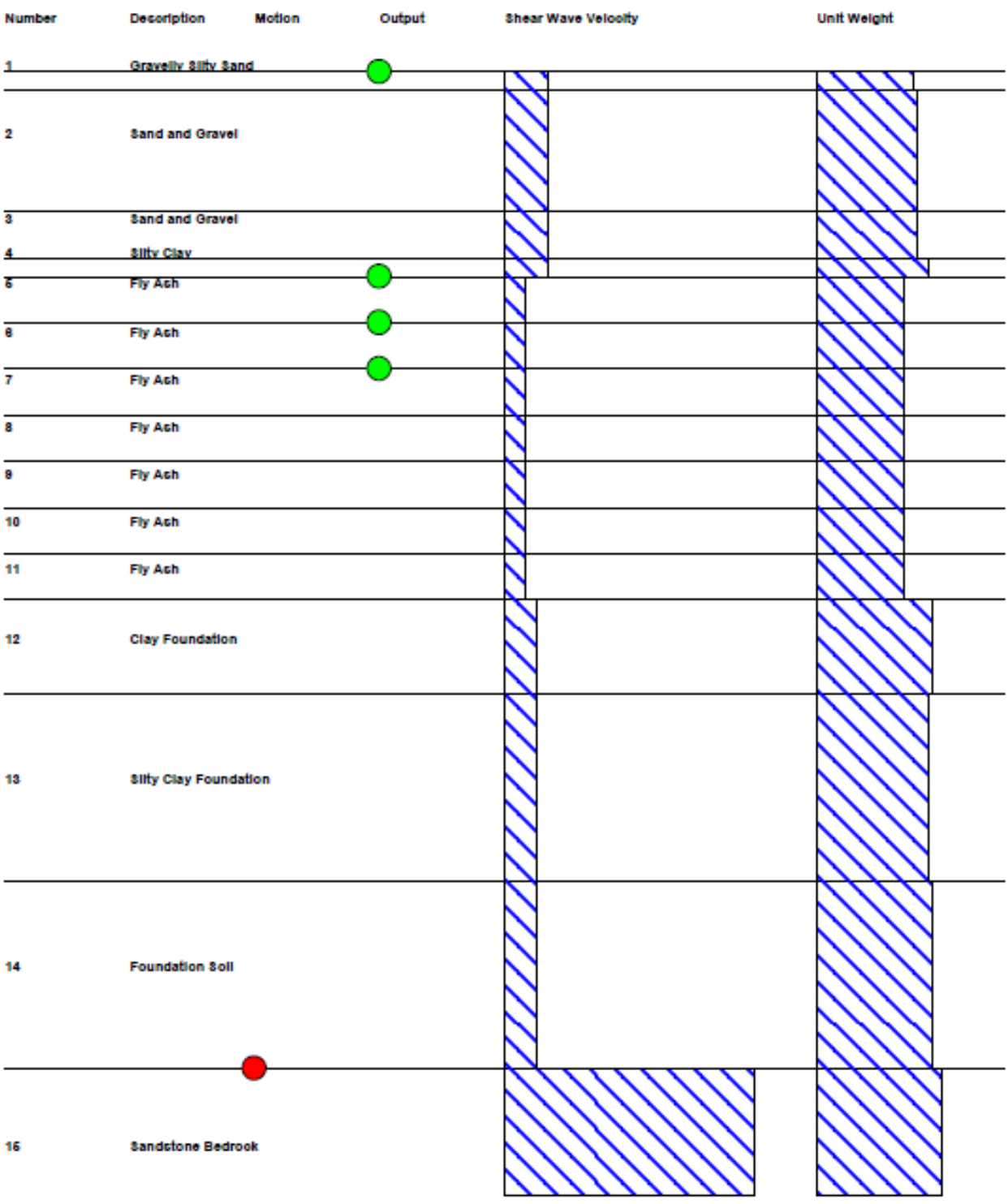

Input B.2: KK-2 Soil Profile Input Results

EduShake Report

Data File: C:\EDUSHAKE\KK2_08EL.DAT

Soil Profile

Profile Name: K-K Mesh - Profile 2
Water Table: 15.00 ft
Number of Layers: 10

Layer Number	Material Name	Thickness (ft)	Unit Weight (pcf)	Gmax (ksf)	Vs (ft/sec)	Modulus Curve	Damping Curve	Mod. Parameter	Damp. Parameter
1	Silty Clay	1.00	125.00	3,718.00	978.26	Clay (Seed and Sun 198	Clay (Idriss 1990)		
2	Bottom Ash	2.00	100.00	2,975.00	978.35	Sand (Seed and Idriss 1	Sand (Idriss 1990)		
3	Gravelly Silty Sand	13.00	110.00	3,391.00	995.91	Sand (Seed & Idriss) - A	Sand (Seed & Idriss) - Ave		
4	Silty Clay	6.00	128.00	1,915.00	693.80	Clay (Seed and Sun 198	Clay - Average (Sun et al.		
5	Fly Ash	6.00	98.00	690.00	475.95	Sand (Seed and Idriss 1	Sand (Idriss 1990)		
6	Fly Ash	6.00	98.00	690.00	475.95	Sand (Seed and Idriss 1	Sand (Idriss 1990)		
7	Bottom Ash	8.00	100.00	2,975.00	978.35	Sand (Seed and Idriss 1	Sand (Idriss 1990)		
8	Silty Clay Foundatic	20.00	125.00	1,870.00	693.77	Clay (Seed and Sun 198	Clay - Average (Sun et al.		
9	Foundation Soil	20.00	130.00	1,944.00	693.63	Clay (Seed and Sun 198	Clay - Average (Sun et al.		
10	Sandstone	Infinite	140.00	135,260.0(	5,575.36	Rock (Idriss)	Rock (Idriss)		

Input Motion

Number of Motions: 1
Numeber of Iterations: 5
Strain Ratio: 0.65
Tolerance: 5.00%

File Name	No of Acc. Values	Max. Acc. (g)	Time Step (sec)	Cuttoff Freq. (Hz)	No of Fourier Terms	Layer	Outcrop
C:\EDUSHAKE\ELCENTRC	4187	0.080	0.020	20.00	8192	10	No

Output Locations

Layer No	Depth (ft)	Outcrop
1	0.00	No
5	22.00	No
6	28.00	No

K-K Mech - Profile 2

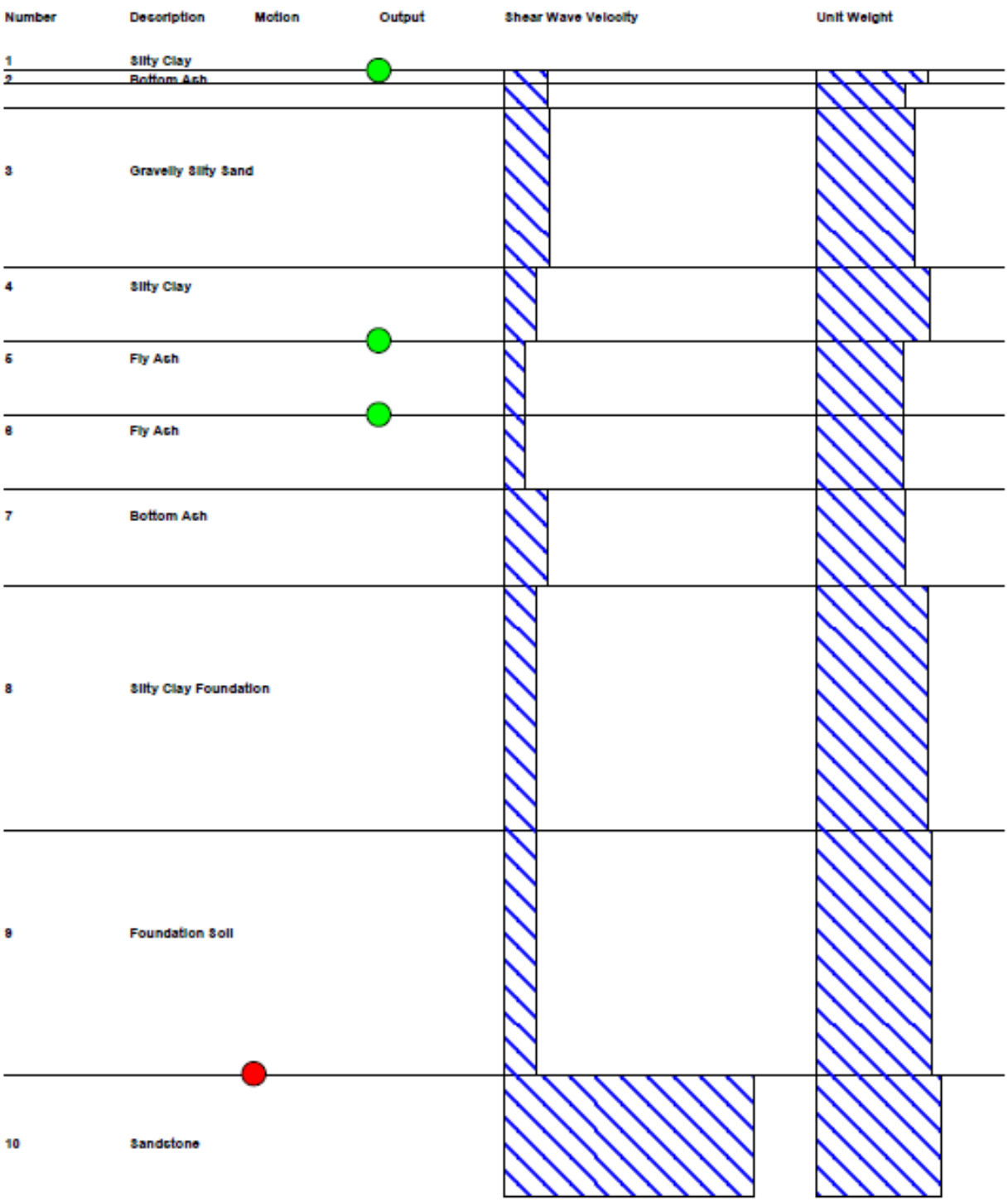

Analysis B.1: KK-1 Profile with El Centro Earthquake Motion at 0.08g Ground Acceleration

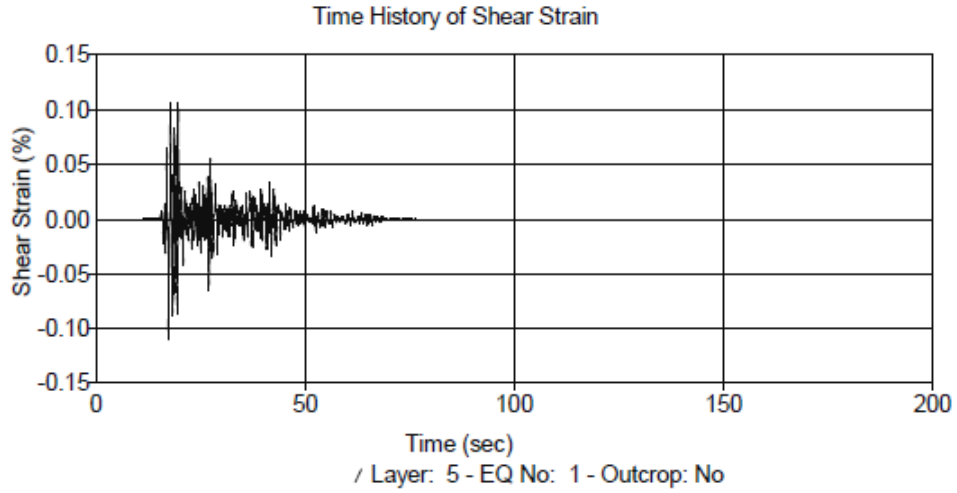

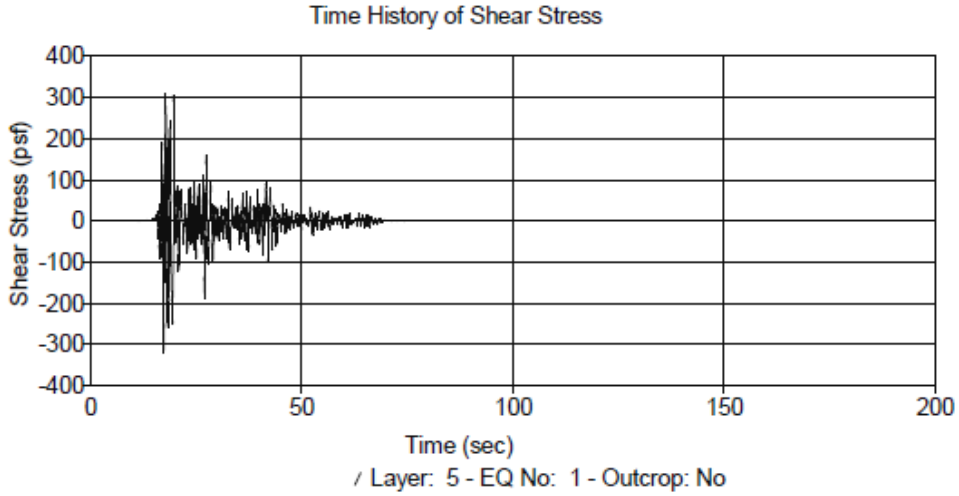

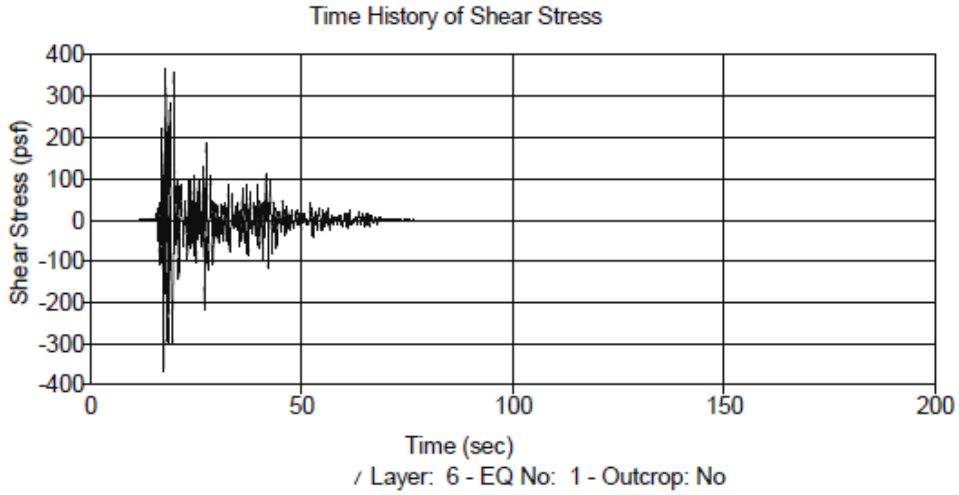

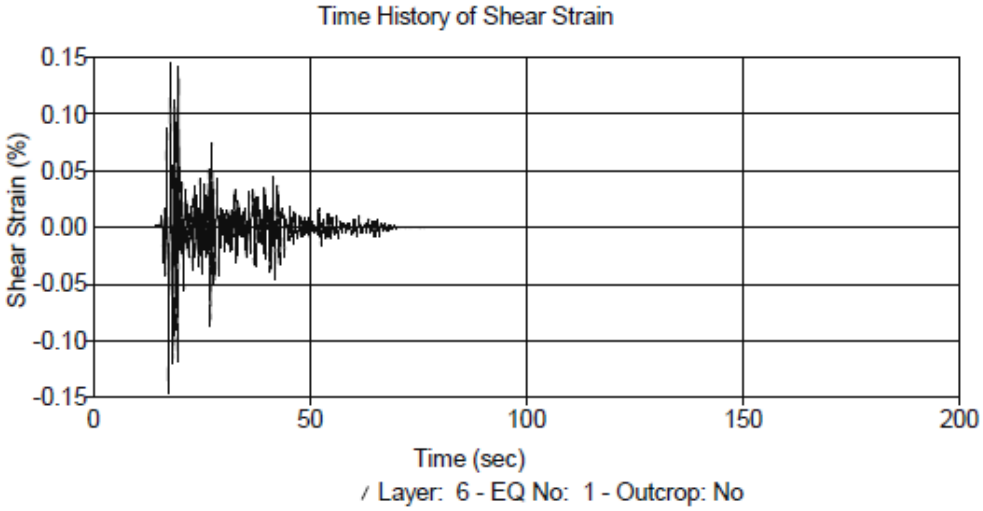
Time History of Shear Strain
Shear Strain (%)
0.15
0.10
0.05
0.00
-0.05
-0.10
-0.15
0
50
100
150
200
Time (sec)
Layer: 6 - EQ No: 1 - Outcrop: No

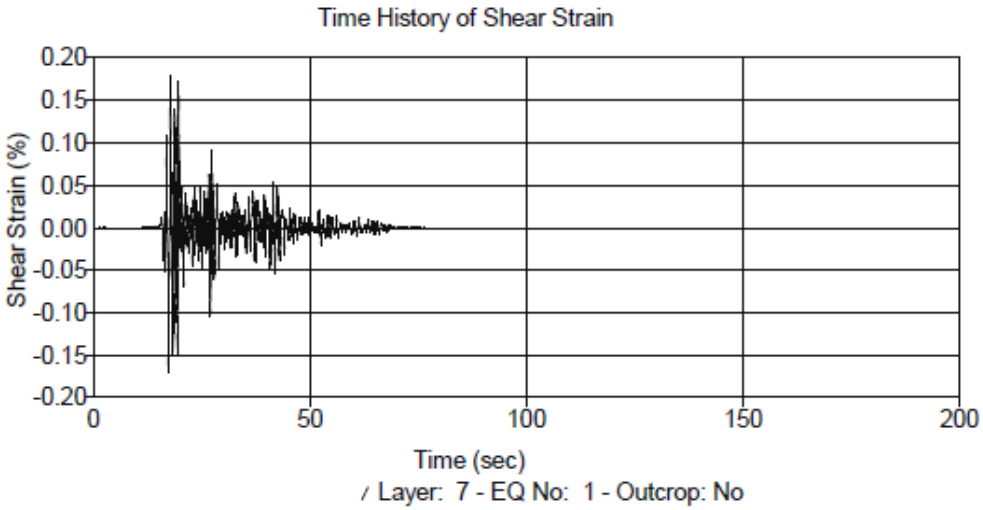
Time History of Shear Strain
Shear Strain (%)
0.20
0.15
0.10
0.05
0.00
-0.05
-0.10
-0.15
-0.20
0
50
100
150
200
Time (sec)
Layer: 7 - EQ No: 1 - Outcrop: No

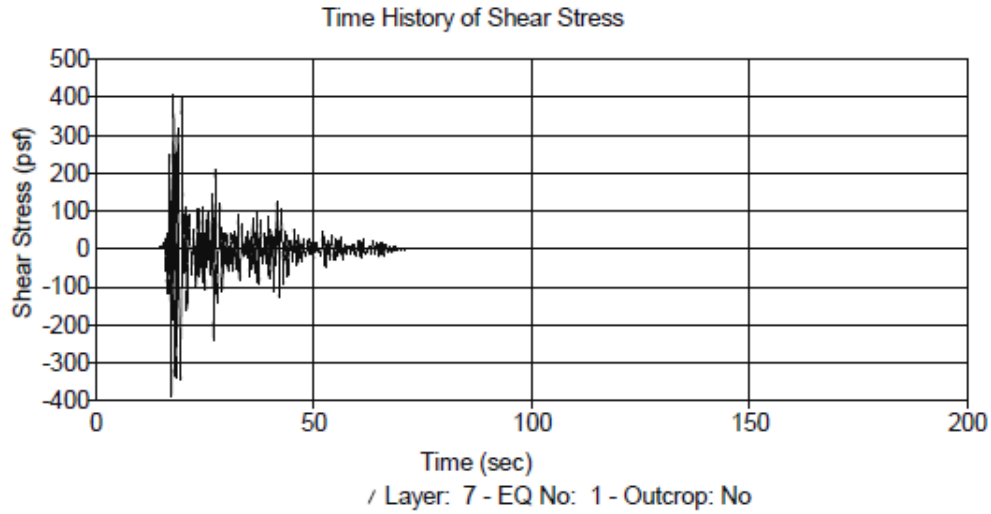
Time History of Shear Stress
Shear Stress (psf)
500
400
300
200
100
0
-100
-200
-300
-400
0
50
100
150
200
Time (sec)
Layer: 7 - EQ No: 1 - Outcrop: No

Peak Shear Stress (psf)

Depth (ft)	EQ No: 1
-1.00	14.01
-8.50	123.75
-17.50	255.07
-21.00	304.65
-24.50	356.80
-29.50	398.33
-34.50	438.50
-39.50	465.93
-44.50	477.43
-49.50	481.23
-54.50	500.50
-62.00	575.13
-77.00	738.56
-97.00	899.64
-107.00	916.80

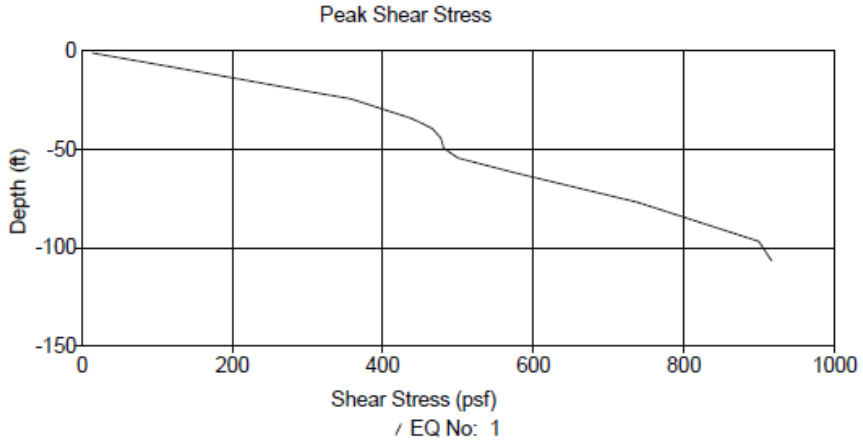

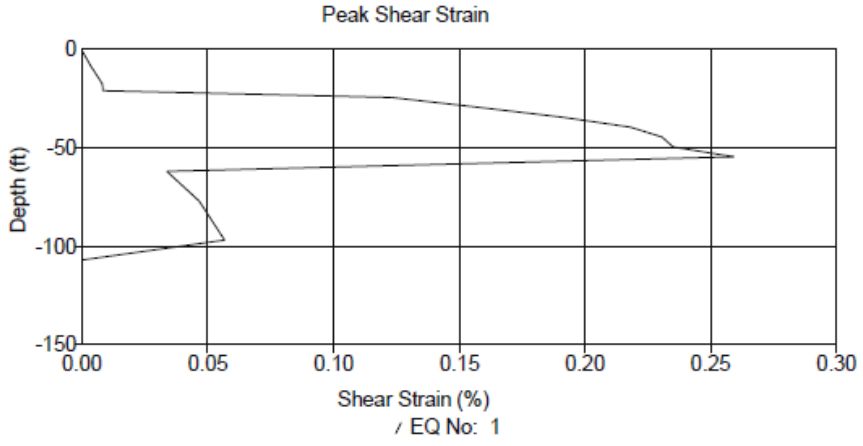

Analysis B.2: KK-1 Profile with Taft Earthquake Motion at 0.08g Ground Acceleration

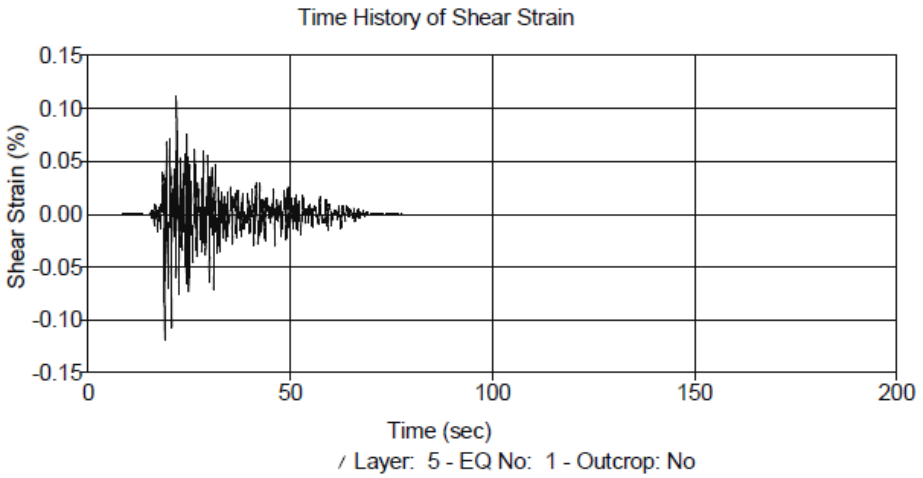

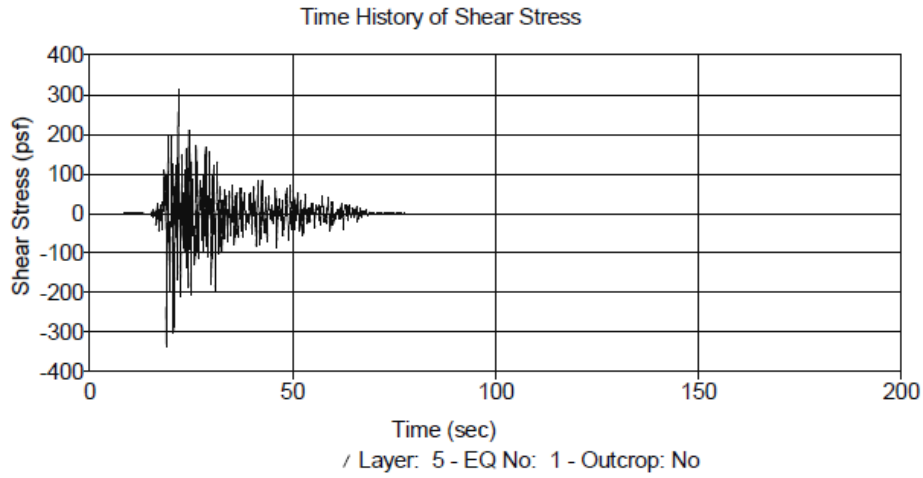

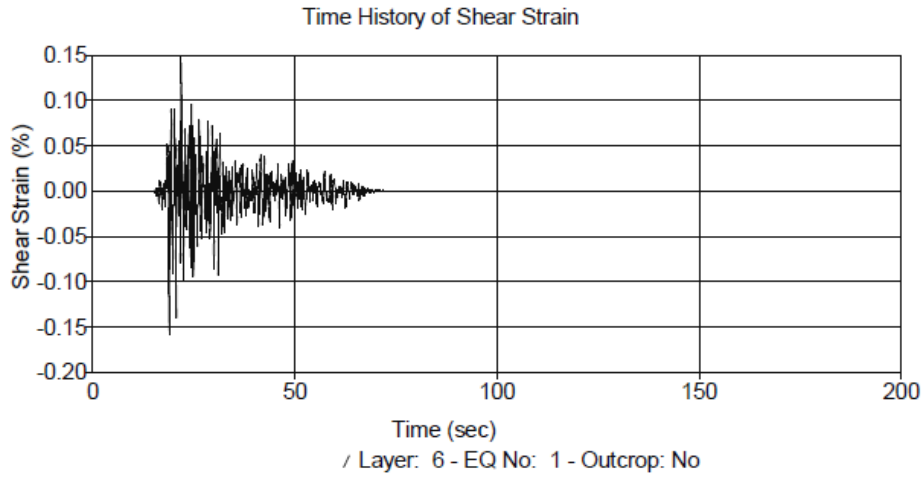

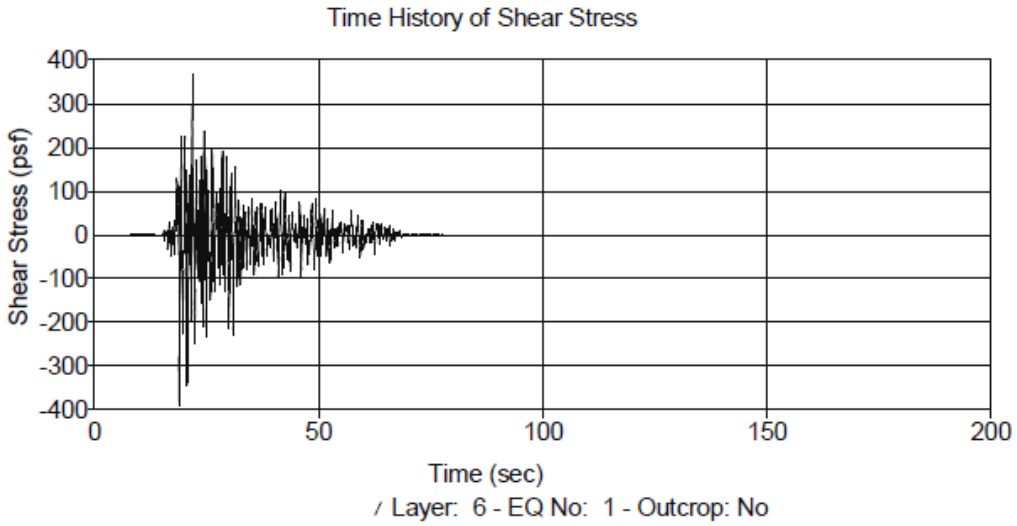
Time History of Shear Stress
Shear Stress (psf)
400
300
200
100
0
-100
-200
-300
-400
0
50
100
150
200
Time (sec)
Layer: 6 - EQ No: 1 - Outcrop: No

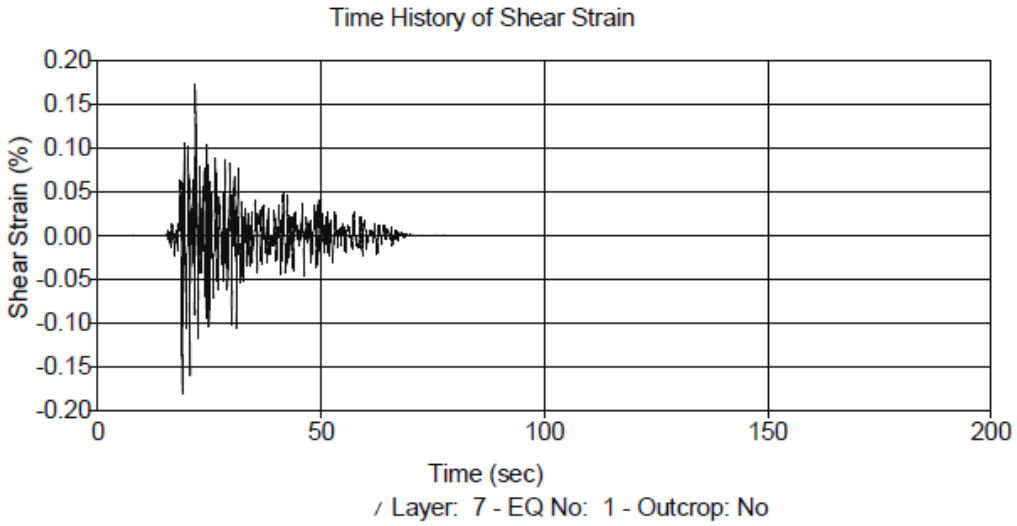
Time History of Shear Strain
Shear Strain (%)
0.20
0.15
0.10
0.05
0.00
-0.05
-0.10
-0.15
-0.20
0
50
100
150
200
Time (sec)
Layer: 7 - EQ No: 1 - Outcrop: No

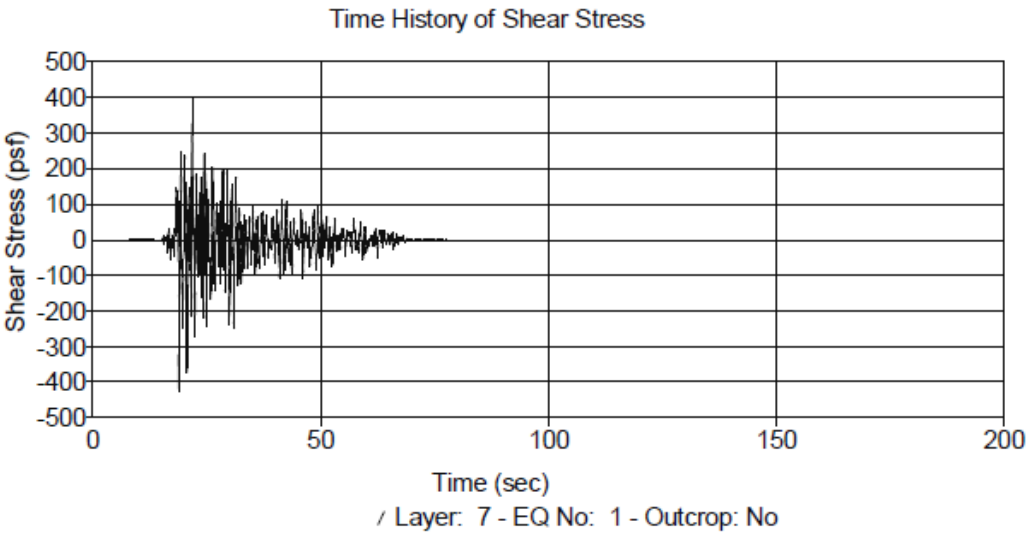
Time History of Shear Stress
Shear Stress (psf)
500
400
300
200
100
0
-100
-200
-300
-400
-500
0
50
100
150
200
Time (sec)
Layer: 7 - EQ No: 1 - Outcrop: No

Peak Shear Stress (psf)

Depth (ft)	EQ No: 1
-1.00	14.94
-8.50	134.17
-17.50	277.78
-21.00	328.76
-24.50	366.85
-29.50	405.70
-34.50	431.22
-39.50	440.64
-44.50	441.83
-49.50	435.56
-54.50	426.56
-62.00	434.12
-77.00	551.33
-97.00	682.72
-107.00	729.74

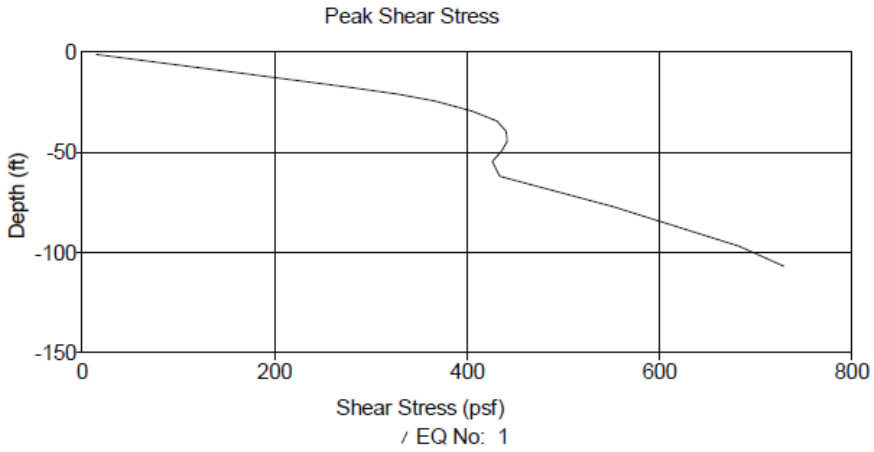

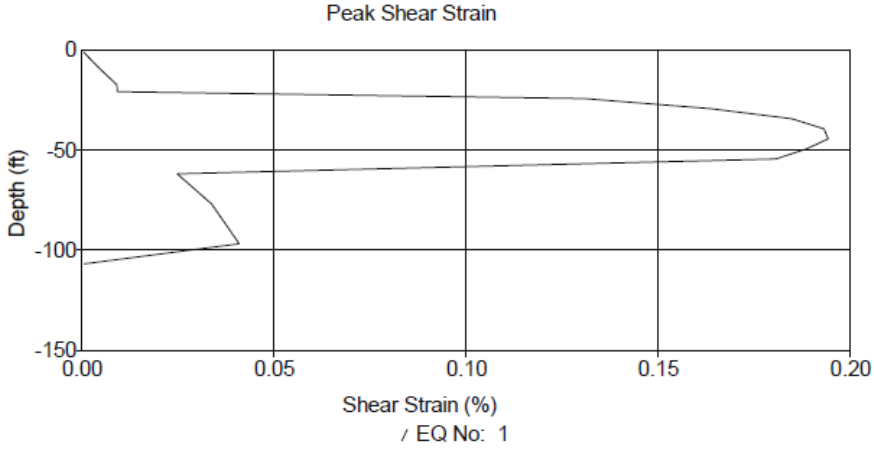

Analysis B.3: KK-1 Profile with El Centro Earthquake Motion at 0.15g Ground Acceleration

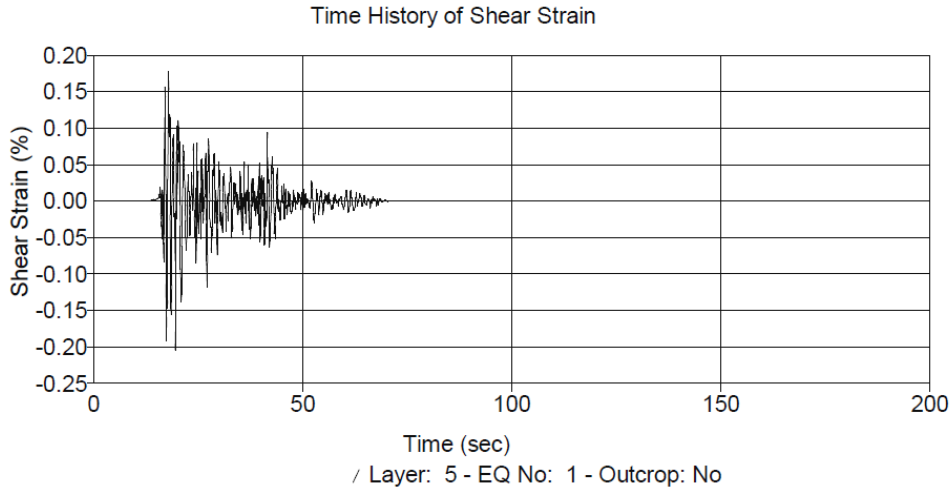

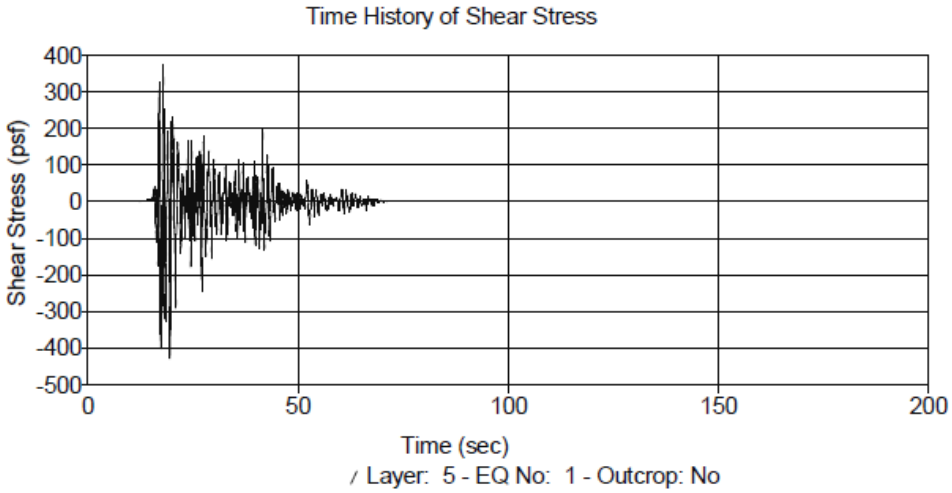

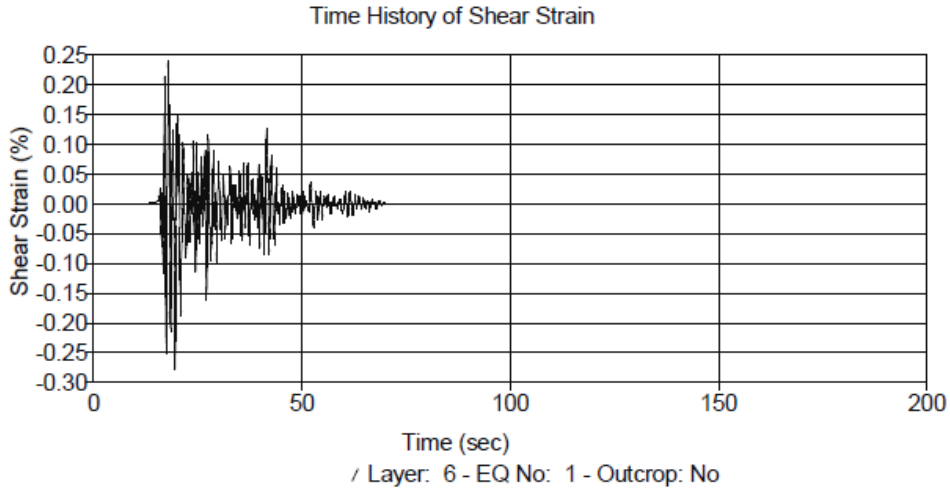

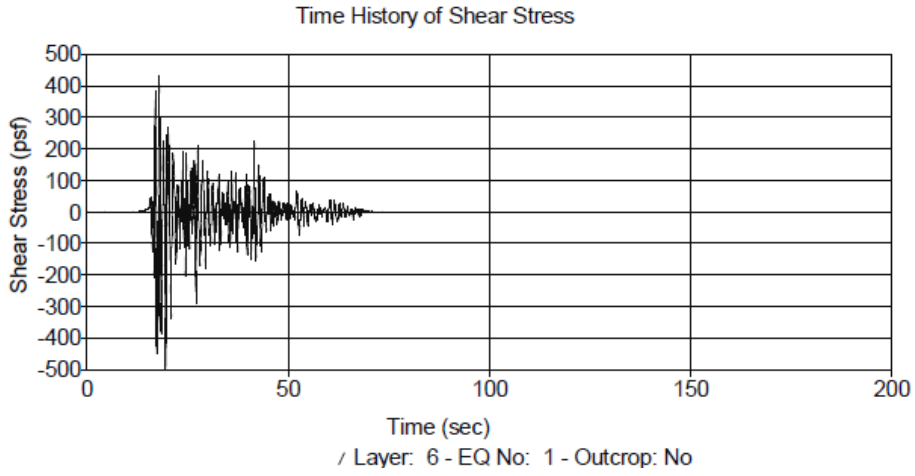
Time History of Shear Stress
Shear Stress (psf)
500
400
300
200
100
0
-100
-200
-300
-400
-500
0
50
100
150
200
Time (sec)
Layer: 6 - EQ No: 1 - Outcrop: No

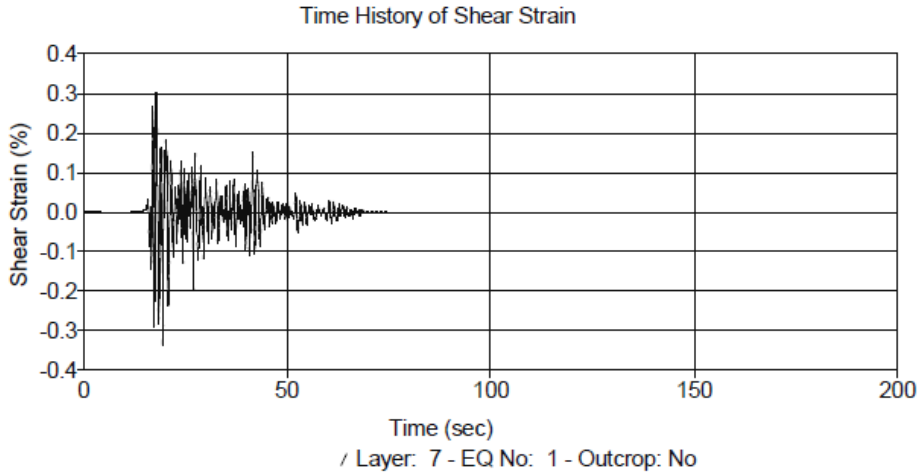
Time History of Shear Strain
Shear Strain (%)
0.4
0.3
0.2
0.1
0.0
-0.1
-0.2
-0.3
-0.4
0
50
100
150
200
Time (sec)
Layer: 7 - EQ No: 1 - Outcrop: No

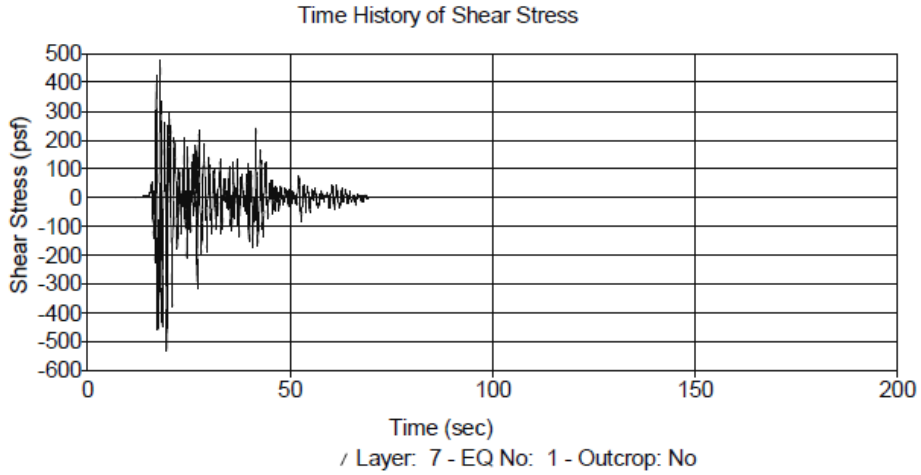
Time History of Shear Stress
Shear Stress (psf)
500
400
300
200
100
0
-100
-200
-300
-400
-500
-600
0
50
100
150
200
Time (sec)
Layer: 7 - EQ No: 1 - Outcrop: No

Peak Shear Stress

Depth (ft)	EQ No: 1
-1.00	17.75
-8.50	158.43
-17.50	333.77
-21.00	388.38
-24.50	472.48
-29.50	520.65
-34.50	548.36
-39.50	556.40
-44.50	556.37
-49.50	564.50
-54.50	607.68
-62.00	715.76
-77.00	1001.09
-97.00	1053.97
-107.00	1076.66

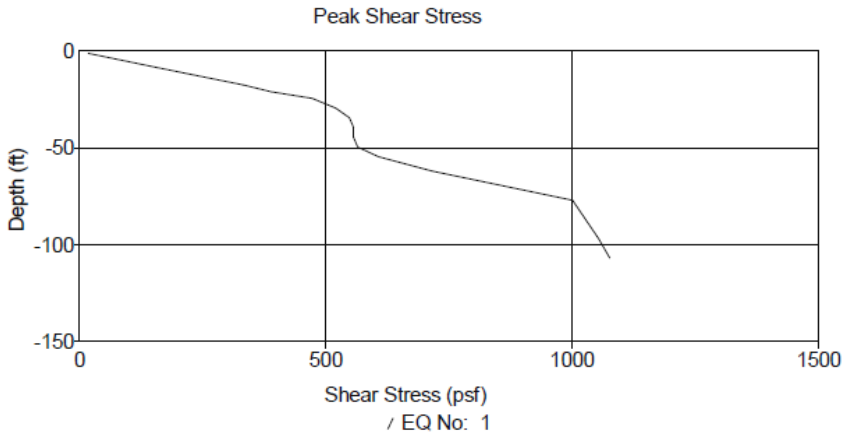

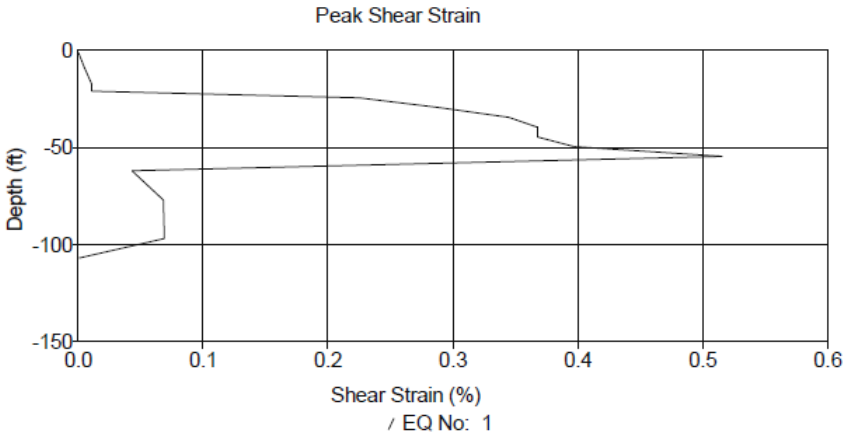

Analysis B.4: KK-1 Profile with Taft Motion at 0.15g Ground Acceleration

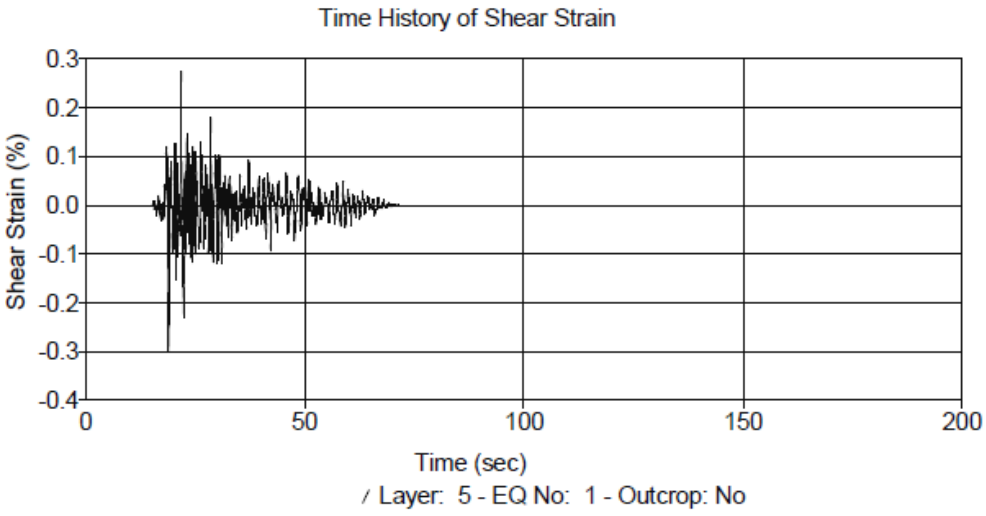

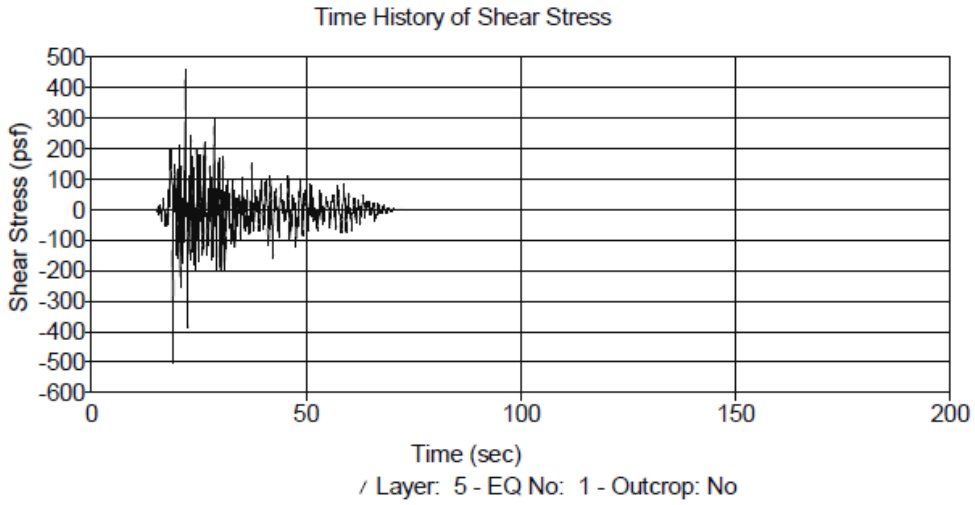

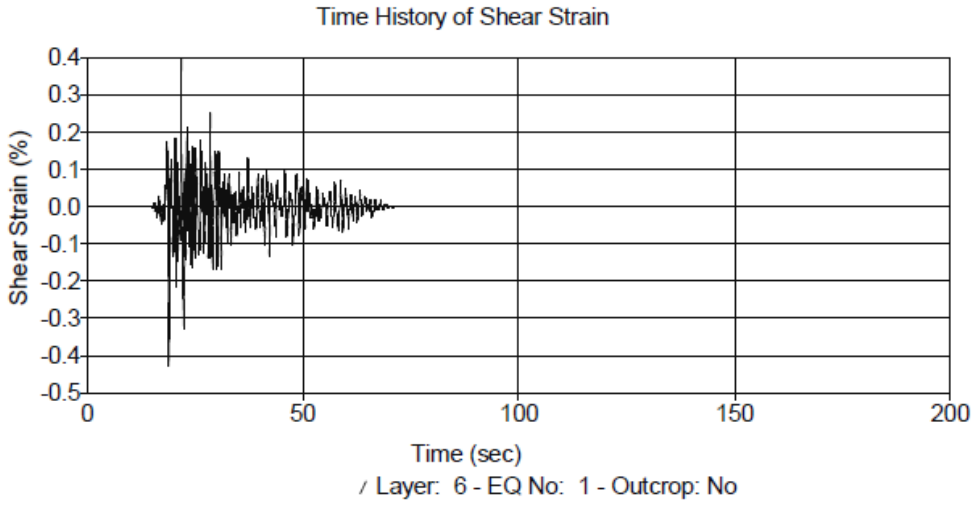

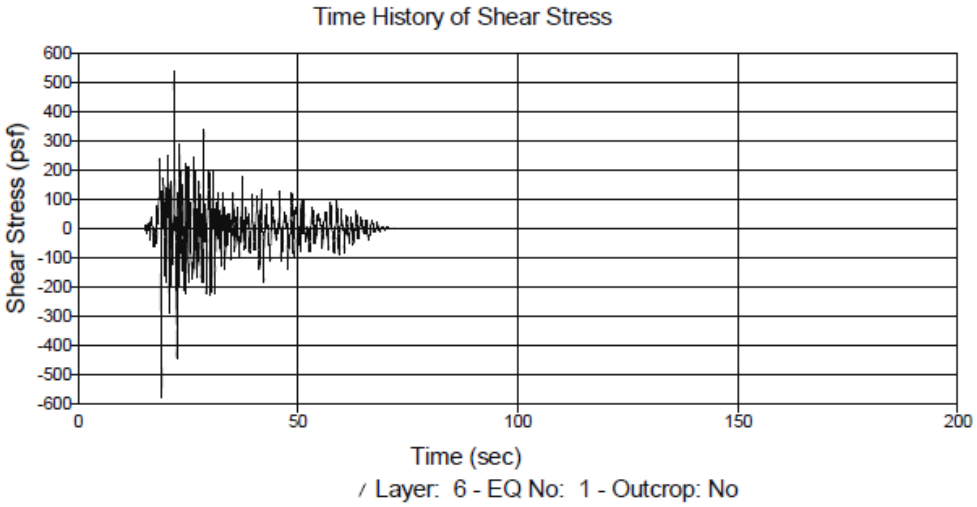
Time History of Shear Stress
Shear Stress (psf)
600
500
400
300
200
100
0
-100
-200
-300
-400
-500
-600
0
50
100
150
200
Time (sec)
Layer: 6 - EQ No: 1 - Outcrop: No

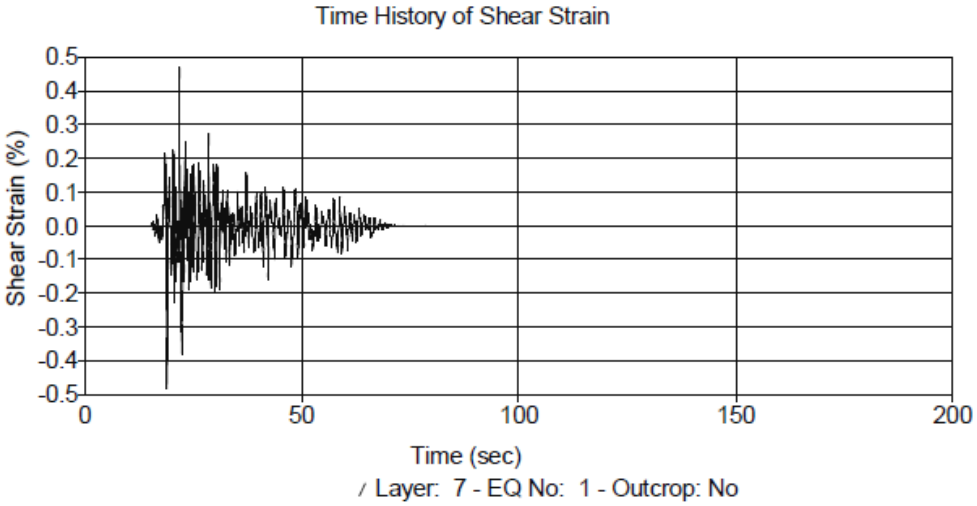
Time History of Shear Strain
Shear Strain (%)
0.5
0.4
0.3
0.2
0.1
0.0
-0.1
-0.2
-0.3
-0.4
-0.5
0
50
100
150
200
Time (sec)
Layer: 7 - EQ No: 1 - Outcrop: No

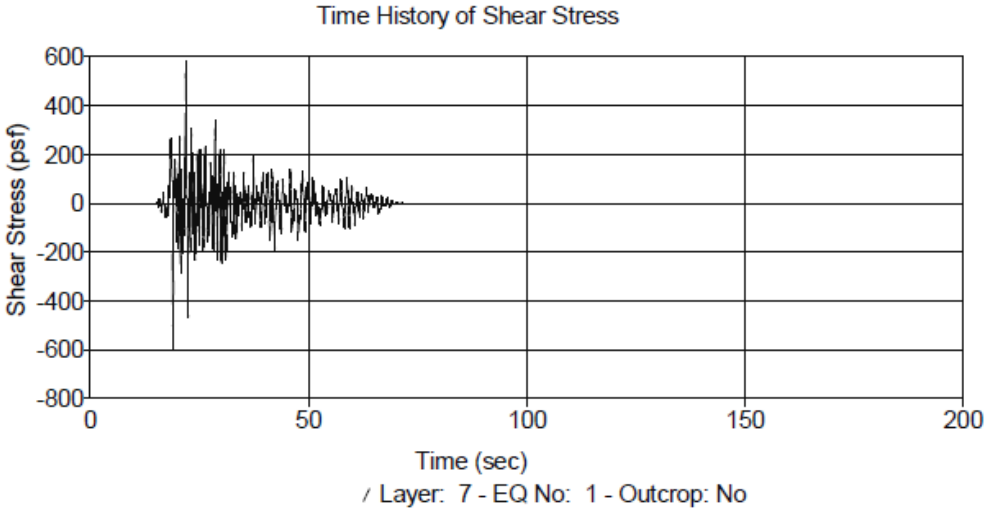
Time History of Shear Stress
Shear Stress (psf)
600
400
200
0
-200
-400
-600
-800
0
50
100
150
200
Time (sec)
Layer: 7 - EQ No: 1 - Outcrop: No

Peak Shear Stress (psf)

Depth (ft)	EQ No: 1
-1.00	22.39
-8.50	197.96
-17.50	404.83
-21.00	488.74
-24.50	537.05
-29.50	569.19
-34.50	574.46
-39.50	569.33
-44.50	556.51
-49.50	535.79
-54.50	532.59
-62.00	596.21
-77.00	843.75
-97.00	1102.50
-107.00	1262.92

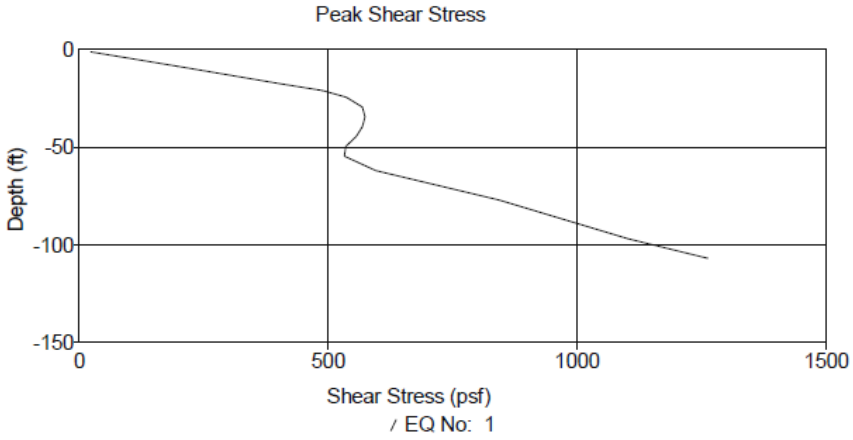

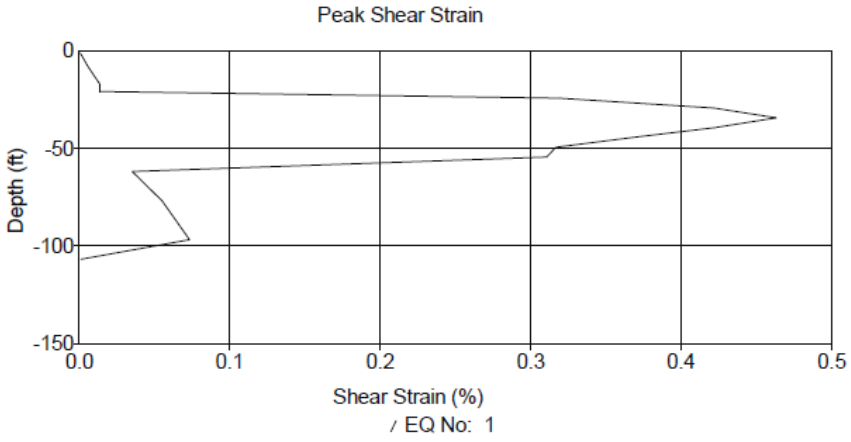

Analysis B.5: KK-2 Profile with El Centro Earthquake Motion at 0.08g Ground Acceleration

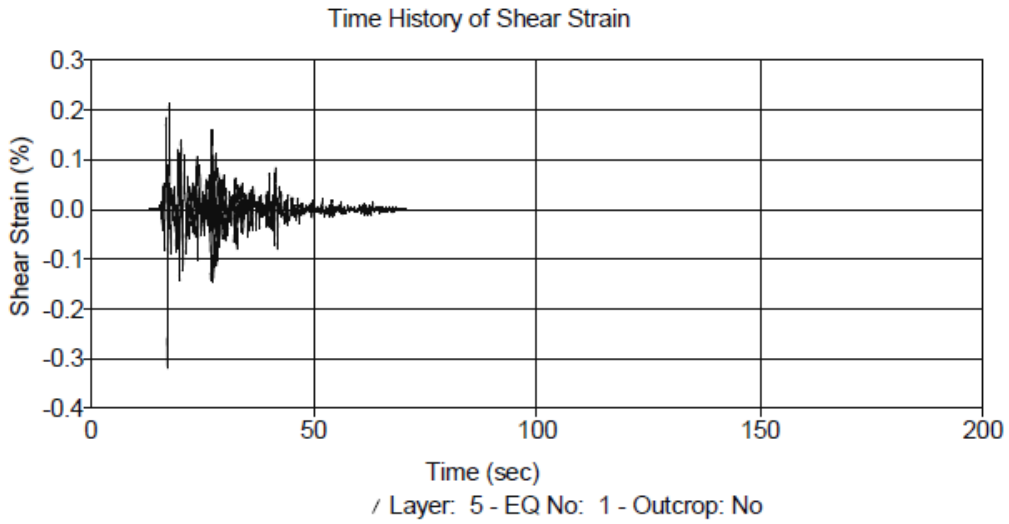

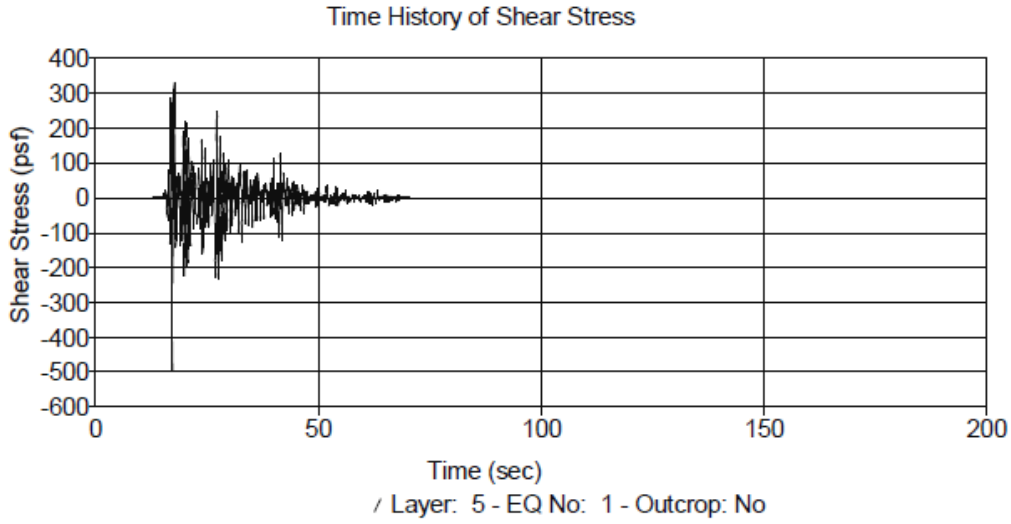

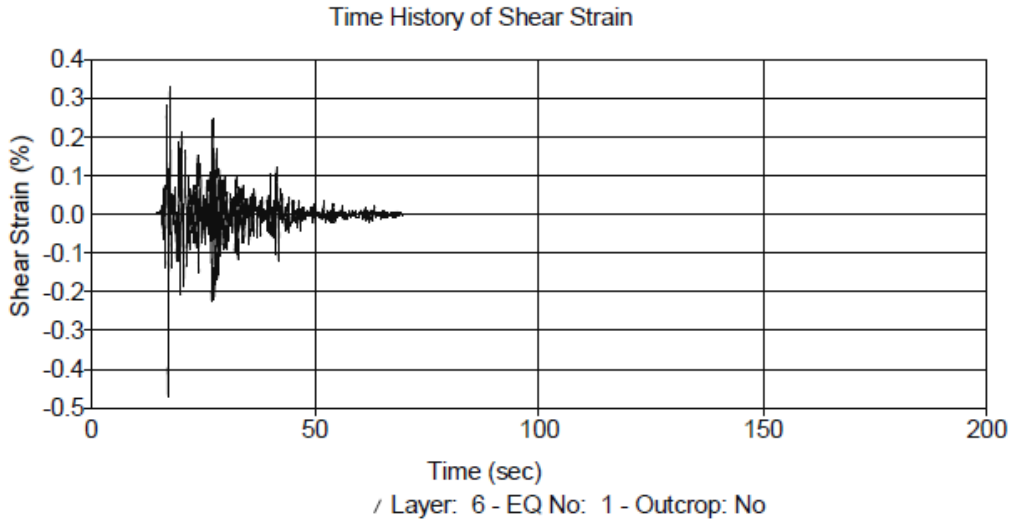

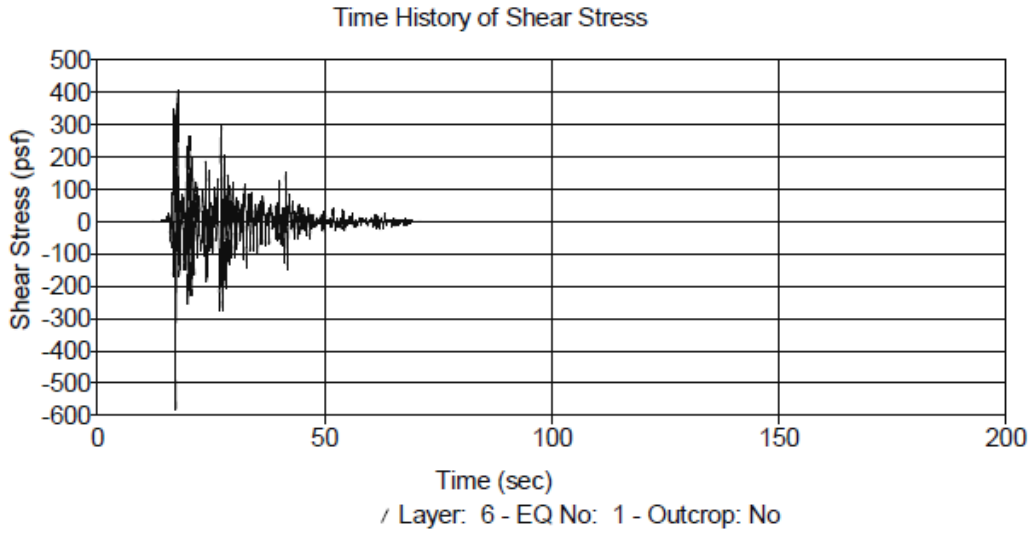

Peak Shear Stress (psf)

Depth (ft)	EQ No: 1
-0.50	12.27
-2.00	44.19
-9.50	207.17
-19.00	424.99
-25.00	551.05
-31.00	579.66
-38.00	623.96
-52.00	731.23
-72.00	898.91
-82.00	996.00

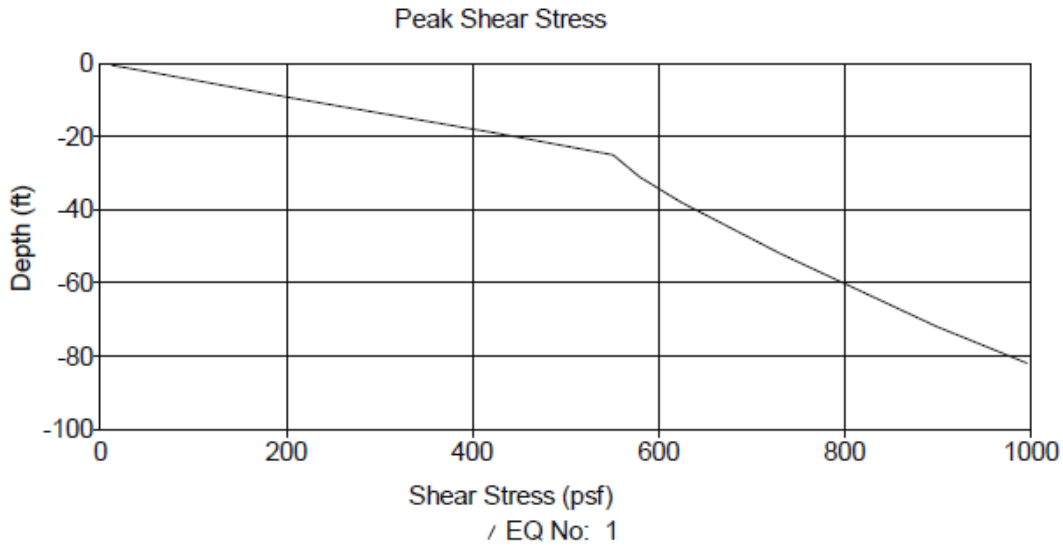
Peak Shear Stress
Depth (ft)
0
-20
-40
-60
-80
-100
0
200
400
600
800
1000
Shear Stress (psf)
EQ No: 1

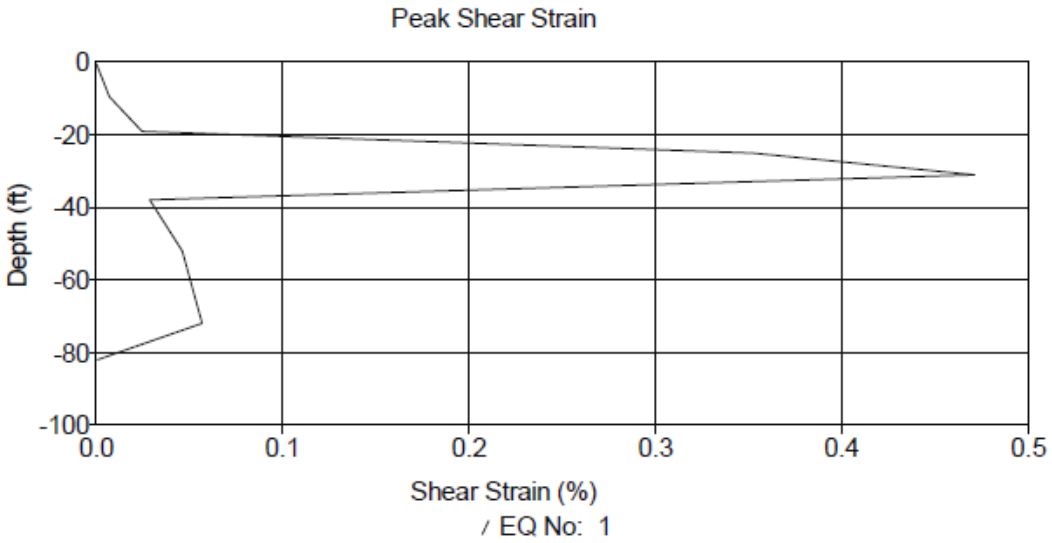
Peak Shear Strain
Depth (ft)
0
-20
-40
-60
-80
-100
0.0
0.1
0.2
0.3
0.4
0.5
Shear Strain (%)
EQ No: 1

Analysis B.6: KK-2 Profile with Taft Earthquake Motion at 0.08g Ground Acceleration

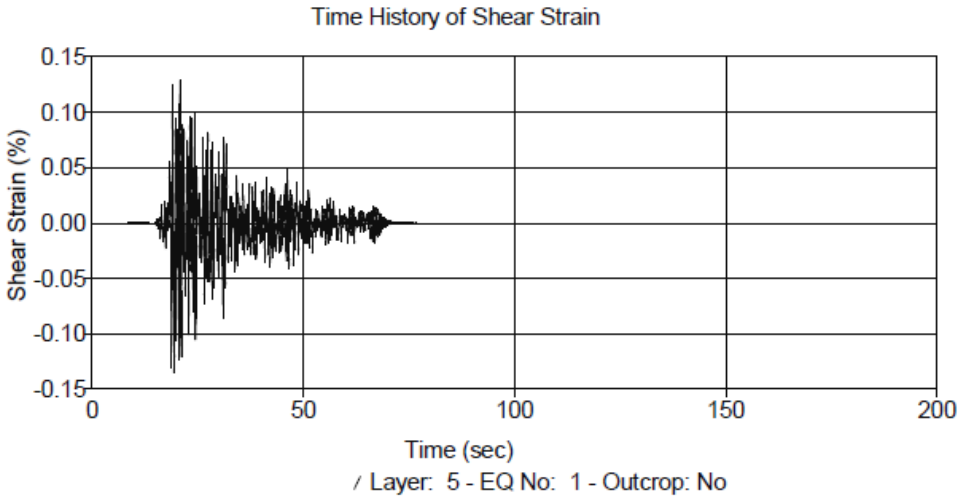

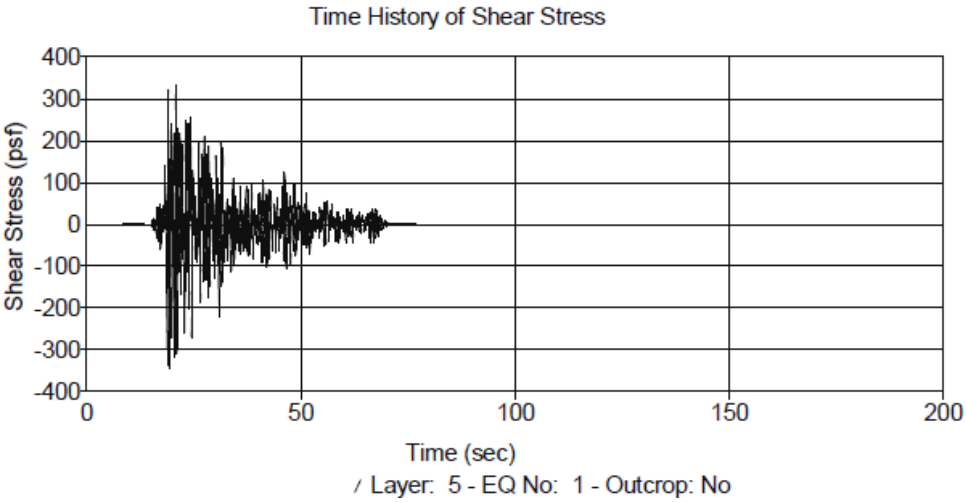

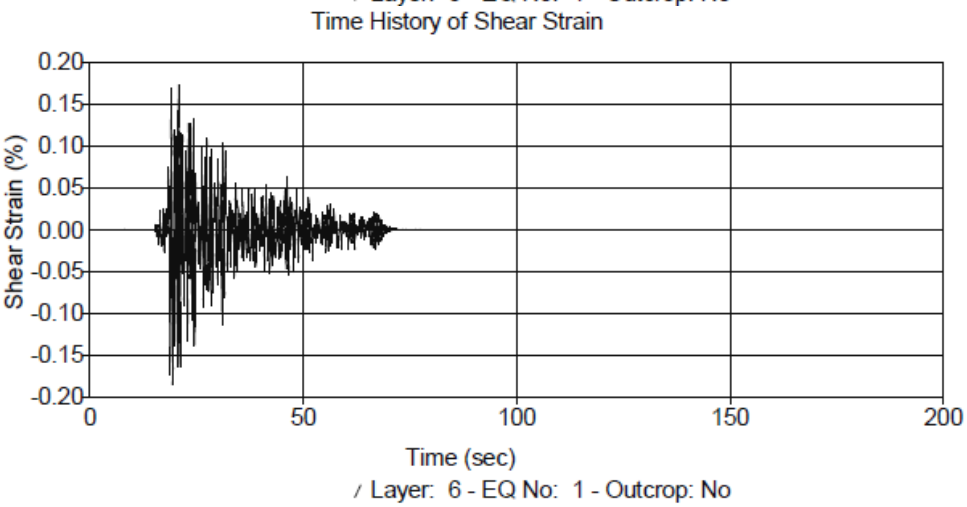

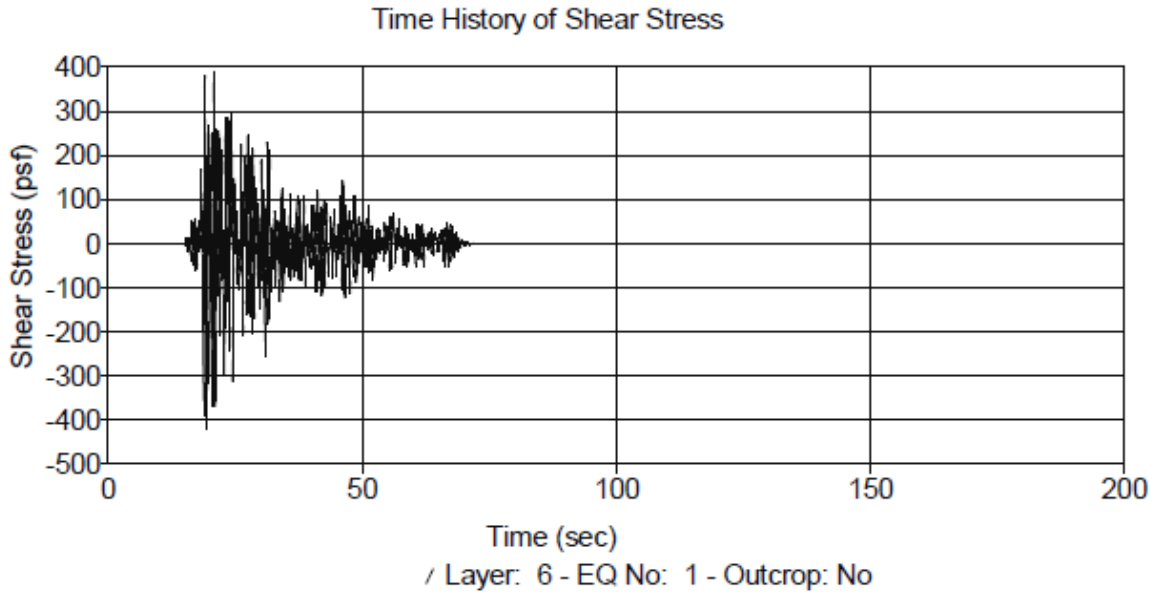

Peak Shear Stress (psf)

Depth (ft)	EQ No: 1
-0.50	9.30
-2.00	33.37
-9.50	151.78
-19.00	308.27
-25.00	391.76
-31.00	445.79
-38.00	500.29
-52.00	568.52
-72.00	666.94
-82.00	729.24

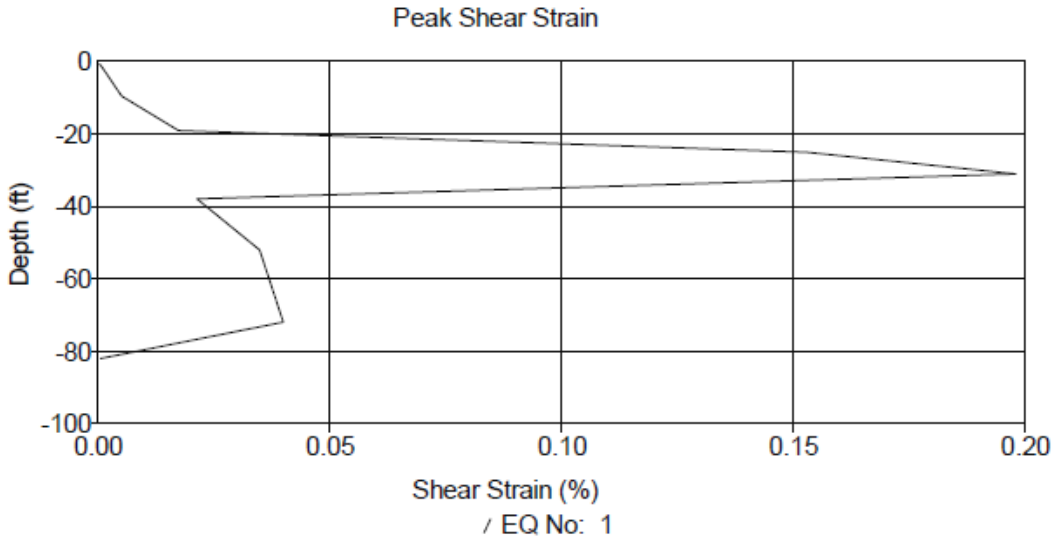
Peak Shear Strain
0
-20
-40
-60
-80
-100
Depth (ft)
0.00
0.05
0.10
0.15
0.20
Shear Strain (%)
EQ No: 1

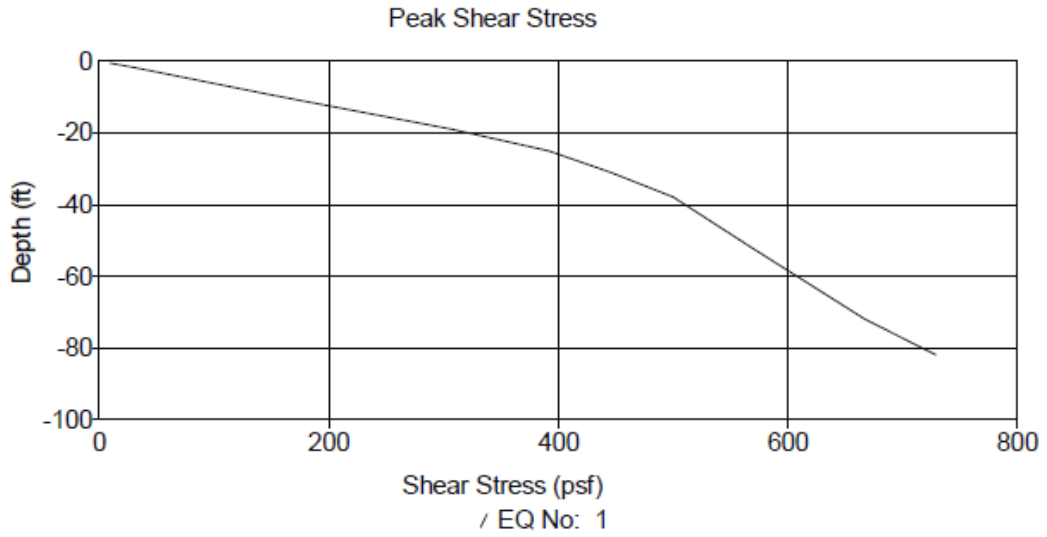
Peak Shear Stress
0
-20
-40
-60
-80
-100
Depth (ft)
0
200
400
600
800
Shear Stress (psf)
EQ No: 1

Analysis B.7: KK-2 Profile with El Centro Earthquake Motion at 0.15g Ground Acceleration

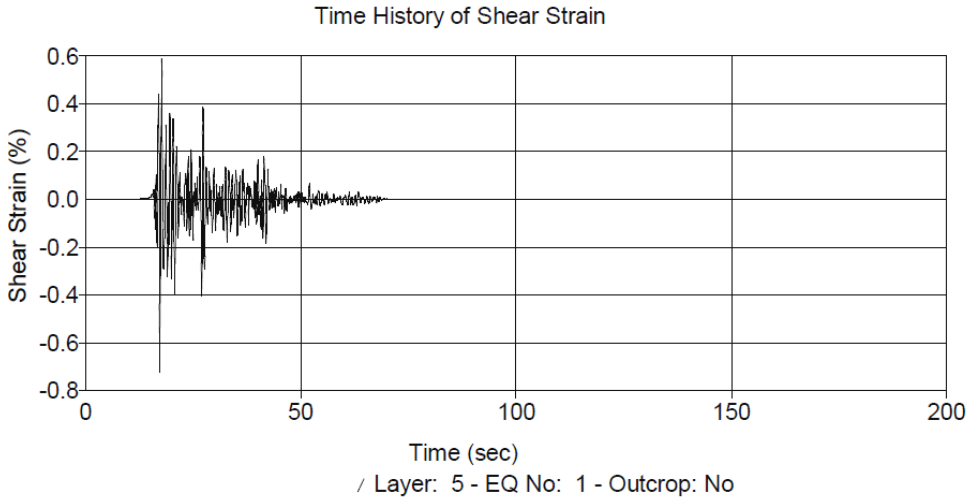

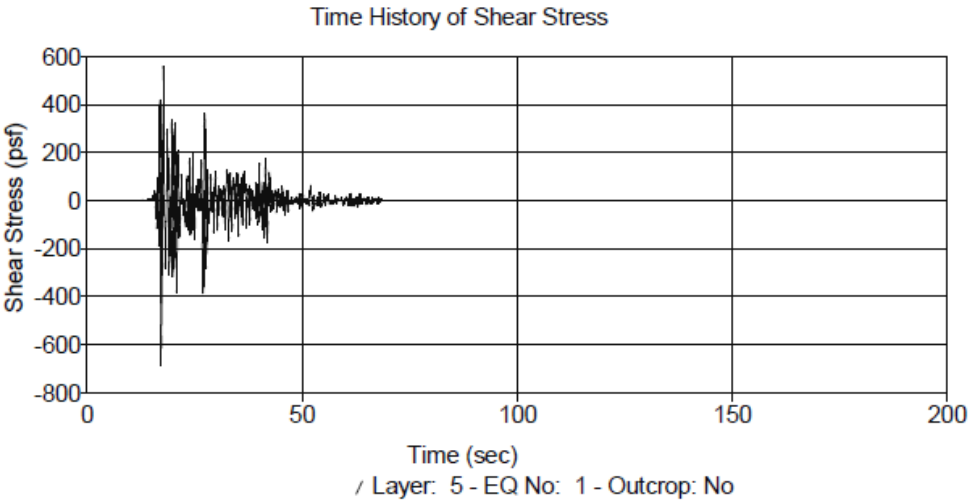

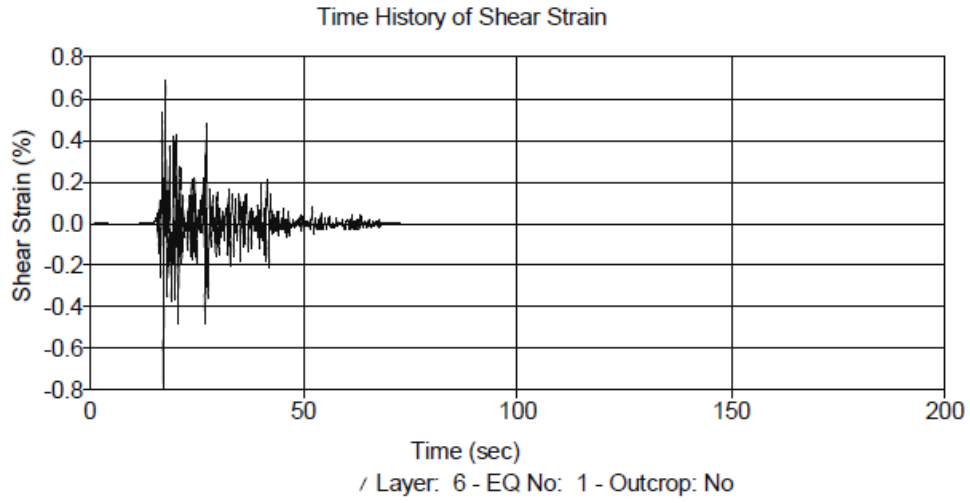

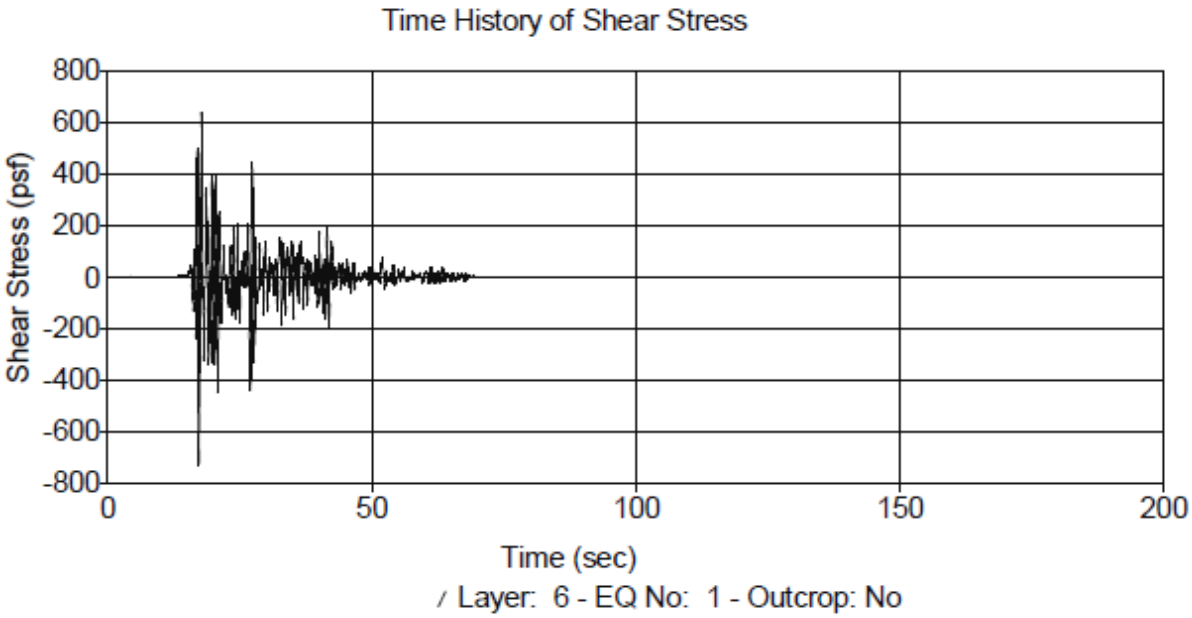

Peak Shear Stress (psf)

Depth (ft)	EQ No: 1
-0.50	17.10
-2.00	62.17
-9.50	290.32
-19.00	588.82
-25.00	729.40
-31.00	742.06
-38.00	772.73
-52.00	929.87
-72.00	1272.58
-82.00	1487.66

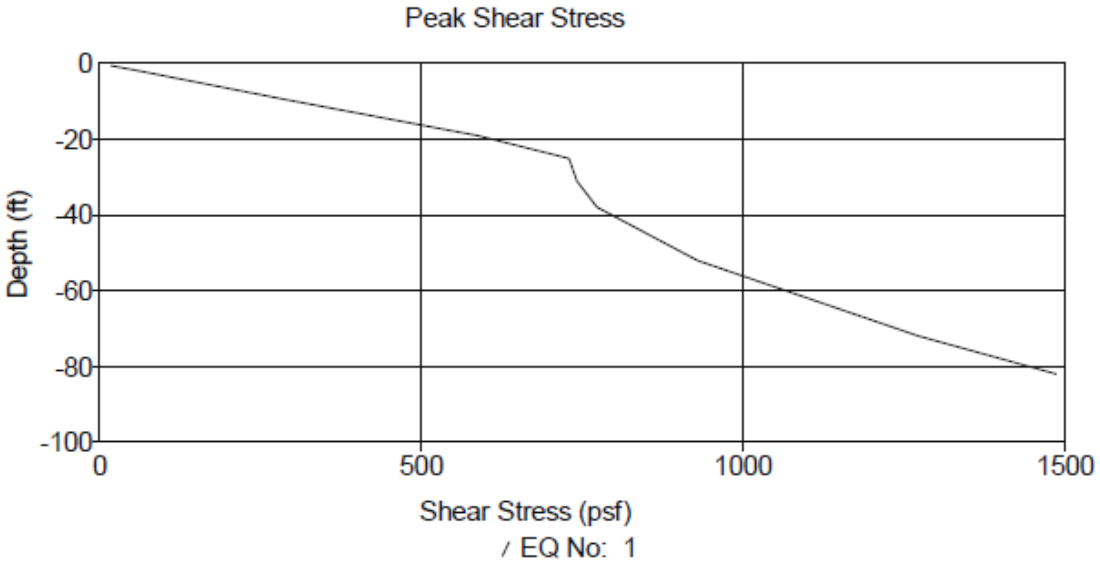
Peak Shear Stress
0
-20
-40
-60
-80
-100
Depth (ft)
0
500
1000
1500
Shear Stress (psf)
EQ No: 1

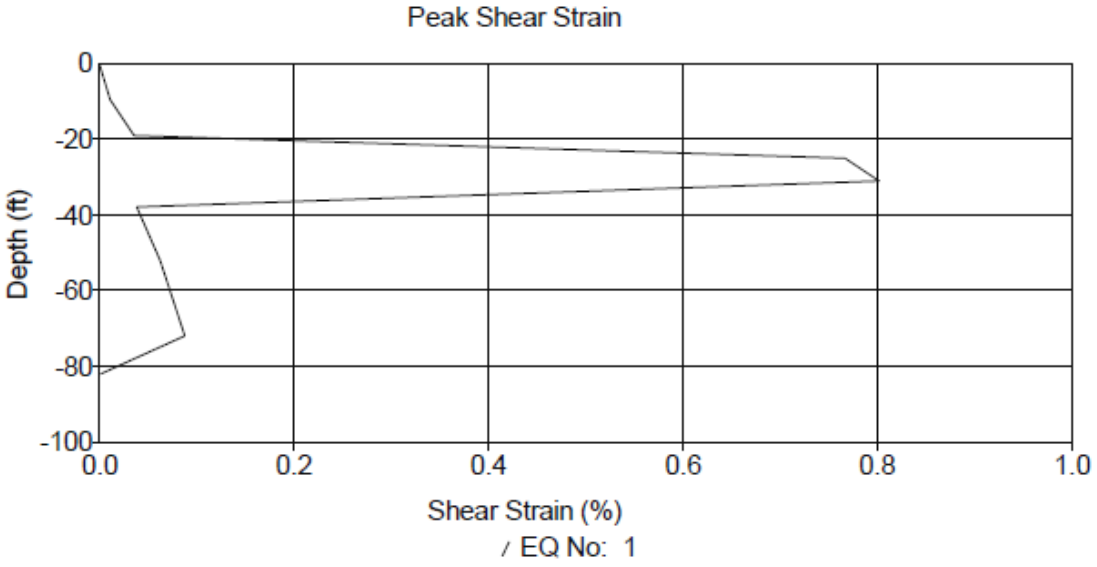
Peak Shear Strain
0
-20
-40
-60
-80
-100
Depth (ft)
0.0
0.2
0.4
0.6
0.8
1.0
Shear Strain (%)
EQ No: 1

Analysis B.8: KK-2 Profile with Taft Earthquake Motion at 0.15g Ground Acceleration

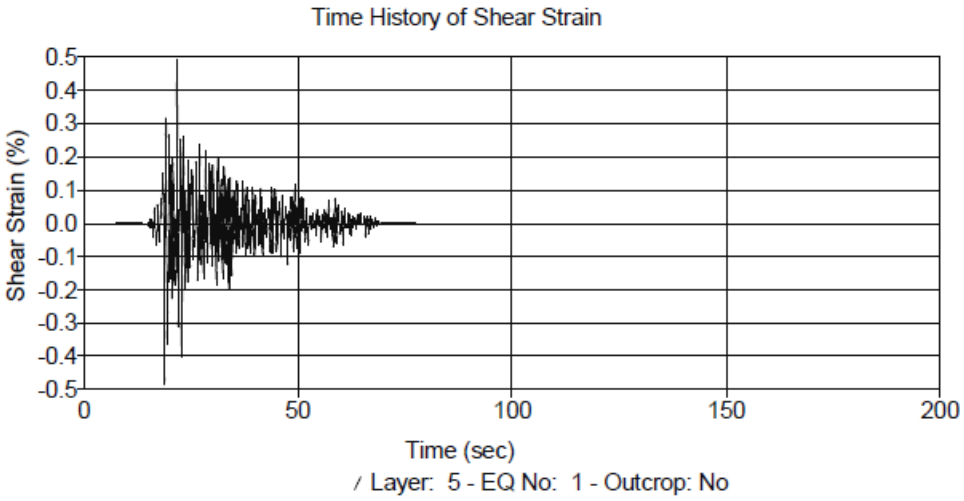

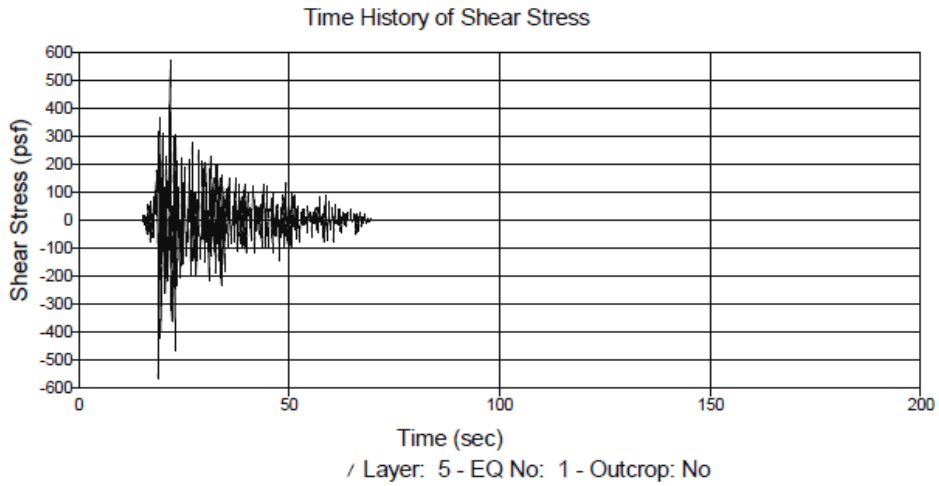

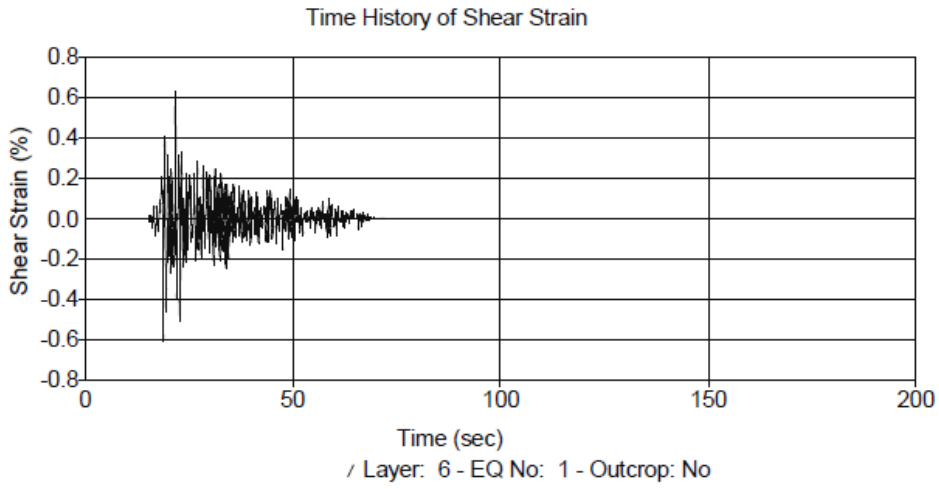

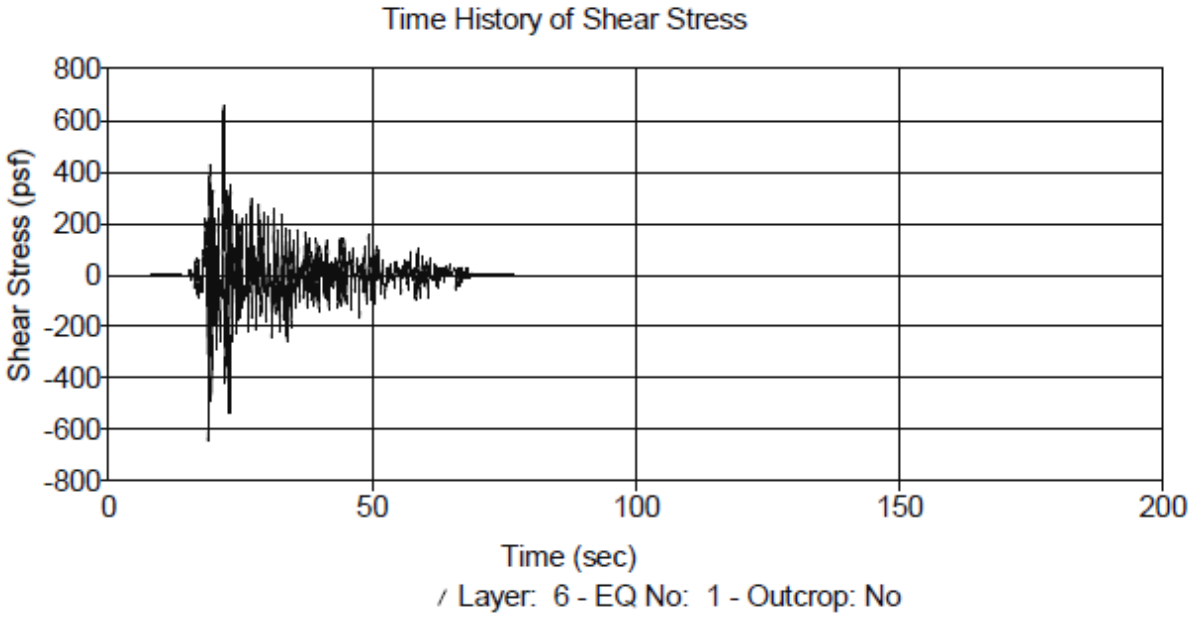

Peak Shear Stress (psf)

Depth (ft)	EQ No: 1
-0.50	14.13
-2.00	51.07
-9.50	239.39
-19.00	485.86
-25.00	616.68
-31.00	674.43
-38.00	669.11
-52.00	847.46
-72.00	1172.66
-82.00	1368.31

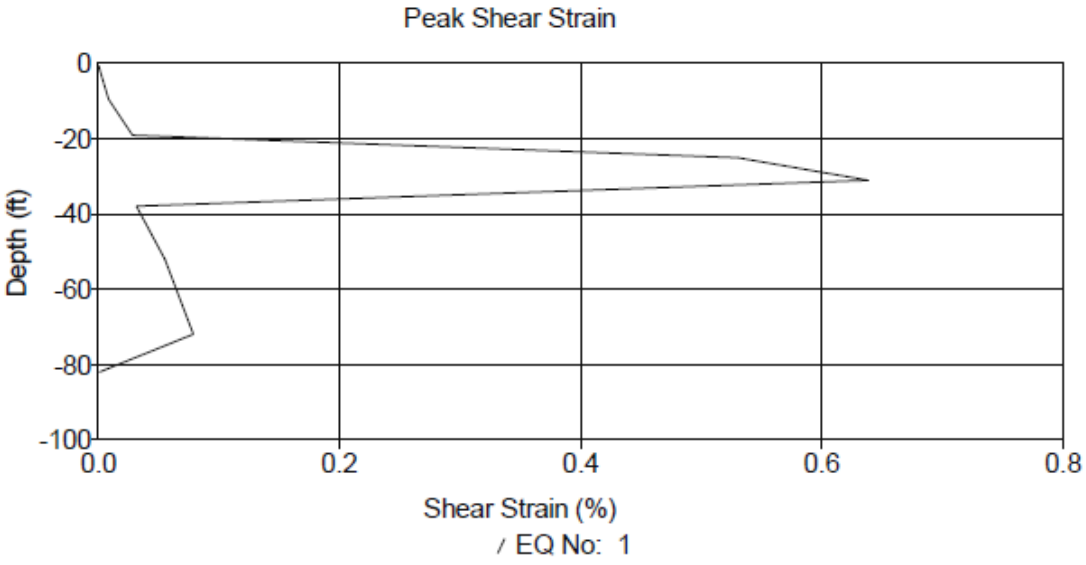
Peak Shear Strain
0
-20
-40
-60
-80
-100
Depth (ft)
0.0
0.2
0.4
0.6
0.8
Shear Strain (%)
EQ No: 1

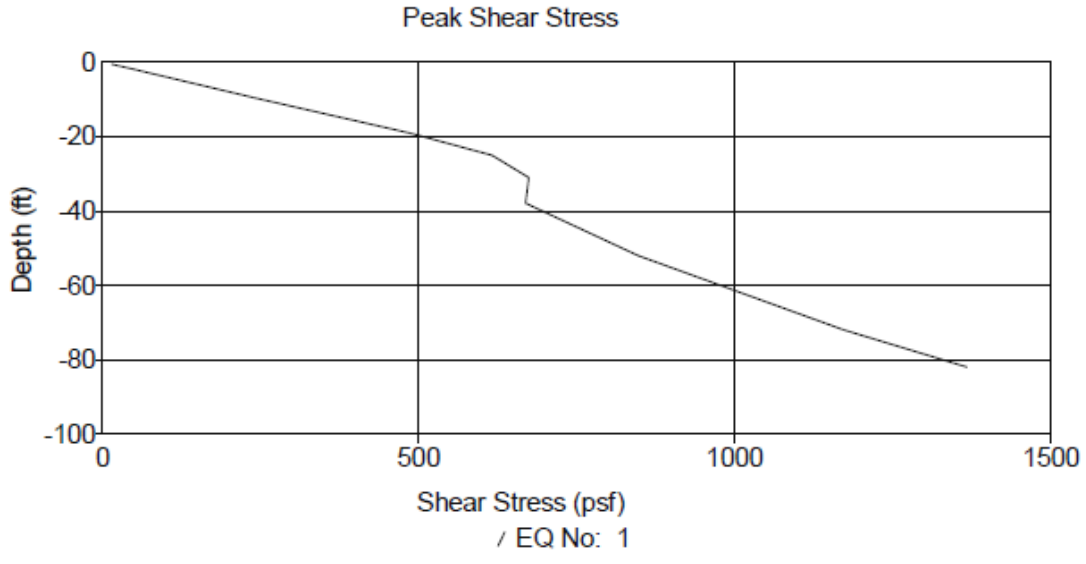
Peak Shear Stress
0
-20
-40
-60
-80
-100
Depth (ft)
0
500
1000
1500
Shear Stress (psf)
EQ No: 1